Dipartimento di Biotecnologie e Scienze della Vita
Laboratorio di Fisiologia Cellulare e Molecolare

DOTTORATO DI RICERCA IN FISIOLOGIA

SPERIMENTALE E CLINICA

XXIV CICLO

A new isoform of PEPT1 (sbPEPT1) and ion channels in touch sensation: Biophysical and Electrophysiological characterization

Tesi di dottorato di: Dott.ssa Rachele Sangaletti

Anni 2008-2011

Tutor: Dott.ssa Elena Bossi

Coordinatore: Prof.ssa Daniela Negrini

The research activity during the PhD program has been reported in the following papers:

1. Sangaletti R, Terova G, Peres A, Bossi E, Corà S, Saroglia M. "Functional expression of the oligopeptide transporter PepT1 from the sea bass (Dicentrarchus labrax)". **Pflugers Arch.** 2009 Nov;459(1):47-54. Epub 2009 Jul 18.
2. Cherubino F, Miszner A, Renna MD, Sangaletti R, Giovannardi S, Bossi E. "GABA transporter lysine 448: a key residue for tricyclic antidepressants interaction". **Cell Mol Life Sci.** 2009 Dec;66(23):3797-808.PMID: 19756379
3. Bossi E, Renna MD, Sangaletti R, D'Antoni F, Cherubino F,Kottra G, Peres A,. " Residues R282 and D341 act as electrostatic gates in the proton-dependent oligopeptide transporter Pept1"**J. Physiology.** 2010 Nov 29 ;PMID:21115649
4. Renna MD, Sangaletti R, Bossi E, Cherubino F,Kottra G,Peres A. "Unified modeling of the mammalian and fish proton-dependent oligopeptide transporter Pept1" **Channels.** 2011 Jan 2; 5(1). PMID:20953145
5. Pérez-Siles G, Núñez E, Morreale A, Leo-Macías A, Pita G, Cherubino F, *Sangaletti R*, Bossi E, Ortíz Ar, Aragón C And López-Corcuera B. "An external vestibule aspartate of glycine transporter 2 (GLYT2) controls cation access and transport coupling" **Biochemical Journal** -2011 (In press)
6. Lu Han, Ying Wang, Rachele Sangaletti, Yun Lu, Shai Shaham and Laura Bianchi
   Two novel DEG/ENaC channel subunits expressed in glia play an essential role in *C. elegans* touch sensitivity (In preparation)

of the following notices at conferences and manuscripts:

- National Meeting of Physiology PhD Students 2009, Santa Croce in Fossabanda (Pisa):
  1) Electrophysiological properties of zebrafish olipeptides transporter PEPT1.
     Rachele Sangaletti, Antonio Peres
- SIF 2009 , Siena :
  1) Electrophysiological properties of the sea bass Dicentrarchus labrax oligopeptides trasporter PEPT1
     Rachele Sangaletti, Elena Bossi, Antonio Peres
- Transportage 2009, Goettinghen (Germania):
  1) Tricyclic Antidepressants interaction with GABA trasporter lysine 448 mutants
     Francesca Cherubino, Maria Daniela Renna, Rachele Sangaletti, Elena Bossi

TABLE OF CONTENTS

Part 2. Ion channels in touch sensation 72

Part 1:

A new isoform of PEPT1 (sbPEPT1): Biophysical and Electrophysiological characterization

SUMMARY

PepT1 is an electrogenic transporter expressed at the small intestinal brush-border membrane. It transports di- and tripeptides derived from diet using a H^+-electrochemical gradient as driving force. The characterization of the oligopeptide transporters is important not only in nutrition science but also in drug delivery because these proteins are also able to transport a large number of peptido-mimetic drugs and therefore they are responsible for the high levels of oral bioavailability of many pharmaceutical compounds. Examples of PepT1 substrates include angiotensin-converting enzyme (ACE) inhibitors, anticancer drugs, penicillin and cephalosporin antibiotics and the antiviral agents Acyclovir.

The research of my PhD was focused on an sea bass isoform PepT1 cloned at the University of Insubria from the intestine of sea bass (*Dicentrarcus labbrax*).

The injection of cRNA into *Xenopus laevis* oocytes allows to obtain a high functional membrane expression of the protein that can be investigated with the use of electrophysiological techniques.

Biophysical and kinetics features of the sea bass oligopeptides transporter 1 were characterized with the two electrode voltage clamp. Exposure of the oocytes to external solutions at different pHs, to substrate concentrations (between 0.03 and 10 mM) and at different membrane voltages allowed to investigate kinetic values as the maximal current (I_{max}) and the substrate apparent affinity ($K_{0.5}$).

sbPepT1, as other peptide transporters, exhibits transport-associated currents when different di- and tripeptides are applied to the external solution and presteady-state currents in the absence of substrate.

To better understand the structure-function relation of sbPepT1, the research was extended to the other oligopeptide transporters classes (zebrafish and mammalian). The comparison of the PepT1 transport cycles among the three considered species showed a similar effect of external pH. In fact the presteady-state currents analysis presented a positive shift in the Q/V and τ/V curves and a slowing down of the decay time constants induced by acidity in all the three tested isoforms, especially in the rabbit transporter. These data were used to propose a new kinetic model.

The simulation curves of the presteady-state and the transport currents calculated with the new model that includes the effect of the acidification of external environment were in good agreement with the experimental data.

Chapter 1:

INTRODUCTION

INTRODUCTION

1.1 PLASMA MEMBRANE TRANSPORT

The plasma membrane is an essential component of all the cells of the organism. It acts as a barrier maintaining the intracellular environment separated from the outside and is selectively permeable to ions and organic molecules. The cell membrane consists of a lipid bilayer containing many integral proteins bounded by electrostatic interactions. These proteins exert the function of transport, enzymatic activity, signal transduction, cell-cell recognition, attachment to the extracellular matrix and the cytoskeleton.

Transport processes are the basis of the cell physiology and fundamental for survival. In mammalian cells the systems mediating nutrient influx are energized by the electrochemical gradient of Na^+ or protons.

In the last years the dipeptide transport mechanism has become an active research area in nutrient delivery. For a long time, it was thought that proteins were completely hydrolyzed in the gut lumen and then absorbed as free amino acids. In the last 20 years, studies on protein digestion in the small human intestine have revealed that the proteins were also absorbed in the small intestine epithelium as di- and tripeptides by a specific peptide transport system.

1.2 OLIGOPEPTIDE TRANSPORTERS: POT/PTR SUPERFAMILY

The POT (proton oligopeptide transporter) superfamily, also called PTR (Peptide transporter family), has been originally proposed in 1994 by Paulsen and Skurray. All peptide transporters (~40 members) from prokaryotes and eukaryotes, including bacteria, yeast, plants, nematodes (*Caernorhabditis elegans*) and vertebrates (Paulsen and Skurray, 1994) are grouped in this family. Members of the SLC15 family are transporters that utilize the proton-motive force to transport short peptides and peptido-mimetic substrates. The SLC transporters (SoLute Carrier) include almost 50 gene families coding for passive transporters, exchangers and co-transporters that show a sequence identity at least of 20-25%. Four transporters belong to the SLC15 family: the oligopeptide transporters, PepT1 and PepT2, and the peptide/histidine transporters PHT1 and PHT2. PEPT1(SLC15A1) and PEPT2(SLC15A2) mediate the transfer of peptide substrates into intestinal and renal epithelia respectively (Steiner et al., 1995). Although the function of PHT1(SLC15A4)

and PHT2(SLC15A3) is still unclear, it is known that they are able to transport histidine and some di- and tripeptides (Yamashita et al., 1997).

SLC15 transporters vary in size from 450 to about 800 amino acids with 12 transmembrane domains (TMD) and the N- and C- termini in the intracellular space.

All POT family members have also three characteristic signature sequences, known as PTR2 family signatures, well conserved during the evolution (Fig. 1.1): the first motif (ExCERFxYYG) is located at the outward-facing end of TMD1 and stretches into the following extracellular loop; the second PTR2 sequence (GxxxADxxxGKxxTI) corresponds to the end of transmembrane domain 2 (TMD2), to the following intracellular loop and reaches TMD3; the third signature (FYING-PTR-motif) includes the core of TM5 and comprises a stretch of 11 amino acid residues (Fei et al., 1998b). Peptide transporter pathways have a distinct evolutionary conservation. In prokariotes, for example, several classes of membrane peptide transporters have been found, including ATP-dependent oligopeptide carriers not identified in eukaryotes. On the contrary di- and tripeptide transporters are found in yeast, invertebrates and vertebrates. In bacteria, three peptide transport systems have been characterized in *Escherichia coli*, in *Salmonella typhimurium* and in *Shewanella oneidensis*: the oligopeptide permease (Opp) and dipeptide permease (Dpp) belonging to the large family of ABC transporters and one for di- and tripeptides belonging to the PTR family, designed as DtpT. In bacteria, peptide transporters are essential not only for metabolic needs but also for chemotaxis, sporulation and for gene expression (Doige and Ames, 1993; Higgins, 1992).

In the yeast *Saccharomyces cerevisae* two peptide transporters are known: one for di- and tripeptides belonging to the PTR family and a second specific for tetra/pentapeptides belonging to the oligopeptide transporter family (OPT) (Hauser et al., 2001).

Fei and colleagues in 1998 cloned two oligopeptide transporters from *Caernorhabditis elegans*, CPTA and CPTB. They are both formed by 796 amino acids with 11 transmembrane spanning regions (TMs), instead of the 12 TMs seen in the other members of the oligopeptide transporter family. It has been observed also that CPTA has high affinity for substrates and a low capacity and it shows a higher similarity and identity to hPepT1 (the lower-affinity mammalian peptide transporter isoform). CPTB instead is a peptide transporter with lower affinity and higher capacity and it is related to hPepT1 no more than to hPepT2 (Fei et al., 1998a).

OPT1 is di- and tripeptide transporter that has been cloned in 1998 from *Drosophila melanogaster*. It transports not only peptides but also aminocephalosporins and aminopenicillins (Roman et al., 1998).

In lower vertebrates the first cloned peptide transporter has been zfPepT1 from Zebrafish (*Danio rerio*) (Verri et al., 2003); zfPepT1is an electrogenic transporter expressed in the intestinal epithelial cells and shows the same characteristics of mammalian PepT1 as a low affinity, high capacity transport.

Later, PepT1 has been isolated and characterized in other fish species such as: antartic haemoglobinless teleost (*Chionodraco hamatus*) (Maffia et al., 2003), atlantic cod (*Gadus morhua*) (Ronnestad et al., 2007), eel (*Anguilla anguilla*) (Kalujnaia et al., 2007) carnivourous fish (*Epinephelis coioides*) (Yuen et al., 2007).

The first cloned mammalian proton-coupled peptide transporter was PepT1 from rabbit's small intestine in 1994 to 1996 (Boll et al., 1996; Fei et al., 1994). The human PepT1 was cloned later and it possesses a similarity of 81% (Covitz et al., 1998) with the rabbit isoform. Subsequently, PepT1 has been isolated by expression-cloning from other mammalian species such as rat (Saito et al., 1995), mouse (Fei et al., 2000), sheep, cow, pig (Chen et al., 1999) and macaco (Zhang et al., 2004).

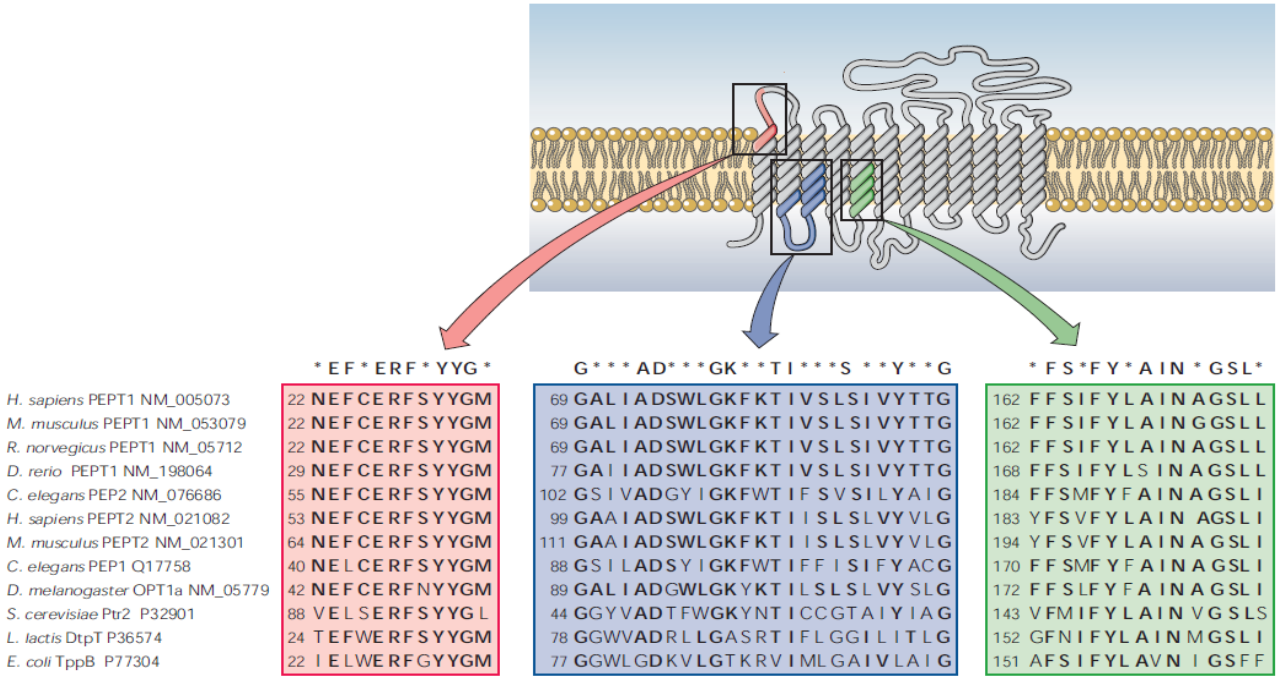

Figure 1.1 Conserved regions and PTR-2 domains in different members of the PTR family: the first motifs at the end of the first TMD (TMD1); the second PTR-2 domain which is less conserved located between the C-terminus of TMD2 and N-terminus of TMD3; the third motifs found in TMD5 (Daniel et al., 2006).

1.3 PepT1

1.3.1 Structure

The gene encoding for human PepT1 consists of 23 exons and is located on the chromosome 13q33-34 (Liang et al., 1995). hPepT1, represented in Figure 1.2, is an intestinal dipeptide transporter of 707 amino acids with 12-transmembrane domains (TMD), a large extracellular loop between TMD9 and TMD10, both N- and C-termini located in the intracellular space, two proteins kinase C (PKC) recognition sites, a protein kinase A (PKA) site (Fei et al., 1994).

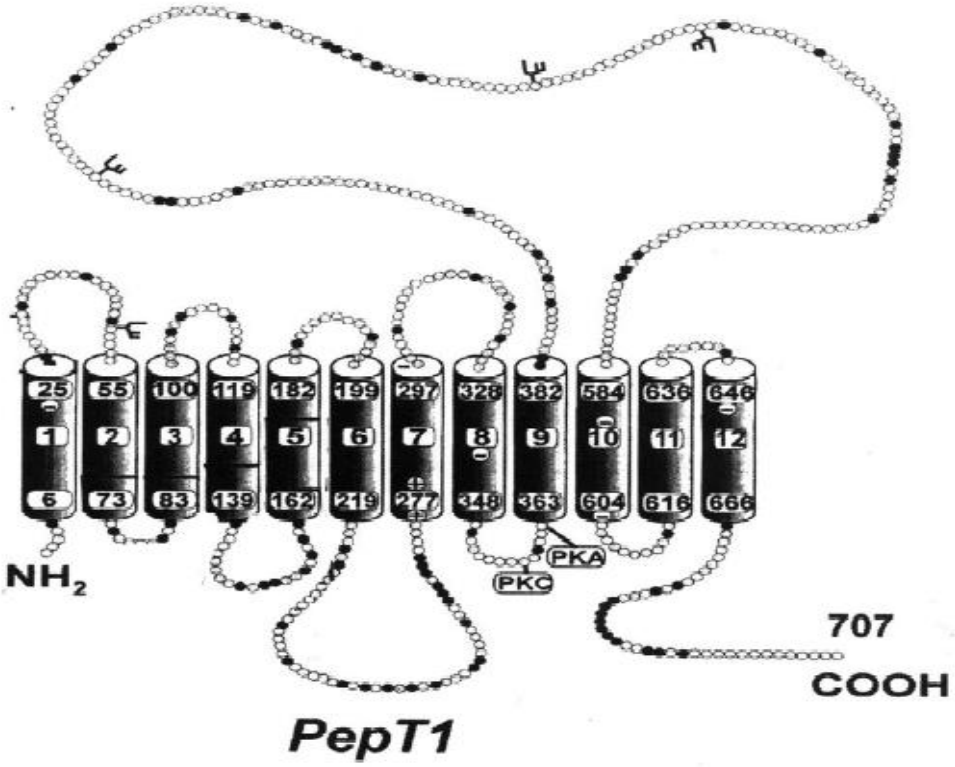

Figure 1.2. A schematic model of PepT1 showing its 12-TM topology (Fei et al.,1994).

Several H^+-coupled solute transporters such as PepT1 are known to possess specific histidine residues essential for their catalytic activity (Ganapathy and Leibach, 1983; Kato et al., 1989). The function of histidine residues in H^+ binding and translocation has first been investigated in 1987 in a typical H^+-coupled solute transport system: *Escherichia coli* Lac permease system (Kaback, 1987). There are three histidine residues conserved in both the intestinal and renal peptide transporters PepT1 and PepT2 between different animal species. In hPepT1 these residues are His-57, His-121 and His-260 corresponding to His-87, His-142 and His-278 in hPepT2 (Fei et al., 1997). Fey and colleagues through site-directed mutagenesis and electrophysiological studies investigated these

mutated histidine residues to clarify their role in PepT1 catalytic function. They found that the extracellular histidine residue His-57 located on the interface between the TMD2 and the extracellular side is mandatory for PepT1 transport function. The His-57 mutants (His-57Asn, His-57Gln) led to a total inactive transporter (Fei et al.,1997). Both His-121 located in the fourth putative transmembrane domain and His-260 in the cytoplasmatic loop between TMD6 and TMD7, are not essential residues in binding and translocation of H^+. Mutations of these residues did not interfere with transport function (Fei et al.,1997). Many mutations have been introduced into PepT1 to identify some critical and essential residues. In summary, the Tyr-64 residue located at TMD2 shown to be involved in substrate translocation. Changing this Tyr residue into Phe abolished the transport of di- and tripeptides (Chen et al., 2000). Mutation of Tyr-56 into Phe, instead, led to a reduction in the affinity for different charged dipeptides (Chen et al., 2000).

A computer modeling approach has been an alternative method to investigate the substrate binding site (Lee et al., 1999). This approach has been applied first to the transmembrane glucose transporter Glut1 (Zeng et al., 1996). Subsequently Bolger proposed a computer modeling for PepT1 based on the essential consideration that the α-helical transmembrane domains were important for substrate/H^+ binding and translocation and that they would bundle against each other in a pairwise manner (Bolger et al., 1998). Minimizing these pairwise interactions, calculating the amphipathicity of the helices and modeling the 12-TM PepT1 structure, Bolger predicted an arrangement of the TMs and the key amino acids that might form a putative channel of the peptide transporter. These amino acids are shown in Figure 1.3: Trp-294, Tyr-588, Glu-26 in the entry from extracellular side to the region termed “bubble”; Tyr-12, Glu-595, Asp-341 and Tyr-91 in the center of the bubble. Into the intracellular side there are Tyr-167 and Arg-282 (Lee et al., 2000). Tyr-167 is a residue located in TMD5 and together with Asn-171 and Ser-174 plays a critical role in substrate binding. Mutating these residues in cysteine abolished the expression on the plasma membrane, suggesting that these amino acids are responsible for a correct packaging and transport of the peptide transporter (Kulkarni et al., 2003).

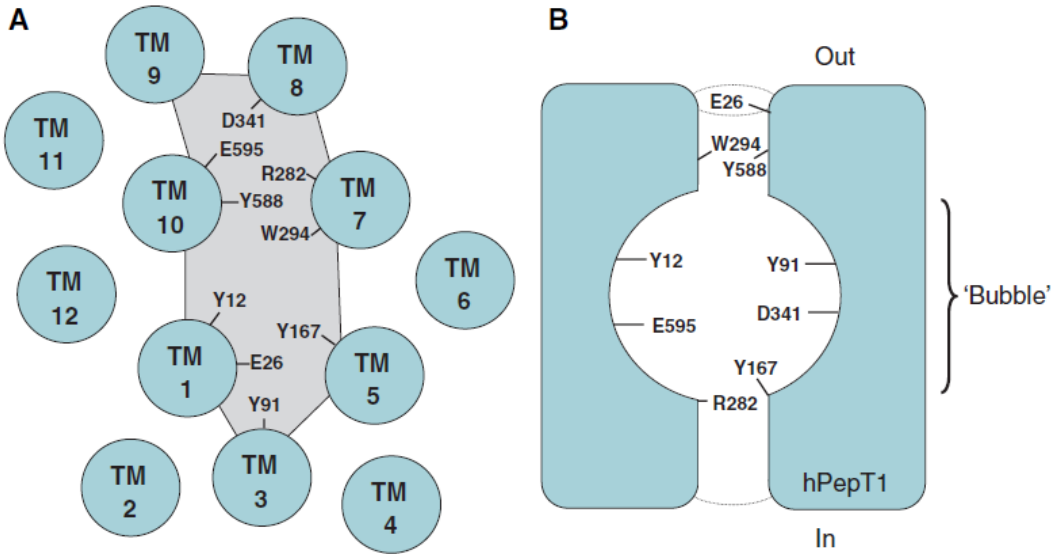

Figure 1.3. (**A**) Amino acidic residues in 12-TM model of hPepT1, predicted to be involved in functional activity of the transporter; (**B**) Schematic diagram of hPepT1, showing the transmembrane channel vestibule labeled 'bubble' in which are indicated amino amino acidic residues necessary in transporter function (Meredith and Price, 2006 adapted from Lee et al., 2000).

Furthermore Meredith before and Kulkarni later have reported that Arg-282 residue, located in the extracellular region of TMD7, plays a key role in the rabbit PepT1 translocation mechanism forming a charged-pair interaction with Asp-341 residue in TMD8. It has been reported that mutations of either Arg-282 and Asp-341 into an oppositely charged amino acid decrease the uptake activity, while mutations at either position into a neutral amino acid does not alter the function (Meredith, 2004); (Kulkarni et al., 2007).

Immunolocalization and single-oocyte chemiluminescence (SOC) experiments performed on mutated Arg-282, Asp-341, His-57 residues showed that all the isoforms were correctly localized in the membrane at levels similar to the wild-type, except for the double mutant Arg-282Asp-Asp-341Arg that gave weak signals in both the experiments (Fig. 1.4) (Uchiyama et al., 2003; Kulkarni et al., 2007; Bossi et al., 2011).

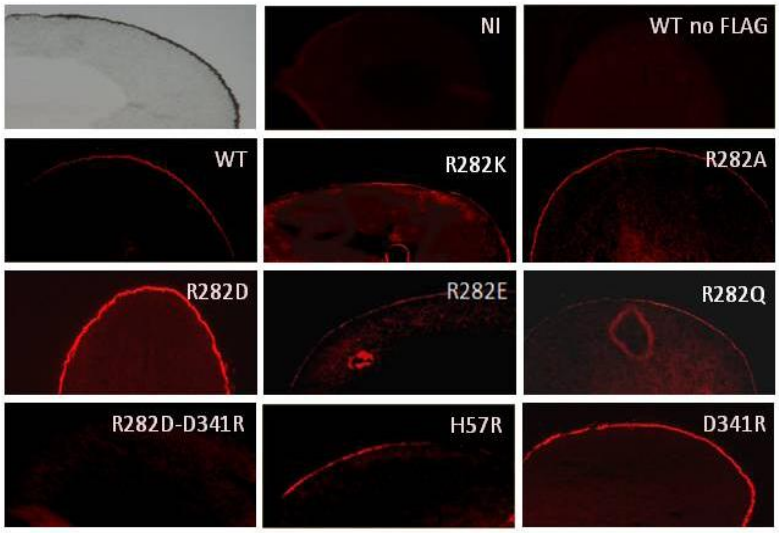

Figure 1.4. (A) Fluorescence microscopy images of the outer membrane of oocytes expressing FLAG-rbPepT1 wild-type (WT) and the indicated mutants. Oocytes non injected and injected with wild-type-non tagged PepT1 are also used as controls (Bossi et al. 2011).

Analysis of chimeric proteins have been conducted in order to determine the role of the large structural domains. In the 1996 Doring and colleagues engineered a recombinant chimeric peptide transporter, CH1PepT that was composed of amino acids 1-401/(TMDs 1-9) from PepT2 and 402-707/(TMDs 10-12) from PepT1. The result has been a PepT2-like transporter, suggesting that the N-terminus region may determine the phenotypical characteristics of Pept2 and that the large extracellular loop between TMD9 and TMD10 was not probably involved in substrate binding (Doring et al., 1996). The same result has been confirmed in 1998 by Fey et al. and in 2000 by Terada et al.

Recently, Newstead and colleagues reported the crystal structure of a peptide transporter from the bacterium *Shewanella oneidensis* (PepTso) that shows the 30% of sequence identity with the mammalian PepT1 and PepT2. PepTso contains 14 TM domains, with the domains H1-H12 observed in all PepT transporters. PepTso has two additional TM domains, HA and HB, located in the cytoplasm (Fig. 1.5A). The role of these domains is still unknown. Two distinct cavities have been also discovered: **1**) the central cavity located in the middle of the membrane and separated from the extracellular space by transmembrane domain TMD1,TMD2,TMD7 and TMD8. This cavity forms the binding site for di- and tri- peptides but not for tetra-peptide and aminoacids.

The binding site is formed by many conserved residues in the family, as the positively charged residues Arg-25, Arg-32, Lys-127 and the tyrosine residues Tyr-29 and Try-68; **2**) the extracellular cavity located between TMD7 and TMD11 domains with a cone shape, the apex at the bottom near

the central cavity and opening outwardly (Fig. 1.5B). The molecular dynamic experiments suggest that the extracellular cavity may represent the vestiges of entrance for substrates (Newstead et al., 2011).

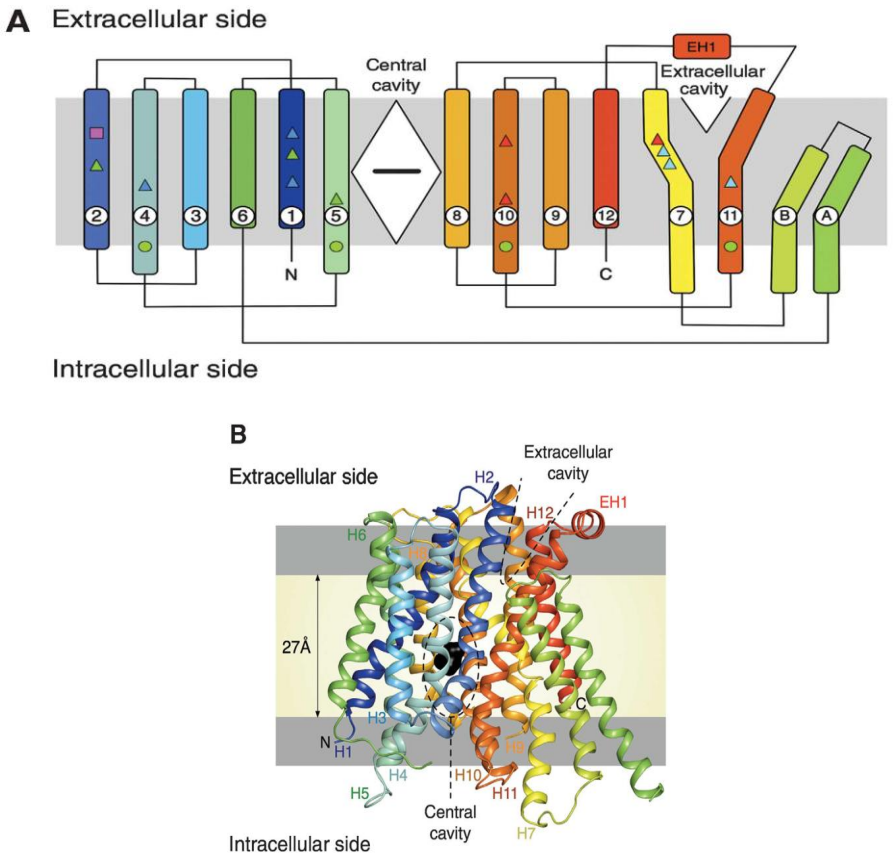

Figure 1.5. Crystal structure of PepTso *Shewanella oneidensis*.(A) 14-TM topology of PepTso. The central and extracellular cavity are represented as a closed diamond and open triangle respectively. The black horizontal bar in central cavity indicate bound ligand. (B) PepTso structure observed in the plane of the membrane in which the two cavities present in the structure are highlighted in dashed line. N and C represent the N- and C- termini, respectively (Newstead et al., 2011)

For the uptake of peptides, the central cavity needs to be connected to the extracellular space through the extracellular cavity from which is separated by an extracellular gate made by TMD2 and TMD3. In this region there are several important residues such as His-61 and Asp-316. Fei and colleagues identified His-61 as the primary protonation site in human PepT1 and PepT2. In fact His-61Arg mutant in human PepT1 is active only at higher pH indicating that the protonation and deprotonation of this residue is essential in peptide transport. The Fig. 1.6 shows the possible mechanism for peptide-proton symport. The presence of a negatively charged residue (Glu-419 and Ser-423) in C-terminal side is important because the arrangement of the opposite charges within the binding site could be a role in the recognition and orientation of peptides through the creation of a dipole moment. The presence of several possible hydrogen-bond donors and acceptors, as the

tyrosine residues, could be advantageous in adapting the peptides of various lengths, sequences and charges (Newstead et al., 2011).

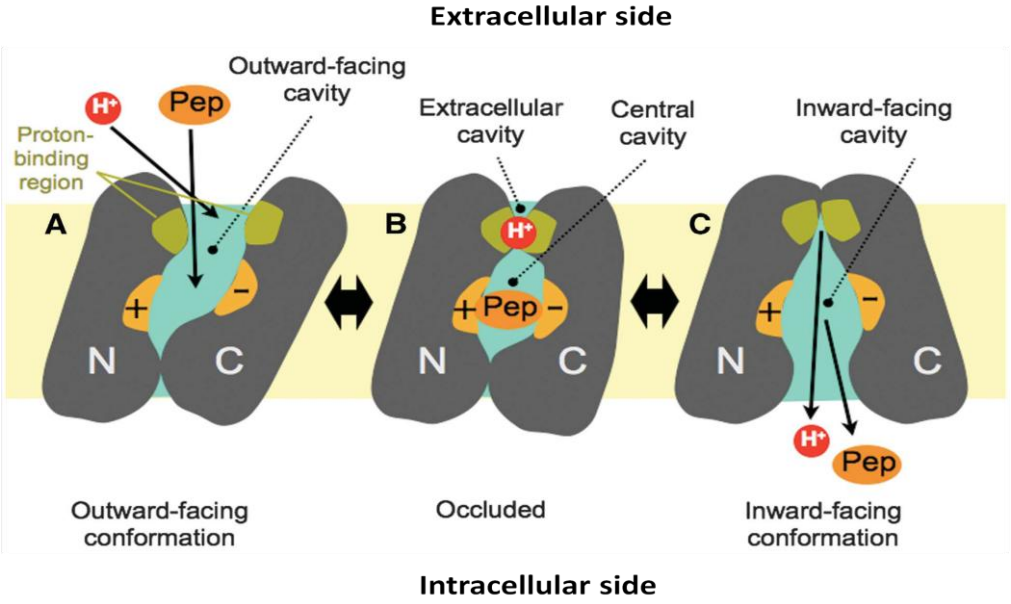

Figure 1.6. A possible mechanism for proton-peptide cotransport. (A) In the outward-facing conformation the central cavity is open and direct towards the extracellular side. Peptide (Pep) and proton (H^+) can access binding sites, the surface of both the N- and C-terminal helix bundle (indicated by + and – signs) and the area close to the extracellular gate respectively. (B) In the occluded state, the peptide is isolated in the central cavity whose both ends are closed. Whereas the proton binding site is still exposed to the extracellular side. (C) The inward-facing conformation represent a conformational change of the transporter. Both peptide and proton are released into the intracellular side thorough the inward-facing cavity (Newstead et al., 2011).

1.3.2 Transporter function

PepT1 is a transmembrane protein with the capability to transport all 400 different dipeptides and 8000 different tripeptides from the 20 L-α- amino acids but is not able to transfer single amino acids (Daniel, 2004).

Di- e tri- peptides, derived from the degradation of ingested proteins, are variable in structure in molecular size, polarity, stoichiometry, solubility and net charge. For example the molecular mass can vary between 132 Da for a di-glycine and 577 Da for a tri-thryptophane. The net charge can range (at pH 7) from neutral to trivalently anionic, as for a triglutamate, or trivalently cationic, as for a tri-lysine (Daniel, 2004). Figure 1.7 shows the structural requirements and/or limitations in substrates for transport via PepT1: **a)** the D- configuration of the amino acid decreases the substrate binding compared to the L- configuration; **b)** an additional carbonyl group incorporated into the

backbone, as realized in delta-aminolevulinic (ALA), increases the substrate affinity of the amino fatty acid; **c)** the α-amino group of the peptide transporter substrates and its spatial location plays a crucial role in binding affinity and translocation. This group may form a salt bridge with either an acidic residue or a histidine residue located in the substrate binding pocket; **d)** 5.5 A° length between N-terminus and C-terminus that explains why neither free amino acids nor tetrapeptides can be bound or transported; **e)** the presence of peptide bond increases the substrate affinity (Bailey et al., 2000).

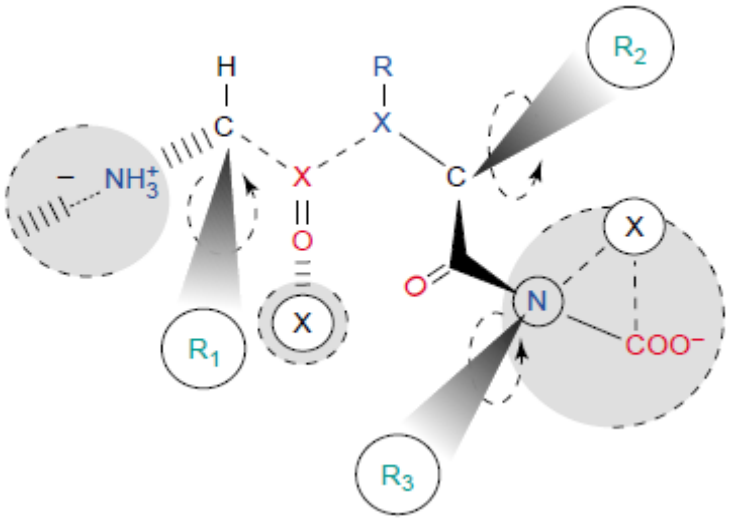

Figure 1.7. Molecular structure of good compounds that serve as substrate of PepT. R1,R2 and R3 are not essential but affect affinity. They represent the backbone carbonyl function and the amino acid side-chains of peptides. The essential substrate properties are: a) the planar length-defined backbone from N-terminal α carbon to R2; b) a free NH3 at the N-terminus of a substrate; c) L-selectivity at the R2 position to allow substrate that need not only a specific orientation but also some hydrophobicity to match with the hydrophobic pocket of the transporter; This allows substrates that do not have a C-terminal COO group and fill this pocket to be transported (Rubio-Aliaga and Daniel, 2002).

The capability of PepT1 to transport substrates via brush border membrane is not limited to di- and tripeptides. In fact several pharmacological compounds that possess good oral availability are delivered by PepT1. Well-characterized peptide mimetic-drug are numerous amino beta-lactam antibiotics of the cephalosporin and penicillin classes (Yang et al., 1999), angiotensin-converting enzyme (ACE) inhibitors such as captopril and the ester prodrugs analpril and fosinopril (Zhu et al., 2000). PepT1 transports also DOPA derivates (DOPA-Phe) and Pro-Phe-esters of bisphosphonates (Ezra et al., 2000); (Tamai et al., 1997). Other drugs substrates of PepT1 are the dipeptide-mimetic bestatin, a peptidase inhibitor that acts as an antitumor agent (Terada et al., 1998) and sulpride that is a selective dopamine D2 receptor antagonist (Watanabe et al., 2002). PepT1 is involved in the

uptake of δ-aminolevulinic acid (ALA) that can be used for tumor therapy (Neumann and Brandsch, 2003) and L-Valacyclovir, an oral active prodrugs of the antiviral drug acyclovir (Ganapathy et al., 1998).

Even if there are many studies on carrier-mediated short peptides transport, its mechanisms are still not well known and characterized.

1.3.3 Tissue distribution

PepT1 is expressed in different tissues. Originally Fey and Liu using Northern- blots and RT-PCR, cloned PepT1 and PepT2 to indicate their tissue distribution (Fei et al., 1994). Subsequent studies confirmed the expression of PepT1 in the human placenta (Adibi et al., 1996), pancreas (Gonzalez et al., 1998), intestine (Freeman et al., 1995) and kidney, where it is specific for the early regions of proximal tubule (pars convoluta) (Smith et al., 1998). Freeman and colleagues by *situ* hybridation on rabbit intestine found that at the cellular level PepT1 is expressed in the epithelial cells especially in the jejunum and duodenum. In contrast PepT1 mRNA was not detected in the stomach, sacculus rotundus or caecum. Microscopic analysis on tissue section identified the presence of PepT1 mRNA along the longitudinal axis of intestinal ephitelium excluding its expression in the lamina propria, muscularis mucosae, muscularis or sierosa (Freeman et al., 1995; Erickson et al., 1995).

Studies on the distribution and developmental changes in rat PepT1 expression, showed that high levels of intestinal mRNA are found in 4-days-old rats, and the levels decrease in the adult by day 28 after birth (Miyamoto et al., 1996). PepT1 has been found not only in the apical plasma membrane but also in the lysosomal membrane suggesting that the compartmentalization of PepT1 in the intestinal epithelial cells is not static (Lee et al., 1999).

1.4 ELECTROPHYSIOLOGICAL PROPERTIES OF PepT1

The expression of different isoforms of PepT1 RNA in heterologous systems such as *Xenopus* oocytes and the use of electrophysiological techniques have allowed to identify some common characteristics. The different isoforms of PepT1 studied present two types of currents: the transport-associated or steady-state current, and presteady-state or transient current.

1.4.1 Presteady-state and transport currents of PepT1

The transport associated currents (I_{tr}) are due to the translocation of the ions across the plasma membrane together with the organic substrate, and depends on the membrane potential.

The presteady-state currents are observed in the absence of the substrate and are due to movements of the ions inside and outside the transporter, or to the rearrangement of the protein conformation itself; they are dependent on the membrane potential, on the presence of the driving ions and represent the initial steps of the transport cycle (Mager et al., 1998; Lester et al., 1996).

The amount of charge that moves inside the membrane electrical field after a voltage change and that generates this current can be measured integrating the transient current over time. The amount of displaced charge, when the potential is moved from the holding level (V_h) to another value, is always the same as the amount of charge displaced in the opposite direction when the voltage returns to its initial value (Peres et al., 2004b). This behavior is reproduced by a single electrical circuit constituted by a resistor (R) and a capacitor (C) in series (Fig. 1.8).

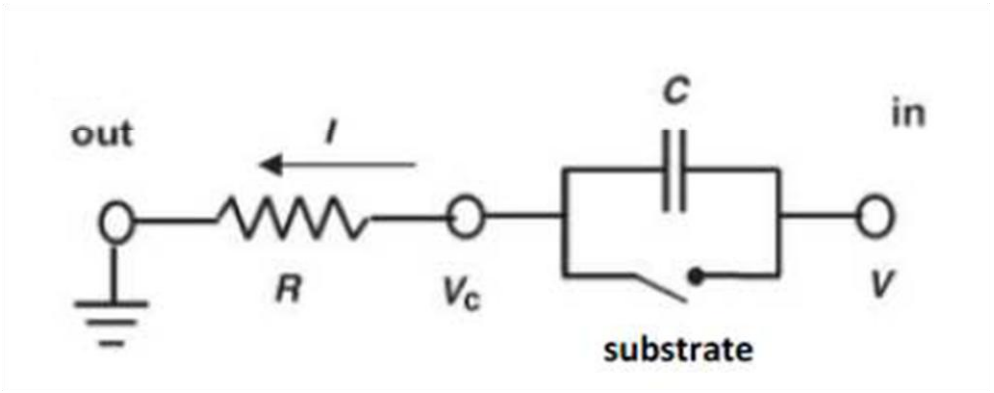

Figure 1.8 : Electrical circuit simulating intramembrane charge movement. (Peres et al., 2004).

The analysis of the presteady-state current is an important biophysical tool to investigate the mechanisms and the kinetics of the transport cycle. In fact from an exponential fitting of the transient currents is obtained the decay time constant (τ), and from the integration the amount of the charge (Q) that moves in the electrical field of the membrane (Peres et al., 2004a).

1.4.2 Transport mechanism of PepT1

In 1996 Mackenzie and colleagues, using two electrode voltage clamp in *Xenopus* oocytes, investigated the transport mechanism of human intestinal PepT1 considering the voltage dependence, steady-state kinetics and transient charge movements. They demonstrated that the transport of glycyl-sarcosine (Gly-Sar) by hPepT1 is electrogenic and coupled to an inward H^+ current. The steady-state measurements indicate that H^+ and oligopeptide are translocated simultaneously in the same reaction step, because, at least at V_m more positive than -70 mV, the affinity of the carrier for substrate (Gly-Sar) deteriorates at diminishing $[H^+]_o$. Moreover, the transporter binds first the H^+ and then the substrate. In fact, the apparent maximal transport rate is significantly attenuated only once $[H^+]_o$ was reduced by 100-fold (Mackenzie et al., 1996). The results show that the apparent affinity constant for Gly-Sar is ~ 0.7 mM at V_m -50 mV (in the pH range 5.0–6.0). At each V_m, Hill coefficients are ~1 for H^+ activation of the Gly-Sar evoked current, suggesting 1 H^+:1 Gly-Sar transport stoichiometry. In the presence of H^+, but in the absence of Gly-Sar, they observe voltage-dependent presteady-state currents. According to their model (Fig.1.9), these transient currents are due to binding/dissociation of H^+ to/from the cotransporter and a conformational change of the unloaded carrier between the external and internal membrane interfaces. Presteady-state analysis indicate that H^+ can bind to the empty carrier in the absence of oligopeptide.

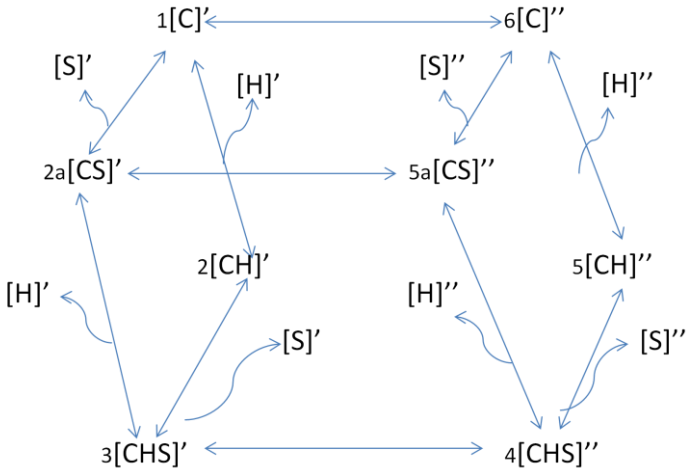

Figure 1.9. An eight-state kinetic model of the human oligopeptide transporter 1 in which carrier states are labeled with numbers. Transporter states at the external face are identified by a prime while at the internal face by double prime. The proton binds first (states 1-2) and then the substrate (states 2-3). The proton and the substrate are translocated simultaneously (3-4). The substrate is released first in the cytoplasm (4-5) and then the proton (5-6). 2a and 5a are states added to a kinetic model previously proposed for SGLT1and represent the possibility that the organic substrate may bind in the absence of proton (Mackenzie et al., 1996).

Electrophysiological and biophysical studies of presteady-state and transport-associated currents have been conducted in parallel to the rbPepT1. Its transport activity is reported to be pH-dependent with external acidic pH having a consistent effect on the uptake of peptide molecules (Fei et al., 1994; Nussberger et al., 1997). More information on the effect of intracellular pH on the kinetics of rabbit PepT1 were obtained studying the behavior of some mutant isoforms. Through electrophysiological experiments on mutated residues Arg-282, Asp-341and His-57, Bossi and colleagues investigated their interaction with ions and their role in the transport activity. All Arg-282 mutants generated presteady-state currents in the absence of substrate and steady-state currents similar to those observed in wild-type. The currents elicited by Asp-341Arg mutant were reduced compared to wt, and the His-57Arg and the double mutant Arg-282Asp-Asp-341Arg were not able to generate any current. In particular, the presteady-state currents of all Arg mutants were pH-dependent with faster decay time constant and both the τ/V and Q/V curves shifted to more positive potentials compared to the wild-type. All the Arg-282 mutants exhibited faster inward and slower outward rates while the opposite occurs replacing the negative Asp-341 with Arg (Bossi et al., 2011). The transport-associated currents were still pH and substrate dependent in all mutant isoforms. While the Arg-282 mutants were able to generate transport currents comparable to the wild-type, Asp-341Arg showed a reduced current. All Arg-282 mutants elicited outward currents with E_{rev} (reversal potential), shifted towards more positive values by substrate concentration and by external pH. These results suggested that the mutants still translocate protons and substrate as a complex (Bossi et al., 2011).

The ability to generate current in the outward direction was already shown in the wild-type rbPepT1 where the current is displayed at alkaline pH and low substrate concentrations (Kottra et al., 2008). Long-lasting voltage and current-clamp experiments show that the outward currents observed in Arg-282 mutants are only temporary and reflect the effects of accumulation and/or depletion of the dipeptides near the membrane (Renna et al., 2011).

Moreover in 2001 Kottra and colleagues through giant patch-clamp experiments demonstrated a possible PepT1 reverse transport in which the maximal velocity appears to be the same of the forward transport, while the binding affinity for the substrate in the cytosol is lower than at the extracellular side (Kottra and Daniel, 2001).

The removal of Arg-282 facilitates the flow of the transported complex in both directions, while the change of Asp-341 with positive residues reduces the transport rate of the wild-type. The ability of Arg-282 and Asp-341 mutants to generate reverse transport was confirmed with a series of experiments injecting substrates in the cytoplasm of the oocytes. Oocytes expressing wild-type,

Arg-282 and Asp-341 mutants were tested under current-clamp conditions. Few minutes after Gly-Sar injection, the registered resting membrane potential became more negative as a consequence of the activation of an outward current by the transporter induced by the increase of the intracellular concentration of the substrate (Renna et al., 2011). The reversal potential and the outward current remained independent of the presence of external cations. Replacing the extracellular Na^+ with different cations (K^+, Li^+ and TMA) did not affect the transport of several neutral organic substrates at different pH values and concentrations. Protons remain the charge carried and the mutants selectivity order for the charged substrates was the same of the wild-type.
All data support the idea that Arg-282 and Asp-341 residues can be part of the electrostatic gate in PepT1 transport cycle (Kulkarni et al., 2007).

1.4.3 Stoichiometry of PepT1

In 1970s it was thought that the force of the active absorption of the small peptides in the mammalian intestine was the transmembrane Na^+ gradient. Only in the 1980s it was observed that the uptake processes for dipeptides was dependent on a proton gradient existing across brush-border membranes (Henderson, 1990); (Hediger, 1994).
The independency of PepT1 uptake from extracellular Na^+, K^+ and Cl^- was confirmed in 1994 (Fei et al., 1994) and the peptide transport was demonstrated to be due to H^+. PepT1 is an electrogenic transporter driven by the electrochemical gradient of protons. The uptake of short peptides and drugs is associated with the proton translocation, therefore with the movement of positive charges that create an acid microenvironment. In 1997, Hediger and colleagues reported a study in which they examined the stoichiometry of neutral and charged dipeptides transported by rabbit PepT1 expressed in *Xenopus* oocytes and the pH dependence of the transporter (Steel et al., 1997). Using membrane vesicles and electrophysiological studies in oocytes, Steel et al suggested a coupling stoichiometry of 1:1 for PepT1 (1 of proton cotransported with 1 molecule of peptide) for the transport of neutral and cationic dipeptides. According to the proposed model (Fig. 1.10), negatively charged dipeptides such as Gly-Glu are cotransported with two protons, one of which is involved in H^+ coupling and the other in neutralizing the charge of the substrate creating a zwitterionic species. On the other hand, a single proton is cotransported with positively charged dipeptides such as Gly-Lys and the transport is shifted towards more basic pH values (Steel et al.,1997). The affinity of PepT1 for charged dipeptides is pH dependent; the affinity for cationic substrates increases with more alkaline pH while the affinity for the anionic peptides with acidic

pH. The compounds with no net charge possess the highest affinity. In case of saturating substrate concentrations, PepT1 is not dependent on the extracellular pH but only on the membrane potential that determines the transport (Steel A. et al.,1997; Kottra et al., 2002).

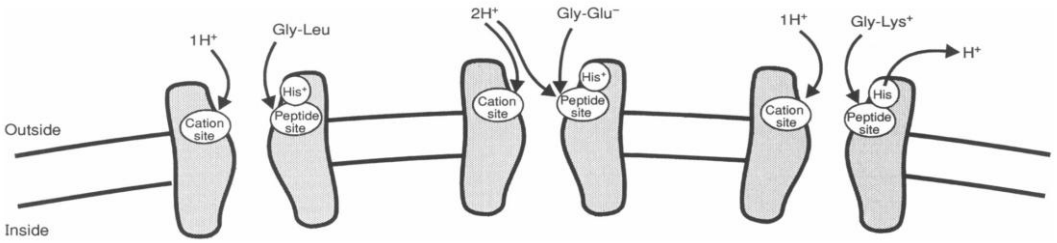

Figura 1.10. Model for coupled transport of neutral and charged dipeptides by PepT1 (Steel et al., 1997).

In 1959, Hobgen et al. suggested the existence of low pH near the luminal surface of the mammalian small intestine (HOGBEN et al., 1959). Subsequently Lucas and colleagues measured an acid microclimate between pH 6.1-6.8 at the luminal surface of the small intestine ephitelium using pH-sensitive microelectrodes (Lucas et al., 1975). In 1995 several proteins were found to be involved in the maintenance of the acidic microclimate required for the peptide transport activity: substrate uptake at the apical membrane by PepT1 causes a proton influx, and the H^+ are carried back to the lumen by the apical sodium-proton exchanger NHE3. The Na^+ rise via NHE3 is regulated by the basolateral Na^+/K^+/ATPase that exchanges sodium with potassium. Incoming potassium leaves the cell by potassium channels (Fig. 1.11).

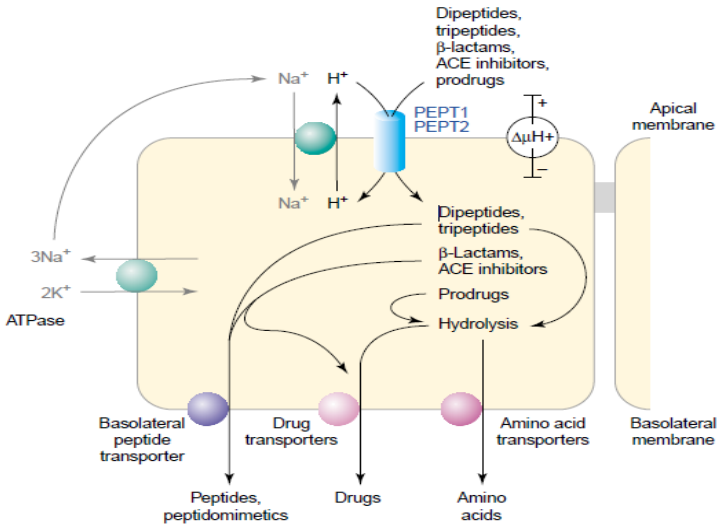

Figure 1.11. Schematic peptide transport in epithelial cells of intestine and kidney. Dipeptides, tripeptides and peptidomimetic drugs are transported through apical membrane by PepT1 and PepT2 that use the inwardly directed proton (H^+) electrochemical gradient as driving force. The proton gradient is generated by a coordinated activity of the apical Na^+-H^+ antiporter and the Na^+-K^+-ATPase pump in the basolateral membrane. Free amino acids and hydrolyzed di-and tripeptides are released into the circulation by basolateral peptide transporter and/or other drug transporting systems that are still unknow.(Rubio-Aliaga and Daniel, 2002).

1.5 REGULATION AND PATHOLOGICAL IMPLICATIONS OF PepT1

The mechanisms of the regulation of PepT1 are not completely clear and occur at different levels: gene transcription, mRNA stability, post-transcriptional modification by second messengers, protein insertion and retrieval from the plasma membrane. At tissue level the regulation consists of hormonal or neuronal signals and in the small intestine may be dependent on diet. Brandsch and colleagues demonstrated that the activation of protein kinase A (PKA) and C (PKC) by second messengers can regulate the activity of PepT1. They showed that the activation of PKC in Caco-2 cell line by phorbol esters inhibited the transport of the peptide Gly-Sar (Brandsch et al., 1994). Wenzel and colleagues focused on the effect of activating PKC by intracellular calcium. In fact PepT1 responds to high levels of $(Ca^{2+})i$ reducing peptides influx (Wenzel et al., 1999). The reason could be that peptides uptake at the brush border membrane by PepT1 causes proton influx; the NHE3 exchanges protons for sodium that is removed from the cell by the basolateral Na^+/K^+-ATPase pump; high levels of intracellular Na^+ lead to an inability of Na^+/Ca^{2+} exchanger to keep $(Ca^{2+})i$ low. The rise of intracellular Ca^{2+} concentration may act to reduce the peptide entry through PepT1 and then open Ca^{2+}-sensitive channels leading to a new polarization of the cell membrane (Thwaites et al., 1999).

It has been reported that exposure to physiological levels of insulin and/or leptin for more than 1h stimulates peptides uptake due to an apparent increase of the transport protein (Thamotharan et al., 1999; Buyse et al., 2001).

Ericson and colleagues found that the level of PepT1 mRNA in rat small intestine was increased in response to a high-protein diet only in the distal portion of the intestine (Erickson et al., 1995). Studies on Caco-2 cells by Walker D. et al observed an increment in the capacity for peptide uptake (Walker et al., 1998) when 4mM Gly-Gln was added. The regulation of PepT1 expression in the presence of high-protein diet could be at gene expression level. The PepT1 gene has several amino acidic/peptide response elements in the promoter region such as the transcription factor AP-1. Shiraga and colleagues suggested that AP-1 levels in Caco-2 cells could be increased by high concentrations of specific amino acids and peptides and consequently lead to an upregulation of PepT1 expression (Shiraga et al., 1999). It is interesting to highlight that under fasting condition there is an increase in peptides uptake. In fact after 1 day of fasting, the uptake of Gly-Gln in rat epithelial intestine is doubled (Thamotharan et al.,1999).

There is no known pathology associated with the malfunction of PepT1, but a functional polymorphism in the PepT1 gene might be of relevance to inflammation and antibacterial responses in inflammatory bowel disease. In the second loop of hPepT1 it was found a coding polymorphism

where the Cysteine to Thymine nucleotide substitution corresponds to an amino acid change from Ser to Asn at residue 117. This single nucleotide polymorphism (SNP) shows a significant and reverse association with inflammatory bowel disease in patients from Sweden and Finland: the common allele C has predisposing and protective effects in the Swedish and Finnish populations, respectively. It was suggested that PepT1-Asn-117 variant operates a more efficient transport of muramyl dipeptide (MDP), the core component of the bacterial peptidoglycan (Zucchelli et al., 2009).

It was also shown a role of Pept1 in inflammation process because of its expression in inflamed colonic tissues and its capability to transport formyl- Met-Leu-Phe (fMLP), a neutrophile attractant peptide derived from some bacterial species (Buyse. et al.,2001).

1.6 SEA BASS PepT1 ISOFORM

Sea bass PepT1 (sbPepT1) has been cloned from the intestine of the sea bass *Dicentrarcus labbrax* (FJ237043). This integral membrane transport protein is homologous to the isoform of Zebrafish PepT1 and is highly expressed in the proximal intestine. The studies on sbPepT1 can be useful to understand the structure-function relationship among vertebrate peptide transporters.

SbPepT1 cDNA has 3014 bp encoding for a protein of 707 amino acids. It consists of 12 transmembrane domains (TMD) with a large extracellular loop between TMD9 and TMD10, intracellular N- and C- terminals, six putative extracellular *N*-glycosylation sites, two intracellular consensus regions containing protein kinase C (PCK) motifs and one intracellular cAMP-dependent protein kinase sequence.

SbPepT1 transports dietary di- and tripeptides in the cells against concentration gradient in a pH-dependent manner.

1.7 OTHER MEMBERS OF SCL15 FAMILY: PEPT2 AND PHTs TRANSPORTERS

PepT1 is not the only reported peptide transporter belonging to SCL15 family, there are also PepT2, PHT1 and PHT2.

The gene that encodes for human PepT2 maps to chromosome 3q13.3-q21 (Ramamoorthy et al., 1995) and consists of 22 exons. The open reading frame of hPepT2 shows a 50 % sequence identity and around 70% similarity to each peptide transporters. hPepT2, differently from hPepT1, has

additional residues found in the amino-terminal cytosolic region and five protein kinase C (PKC) recognition sites. PepT2 has been cloned from C. *elegans* and from vertebrates as fish and mammalians (Liu et al., 1995; Fei et al., 1998a); Romano et al., 2006). Mammalian PepT2 is differently expressed than PepT1. It is located in the type II pneumocytes and in the brush-border membrane vesicles (Meredith and Boyd, 1995) in the lateral region of proximal tube of the kidney (Smith, 1998), in the mammary gland and in the central nervous system (Wang et al., 1998).

The peptide carrier 2 transports not only di- and tripeptides, but also peptidomimetic drugs such as β-lactam antibiotics, valacyclovir, certain angiotensin-converting enzyme (ACE) inhibitors and antineoplastic agent bestain (Doring et al., 1998; Ganapathy et al., 1998; Terada et al., 2000). PepT2 is not able to transport amino acids and tetrapeptides (Daniel and Kottra, 2004).

Contrary to PepT1, the proton to substrate stoichiometric ratio for the cotransport of neutral substrates was found to be 2:1, while the charged substrates show variable coupling ratios (Chen et. al., 2000). During the transport cycle, in PepT2 one H^+ is bound prior to substrate binding by an overall transfer of two protons in one cycle (Kottra et al., 2001). As well PepT1, at saturating concentration of compounds, the transport cycle of PepT2 is not dependent on the extracellular pH but only on the membrane potential.

PHT1 and PHT2 are proton-coupled proteins with 12 TMD, potentials sites for Asn-linked glycosylation located in the third, fourth and fifth extracellular loops, four sites for protein kinase C-dependent phosphorylation, two sites for protein kinase A-dependent phosphorylation, a PTR2 consensus domain and an overall amino acid identity with PepT series of 20 to 25% (Fig. 1.10). PHT1 and PHT2 were shown to mediate histidine and free amino acids (Glu, Gly, Leu, Met, or Asp) transport and they are inhibited by di- and tripeptide (Yamashita et al., 1997).

The cDNA of rPHT1 was cloned in 1997 and is 2751 bp long with an open reading frame of 1719 pb encoding for a protein of 572 amino acids. rPHT1 is a neuro-specific peptide/histidine transporter expressed in the brain, with high levels in the hippocampus, choroid plexus, pontine nucleus and cerebellum and in retina (Yamashita. et al., 1997). Sakata and colleagues cloned the cDNA of the histidine/transporter 2 found in rat (rPHT2). rPHT2 shares a 49,2% sequence identity with the brain PHT1 (Fig. 1.12) (Sakata et al., 2001) and it was found especially in spleen, lung and thymus and faintly in liver, brain, adrenal gland and heart by Northern- blot analysis.

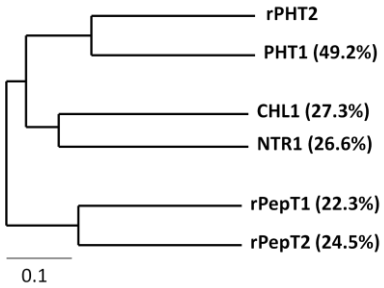

Figure 1.12. Amino acidic identities percentages between representative proteins of the PTR family (Sakata et al. 2001).

1.8 BASOLATERAL MEMBRANE TRANSPORT

The step in which peptides and peptidomimetics cross the cell basolateral membrane is not identified yet. Di- and tripeptides transported into the cell by PepT1 are hydrolyzed by the activity of intracellular dipeptidases and they leave the cell via basolateral amino acids transporters. Peptidomimetics are partially degraded by esterase enzymes and exit the intracellular compartment through several unknown basolateral drug transporters (Daniel, 2004). Terada and colleagues demonstrated that the transport of Gly-Sar at the basolateral membrane of Caco-2 cells is less sensitive to the external pH changes than the transport via the apical membrane of the same cells (Terada et al., 1999). Further studies conducted on Caco-2 cells showed that the affinities for transport of B-lactam antibiotics differed at the apical and the basolateral membranes, suggesting that the drugs transport may be H^+ - independent (Matsumoto et al., 1994).

1.9 XENOPUS LAEVIS

PepT1 is a peptide transporter normally expressed in intestinal and epithelial cells with low protein levels. For this reason heterologous expression systems are very useful to characterize the structure and function of the carrier proteins. The yeast is one heterologous system that is used for functional analysis of the transporters. It possesses the advantage of rapidly obtain large quantities of transgenic cells and subsequently large amounts of the carrier proteins (Theis et al., 2001).

The heterologous systems used in this work are the oocytes deriving from *Xenopus laevis*. *Xenopus* oocytes provide an important expression system for molecular biology. By injecting DNA or mRNA into the oocyte or developing embryo, scientists can study the protein products such as ion channels, transporters and membrane receptors in a controlled system. This allows rapid functional

expression of manipulated DNAs (or mRNA) and is particularly useful in electrophysiology (two electrode voltage clamp technique).

The oocytes are an excellent and convenient heterologous expression system for several reasons: 1) they possess all the machinery required for the synthesis, directed by a foreign mRNA, of a specific protein; 2) it is possible to isolate a large amount cells from one *Xenopus laevis* female*;* 3) the large size (~ 1.3 mm of diameter) makes them easy to handle and to microinject with different molecules such as natural mRNA, cRNA and antibodies; 4) they can survive *in vitro* in favorable condition for more than two weeks.

The oocytes posses also negative characteristics: 1) they posses native proteins such as membrane channels that might confound results and interfere with the records of small currents of the exogenous proteins; 2) they have a life temperature lower than the physiological conditions in which the mammalian proteins usually survive (16° instead of 37°C); 3) the post-translation modifications can be different in the oocytes compared to mammalian cells and this can lead to a change in the protein function.

1.10 AIM OF THE PROJECT

In the last decade, carrier-mediate transport has become a research area of interest in nutrient delivery. Nutrient transport into the cells is a critical step in the life of all organisms and occurs with expense of energy; it is often driven by a transmembrane electrochemical proton gradient.

Over recent years, a large number of H^+-coupled cotransport mechanisms have been identified in the luminal membrane of the mammalian small intestine. These transporters are considered to be a major route of dietary molecules absorption in the intestine (Meredith and Boyd 2000).

The most representative proton-coupled system is the di- and tripeptide transporter PepT1 belonging to the SLC15 family, identified by gene expression and cloned from mammals in 1990 (Fei et al., 1994; Lui et al., 1995; Covitz et al., 1998).

My PhD project had two main aims: in general it is known that more detailed information about the structure-function relationship can be obtained comparing different isoforms of a protein. In this case, the fish isoform of the peptide transporter PepT1 cloned from sea bass and investigated in my work for the first time, was compared to zebrafish and rabbit isoforms. The biophysical characteristics were likened in order to identify a common scheme of transport.

The second aim was to better understand the role of sbPepT1 in nutrient adsorption. The role of small peptides in nutrition is very relevant in aquaculture technology. In fish farming good nutrition

is essential to obtain healthy, high quality products but it is also critical because of its high costs. In particular, proteins represent the most expensive part of fish feed. The determination of the proteins and of the essential amino acid requirements for each fish species is fundamental.

Recent studies have shown that the incorporation of short peptides into the fish diet improves the development and the nutritional status of the larvae (Chatelier et al., 2006). On the other hand, it is also important to avoid the overfeeding for some reasons: first at all, it is a waste of expensive feed; second, the proteins in uneaten food and fish waste are broken down in ammonia and nitrogen that are toxic for the fish; the organic material uses oxygen to rot producing carbon dioxide resulting in water pollution low oxygen level, and increases bacterial load.

Chapter 2:

METHODS

METHODS

2.1 PepT1-pSPORT CONSTRUCTS

2.1.1 Plasmidic vectors

Plasmidic vectors are useful tools used in genetic and biotechnology lab to amplify and transfer DNA inside an organism, where it will express.

They generally are double-stranded and, in many cases, circular DNA. Plasmidic vectors usually derive from bacterial plasmids but are sometimes found in eukaryotic organisms and they show three common features:

- A replication origin, recognized by the host cell, for example ori C if the plasmid must replicate in *E. Coli*;
- A poli-linker or multi cloning site (MCS), composed by restriction sites grouped together and where the insertion happens. The insertion process happens when the plasmid and the DNA are cut with the same restriction enzyme and after a ligation reaction;
- A selective marker that make cells containing the plasmid able to be distinguished from the others. Generally genes conferring to the host a particular antibiotic resistance are used, for example the Amp^R gene gives to the host cell ampicilline resistance.

To obtain a good level of transcription some specific sequences are required in order to express the cloning vector in heterologous system such as *Xenopus laevis* oocytes: a) a promoter recognized by the RNA-polimerase (T3,T7 or SP6); b) the lack of initial codon (ATG), between promoter and the gene in order to avoid an early transcription; c) the lack of long non codifying DNA to limit the formation of secondary structures that may reduce the polymerase functionality; d) two post-transcriptional modifications: adding the cap at 5' and poliadenilation at 3'. The cap is a molecule of 7-metiloguanosine that protects the transcript from degradation and favorites the association of ribosomes with the 5' of mRNA. The poliadenilation consists in adding 150-300 adenosine at the 3'. The poli- A is not essential for transcription but it protects mRNA form ribonuclease and facilitates the transport of the mRNA from the nucleus to the cytoplasm.

2.1.2 PepT1 cDNAs preparation

cDNAs encoding rabbitPepT1 were cloned in pSPORT1 vector between *Sal*I and *Not*I sites (Mertl *et al.*,2008) and zbPepT1cDNAs between *Sal*I and *Hind*III sites.

cDNA encoding sbPepT1 was first cloned in pcDNA3.1 plus vector (Fig.2.1) between *EcoRI* and *NotI* sites. Because this vector did not allow the expression of the transporter on the membrane surface of the *Xenopus* oocytes, sbPepT1 was then cloned in pSPORT vector between *Sal*I and *Hind*III sites.

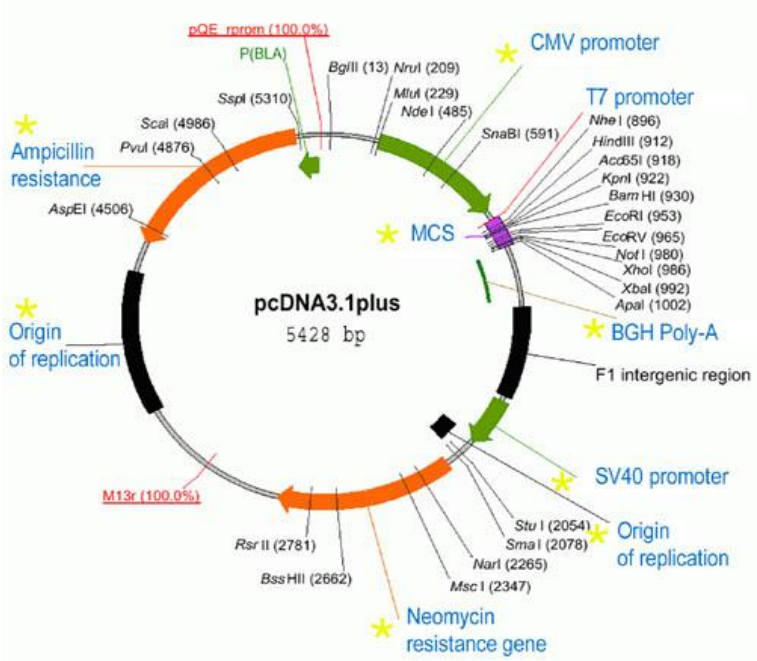

Figure 2.1. pcDNA3.1+ vector

pSPORT1 (Fig. 2.2) is an expression vector that presents the ampicillin resistance (APR) and the reported multi cloning site (MCS). At both ends of the MCS there are promotor sites for T7, T3 and M13 RNA polymerases.

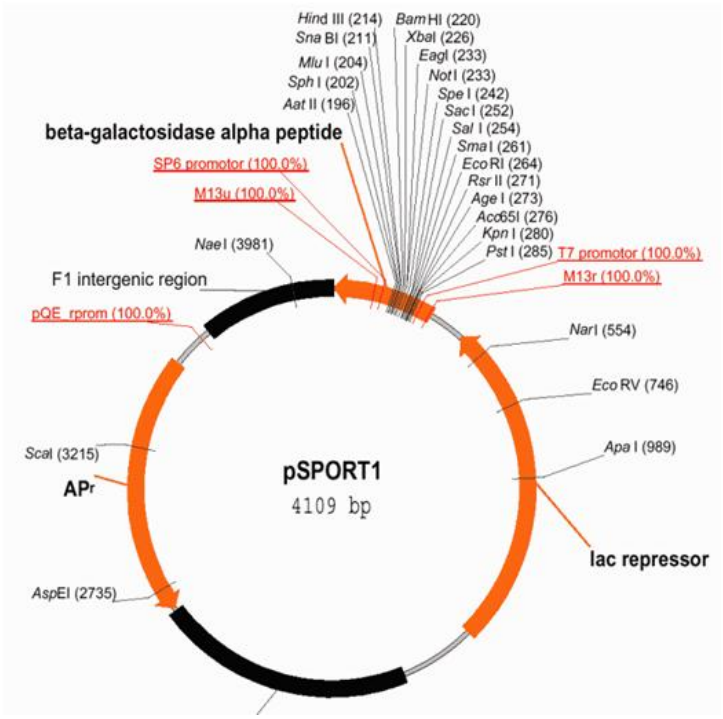

Figure 2.2. pSPORT vector.

2.1.3 Plasmid amplification and purification

The vectors containing PepT1 cDNAs were introduced into JM109 strain of *E. Coli* by the means of the heat-shock procedure following the instructions of the bacteria supplier (Promega). Transformed bacteria were then left to grow for about 1 h in SOC medium (tryptone 2% (w/v), yeast extract 0.5% (w/v), NaCl 10 mM, KCl 2.5 mM, glucose 20 mM), centrifuged, plated on plates containing selective medium (LB-Agar added with 50 mg/ml ampicillin) and incubated over night at 37°C. The day after, colonies were picked up and inoculated in liquid selective medium (LB added with 50 mg/ml ampicillin). Bacteria were left to grow over night at 37°C and then the plasmid DNA was extracted using Wizard® *Plus* SV Miniprep (Promega) following supplier's instruction. The extracted DNA was loaded on a 1% agarose gel in TAE 1X buffer to check the quality and to estimate the concentration.

2.2 mRNAs PREPARATION

In order to achieve an efficient *in vitro* transcription, the clone containing the cDNA of interest has to be linearized in 3' direction with respect to the coding region. The cDNAs encoding sea bass and zebrafish transporters were both linearized with *Hind* III, the cDNA encoding rabbit PepT1

transporter with *Not*I. 8-10 mg of plasmid DNA were digested, then purified using the Wizard® SV Gel and PCR Clean-Up System (Promega) and eluted in 35 µl of nuclease free water. 3 µl were loaded on a 1% agarose gel in TAE 1X buffer to check the linearization. The remaining DNA was used for the *in vitro* transcription. Briefly, the linearized DNA was incubated at 37°C for 3h in presence of 200 units of T7 RNA polymerase, 18 µl of 5X Trascription Buffer, 8 µl of 100 mM DTT, 2.5 µl of RNasin 30 U/µl, 13 µL NTPs mix (ATP, CTP, UTP 10 mM and GTP 0.5 mM), 6.5 µL of 10 mM Cap Analog (Promega), 10 µl RNA polymerase 20 U/µl (final volume 90 µL). After 10, 20, and 40 minutes from the beginning of the incubation, 1 µL of 25 mM GTP was added to the reaction. After 1 h from the start of the transcription, a mix of 4 µl of 5X TB, 1 µl of 100 mM DTT, 1 µl of RNasin 30 U/µl, 5 µl of NTPs mix, 1 µl of T7 RNA polymerase20 U/µl, 1 µl of 25 mM GTP, 4 µl of nuclease-free water was added to each sample. At the end of 3 h, the reaction was stopped by adding nuclease-free to a volume of 200 µl. All enzymes were supplied by Promega Italia, Milan, Italy.

The transcribed cRNA was extracted with phenol: chloroform: isoamyl alcohol, 25:24:1, pH 6.6, precipitated with LiCl 8 M and washed with 70% EtOH. The dried cRNA was then resuspended in a small volume of nuclease-free water and the concentration estimated using a spectrophotometer (1 A260nm unit = 40µg/ml).

Transcribed cRNAs had a modifications which mimic *in vivo* conditions: the process of 5' capping. The so called "Cap Analog" is a modified guanine (m7G(5')ppp(5')G) which, although is not necessary for the protein expression, increases the translation efficiency and also protects the mRNA from degradation.

2.3 XENOPUS LAEVIS OOCYTE EXPRESSION

2.3.1 Xenopus laevis maintenance

Xenopus laevis is a member of the Piped family originally from South Africa and able to adapt to the conditions of the stabulary .

Xenopus females are kept in the laboratory in dark plastic aquaria containing chloride free water, because chloride causes the inactivation of magainine, an antibiotic that helps the epidermis prevent bacterial infections. The water needs to be changed every three days and the animals showing infections need to be isolated and cured. The water temperature is kept between 18 and 21°C. The salinity must be controlled to avoid the loss of salts from epidermis and it is necessary to keep the

stabulary in a light-dark cycle of 12 hours, in order to attenuate the natural annual cycles avoiding variability in oocytes production.
The frog nutrition is variable: it consist of food containing worms and raw meet such as pork liver. The food is provided 3 times a week.

2.3.2 Frog surgery

Xenopus laevis frog is anaesthetized in MS222 (tricaine methansulfonate) 0.10 % (w/v) solution in 500 ml of tap water. After 20 minutes the frog is rinsed under sink and put on ice in order to elongate the hypothermia of the anesthetic.
The surgery tools are disinfected with ethanol 70% and rinsed with water right before use. The epidermis is lifted up with a paper tissue and a small incision on the abdomen is made. After isolating the muscular tissue from connective, a second small incision is made reaching the ovary. The oocytes are extracted without hurting the surrounding organs as pancreas, intestine and blood capillaries.
Only oocytes necessary for the experiment are taken, leaving the other ovaric lobes able to produce new cells. At this point the silk is used to sew first the muscular and connective tissues and then the epidermis. The animal is rinsed with and put in a small chamber containing water. After few hours, when the frog is totally awake, it is transferred to a aquarium containing decanted water with methilene blue to avoid any bacterial infection. After some days the animal is put back together with the other frogs.

2.3.3 Oocytes treatment and selection

The preserved oocytes are put in Petri dishes (9cm diameter) containing ND96ØCa^{2} solution (NaCl 96 mM, KCl 2 mM, $MgCl_2$ 1 mM, Hepes 5 mM pH 7.6), in order to inhibit the activation of proteases released by some damaged oocytes that could hurt the oocytes membranes or inhibit the collagenase (1gr in 1 l of ND96ØCa^{2+}).The ovary portions are quickly rinsed to remove cytoplasm and blood, and they are seized in groups of 10-15 oocytes kept together by follicular cells.
The small isolated groups are put in 5mL tubes containing a collagenase 1mg/ml solution (type A, Sigma) in ND96øCa^{2+}. They are incubated in dark at 18°C for about 1 hour on a shaker in order to remove the follicular cells and the connective tissue.

Usually the separation state is often controlled, avoiding a too long treatments that could damage the oocytes. When the separation is enough, the oocytes are washed in ND96ØCa^{2+} solution and in calcium containing NDE (NaCl 96 mM, KCl 2 mM, $MgCl_2$ 1m M, $CaCl_2$ 1.8 mM, Hepes 5m M, Gentamicine 20µg/ml, Piruvate 2.5 mM pH 7.6) at list three time. The oocytes are now put in a NDE containing Petri dishes and selected with a stereoscope and a Pasteur pipette. Only the oocytes that appear round shaped and with a good color separation of the two poles are selected; these two features are in fact sign of good health. The other oocytes should not be used for injection.

Some oocytes may be still surrounded by follicular membrane that needs to be removed; it is possible to remove it by sucking few times the oocytes inside a Pasteur pipette with a diameter slightly smaller than the oocytes.

The selected oocytes are stored in 6 cm diameter Petri dish containing NDE at 18°C for at list 12 hours before injection.

2.3.4 cRNAs microinjection

The injection is operated with a constant volume mechanic injector (Drummond Nanoject) and a dissection stereoscope.

The glass capillary are pulled with a horizontal puller (Narishige), obtaining tips of about 5 µm diameter. The tips are then broken with a sterilized Petri dish lid. The capillary is filled up with liquid paraffin and put on the micronjector piston. The oocytes are put in a special Petri dish, with at the bottom a nest 1 mm wide and containing NDE. Every oocytes is injected with 50 nl of the transporter cRNA diluted to a final concentration of 0.25 µg/µl for a quantity of 12,5 ng per oocyte. The injected oocytes are stored in groups of 20 in NDE Petri dishes for 72-96 hours. During incubation the solution is changed every 24 hours.

2.4 TWO ELECTRODES VOLTAGE CLAMP

The “voltage-clamp” technique was introduced by Marmont and Cole (Cole and Curtis, 1941) and by Hodgkin, Huxley and Katz (HODGKIN et al., 1952) to study the ionic currents underlying the action potential in nerve axons, and it has been extended to the study of transporters soon after the cloning and expression of the first transporters in *Xenopus laevis* oocytes (Hediger et al., 1987); (Ikeda et al., 1989); (Parent et al., 1992); Mager et al., 1993).

The TEVC technique is based on the use of two microelectrodes, one for recording the transmembrane voltage and one for passing current (Fig. 2.3). The recorded membrane voltage is compared to the desired (command) voltage and a compensating current is automatically injected into the cell by the appropriate electronic apparatus. In this technique the independent (controlled) variable is the membrane voltage, controlled by the experimenter, while the dependent (measured) variable is the membrane current.

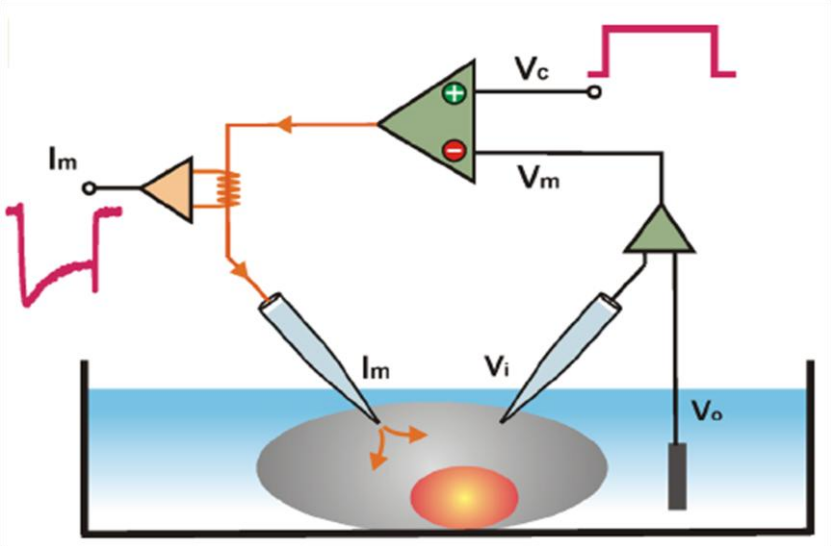

Figure 2.3. Two electrode voltage clamp. I_m is the membrane current, V_i is the membrane voltage and V_c is the command voltage.

When a current takes place due to the activity of the transport systems located in the membrane, a negative feedback in the circuitry injects into the oocyte a current that exactly compensates the charge flow through the cell membrane, in order to maintain transmembrane voltage under control. In addition to keeping the membrane potential constant, membrane voltage changes of any desired form can be applied to the cell by the TEVC technique. In the case of ion-coupled transporters, the transmembrane current is an indication of the transport activity, and the possibility of accurately controlling the membrane potential is particularly crucial in voltage-dependent processes.

The *ideal* voltage clamp simply consists of a battery, a switch, a wire, the cell and an ammeter (Fig. 2.4). Since the wire has zero resistance when the switch is closed, the membrane potential steps instantly to the battery voltage. This generates an impulse of current that charges the membrane capacitance ($Q = C_m V_{cmd}$), followed by a steady-state current ($I_m = V_{cmd}/R_m$) to sustain the voltage across the membrane resistance.

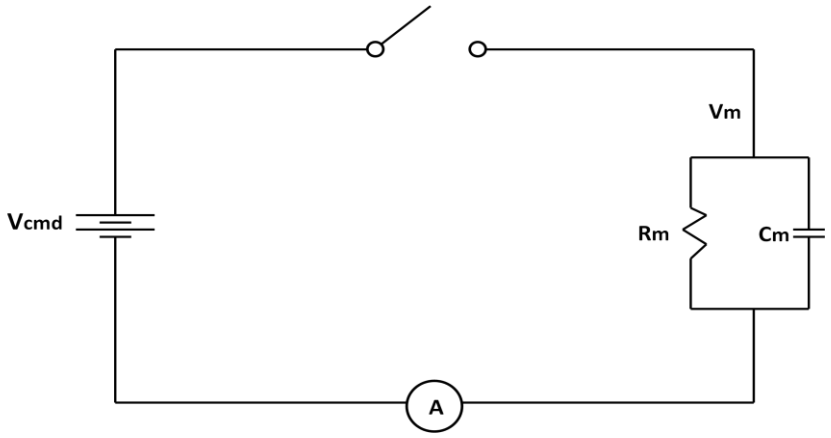

Figure 2.4. The ideal Voltage Clamp.

2.4.1 TEVC setup

The electrophysiological recordings are conduced inside a Faraday chamber whose function is to minimize the outside electromagnetic noise. The Faraday cage is grounded as are all the other metal objects inside it. The oocyte is put at the bottom of a recording chamber where there is a small nest that keeps it still even when penetrated by electrodes. The oocyte chamber is connected to two plates containing KCl 3 M trough two 1% KCl 3 M agar bridges. In the plates two external electrodes minimize the chloride effect on junction potentials.

The perfusion system is made of 30 ml syringes connected to the chamber by small plastic tubes: the applied solution is immediately sucked away by an aspiration pump connected to a lateral pool in connection with the central chamber.

Electrovalves control the release of solutions and make it possible to alternate them. The microelectrodes are made of borosilicate glass capillaries with a 1mm diameter. They are pulled by a horizontal puller that heats the central part while applying a constant tension. The obtained electrodes are filled with a KCl 3M solution (a ionic conductive solution) and put on two holders. In this way a thin $Ag/AgCl_2$ electrode can be inserted inside the electrodes.

The holders are put on the machinery and the electrodes tips are gently broken against the chamber bottom moving the micromanipulators. The optimal dimension is referred to resistance values: 0.8-1.0 MΩ for current electrode and 4 MΩ for the voltage one. Now the electrodes are inserted in the oocytes, damaging as little as possible its membrane. When both the electrodes are inserted, the voltage electrode measures the resting potential, which for oocytes in good shape, varies between -40 and -60 mV. After the oocytes is stable, the voltage clamp can be applied. While clamping the membrane potential, data about the currents crossing the membrane can be obtained, depending on the previously chosen experimental protocol.

We have used the program Clampex 8.1 (Axon Instrument Foster City, CA, USA). The software generates digital inputs that are then translated in analogical output and sent to the oocytes.
The currents induced by potential changes are recorded and amplified through the voltage-clamp amplifier (GeneClamp, Axon Instruments Foster City, CA, USA or Oocyte Clamp OC-725B, Warner Instruments, Hamden, CT, USA). The signal is filtered at 1 kHz in order to eliminate high frequency "noise" and it is sent to a oscilloscope that visualizes the current. The oscilloscope sends the current to an AD/DA (analog-digital, digital-analog) converter (DIgiData 1200, Axon Instr.). The signal is converted in digital one that can be stored by the computer.

2.4.2 TEVC protocols

In voltage-clamp mode the holding potential (V_h) was generally -60 mV, unless otherwise indicated. The pulse protocol used consisted of 20 mV steps covering a voltage range from -160 to +20 mV or from -140 mV to +40 mV and lasting in 200 ms. The current signal was filtered at 1 kHz before sampling at 2 kHz. Two methods were used to isolate the presteady-state currents elicited by voltage jumps (Mertl et al., 2008): the first method consisted of a double-exponential fitting, while in the second the current obtained from the subtraction of the traces in the presence from those in the absence of substrate were fitted with a single exponential. The isolated traces were than integrated to calculate the amount of displaced charge, after zeroing any residual steady-state transport current. Even if the two methods gave generally equivalent results, the subtraction method was preferred when the presteady-state currents were fast.

2.5 SOLUTIONS

The oocyte culture and washing solutions had the following composition (in mM), ND96: NaCl 96, KCl 2, MgCl2 1, CaCl2 1.8, Hepes 5, pH 7.6; MBS: NaCl 88, KCl 1, NaHCO3 2.4, Hepes 15, Ca(NO3)2 0.30, CaCl2 0.41, MgSO4 0.82, sodium penicillin 10 μg/ml, streptomycin sulphate 10 μg/ml, gentamycin sulphate 100 μg/ml, nystatin 10 U/ml, pH 7.6; PBS: NaCl 138, KCl 2.7, Na2HPO4 8.1, KH2PO4 1.9, pH 7.6. The external control solution had the following composition (mM): NaCl, 98; MgCl2, 1; CaCl2, 1.8. Different pH buffers were used for the various pH values: for pH 6.5, Mes 5 mM was used; Hepes 5 mM was employed for pH 7.0 and 7.5, while for pH 8.0 the buffer was Taps 5 mM. The final pH values were adjusted with HCl and NaOH. Substrate amino acids (histidine and threonine) and oligopeptides (Table 2.1) were added at the indicated

concentrations (between 0.3 and 3 mM) to the appropriate solutions. All substrates for electrophysiology experiments were supplied from Sigma, Milan, Italy. Experiments were performed at room temperature (20–25 °C).

Oligopeptides	
Gly-Gln	Glicine-Glutamine
Gly-Sar	Glicine-Sarcosine
Ala-Ala	Alanine-Alanine
Gly-Gly-Gly	Glicine-Glicine-Glicine
Leu-Gly-Gly	Leucine-Glicine-Glicine
Gly-Gly-Gly-Gly	Glicine-Glicine-Glicine-Glicine

Table 2.1. Oligopeptides used during the electrophysiological analysis.

2.6 DATA ANALYSIS

Data were analyzed using Clampfit 8.2 (Axon Instruments), and figures were prepared with Origin 7.5 (Microcal Software Inc.,Northampton, MA, USA).

Chapter 3:

RESULTS

RESULTS

The aim of my research was the electrophysiological characterization of PepT1 transporters focusing particularly on the sea bass isoform. The identification of the functional mechanisms of PepT1 is important because of its role in the absorption of nutrients and of several therapeutic drugs. The characterization has been conducted using the voltage clamp technique on *Xenopus laevis* oocytes injected with cRNA coding for transport proteins.

Most of the functional information have been obtained from electrophysiological measurements of the substrate-dependent transport currents and from the presteady-state currents. Both types of currents have been recorded in different conditions: varying the type and the concentration of the organic substrate, the pH of the bathing solution, the number and the position of the amino acids composing the peptide.

3.1 sbPepT1

The peptide transporters are able to bind and translocate an enormous number of peptides (Ganapathy and Leibach, 1982). In the recent years, the effect of dietary protein on PepT1 expression and activity has been an area of active research. In low vertebrates members of the PTR family have not been described at the molecular level yet. Sea bass might represent a useful tool not only to reach new insight into the molecular structure and function of vertebrates peptide transporters, but particularly for its importance in nutrition i.e. in amino acid supplements. In fact the characterization of sea bass intestinal peptide adsorption is of considerable interest in aquaculture technology for dietary purpose.

3.1.1 sbPepT1 transport associated currents

Numerous studies have been conducted during the past decade to investigate the structural requirements for PepT1 binding (Daniel et al., 2004; Bailey et al., 2005). Dipeptide transport is influenced by charge, hydrophobicity, size, and side chain flexibility. Vig and co-workers classified the dipeptides on the basis of the maximum depolarization achieved in a functional assay relative to the Gly-Sar response (%GSmax/EC50): best substrates >1000, good substrates = 300-1000, intermediate substrates = 100-300. In addition they determined the compound binding affinity, expressed as the IC50 value (mM). Thus, higher %GSmax/EC50 values generally correspond to higher affinities (lower IC50) for PepT1. For example, in their experiments, all compounds with IC50 values >3 mM had a %GSmax/EC50 < 50 (poor substrates) (Vig et al., 2006).

The dipeptides used in the present work were chosen on the basis of the structural features summarized in the Introduction and of the values of the %GSmax/EC50 and IC50 (Fig. 3.1).
All the oocytes in the reported experiments were tested 72h after the cRNA injection in the presence of NaCl 98 mM.
Figure 3.1 shows records of membrane currents from an oocyte kept at -60 mV holding potential expressing sbPepT1 and exposed to different dipeptides and to two amino acids all at concentration of 1mM. As expected, the dipeptides are able to generate transmembrane currents; the effect of Gly-Sar on sbPepT1 transport activity is lower than that of Gly-Gln and Ala-Ala. Oocytes exposed to 1mM threonine (data not shown) or histidine do not exhibit transport currents in sbPepT1. This last result is similar to the data obtained from the mammalian PepT1, that is not able to transport any amino acids. The amino acid were tested because the other two members of the SLC15 family PHT1 and PHT2 are able to transport histidine (Yamashita et al., 1997). A non-injected oocyte was tested as control with the same substrates and, as it is possible to see in the last traces of Figure 3.1 it does not generate any current, confirming that the currents recorded and showed in Fig. 3.1 are due to the expression of peptide transport exogenous proteins. In Figure 3.1 it is also presented the effect of external pH (form 7.5 to 6.5). Acidic pH leads to a slight increase in the currents generated by substrates, confirming for the sea bass transporter the pH sensitivity present in the mammalian PepTs (Fei et al., 1994; Steel et al., 1997).

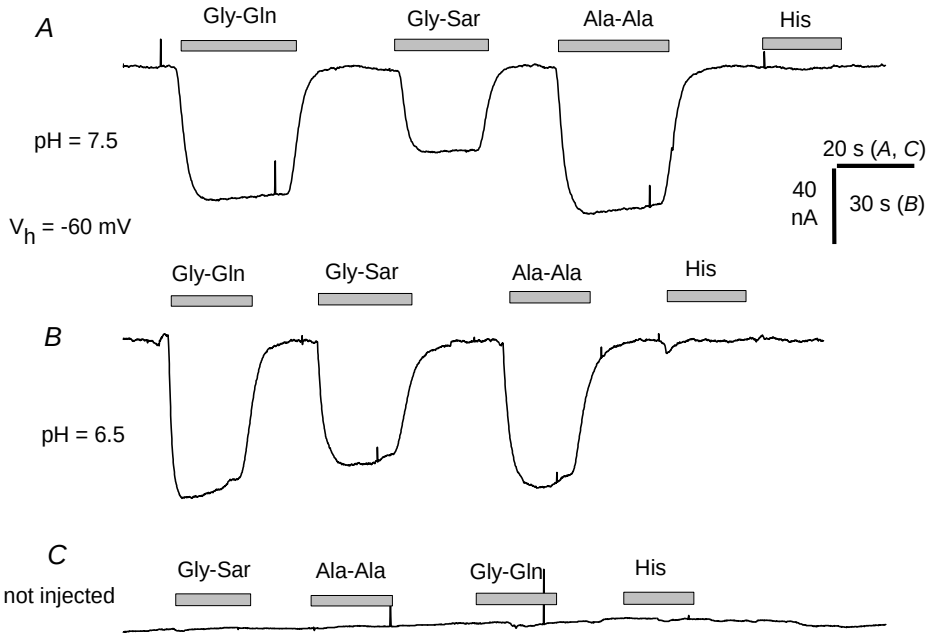

DIPEPTIDES	%GSmax/EC50	IC50
Gly-Sar	190	0.91
Gly-Gln	3100	0.08
Ala-Ala	150	0.95

Figure 3.1. A) and **B)** Representatives traces from an oocyte transfected with sbPepT1 kept a -60 mV holding potential and exposed to histidine and three different dipeptides all at 1mM. Gray bars is the periods of exposure to the substrates. Top trace is recorded at pH 7.5, while bottom traces at pH 6.5. **C)** a non injected oocyte exposed to the same substrates. The %GSmax/EC50 and IC50 values are shown in the table below the graph.

Among the eight thousands different tripeptides that PepT1 is able to transport, some of them have been selected and tested on the basis of their Km values and their commercial availability. Furthermore, as already observed for dipeptides, tripeptides containing a charged amino acids in third position or hydrophobic amino acid residues show the highest binding affinity for PepT1 (Terada et al., 2000). In Figure 3.2, a representative oocyte kept at -60 mV holding potential was perfused with two different tripeptides and one tetrapeptide. Both two tripeptides generate inward currents comparable to those elicited by dipeptide Gly-Gln used as reference, instead the tetrapeptide Gly-Gly-Gly-Gly at the same concentration gives rise only to a small inward current. As expected, the same effect of pH observed in Figure 3.1 is seen also for the transport current induced by tripeptides.

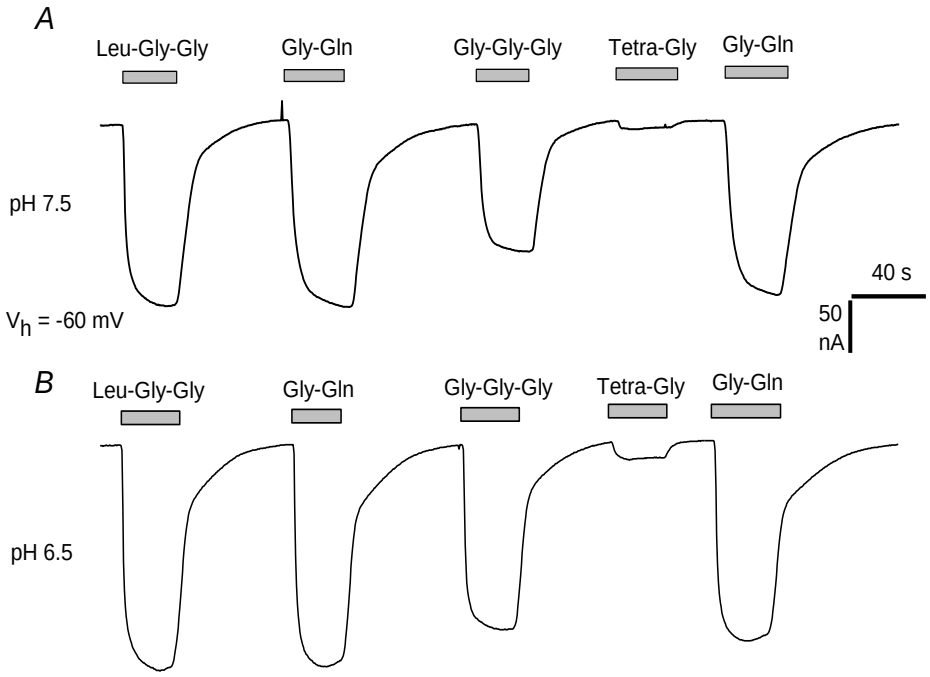

Figure 3.2. A) and **B)** Representatives traces from an oocyte injected with sbPepT1 kept a -60 mV holding potential and exposed to two different tripeptides and one tetrapeptides all at 1mM. Gray bars is the period of exposure to the substrates. Top trace is recorded at pH 7.5, while bottom traces at pH 6.5. The oocyte was also exposed to 1 mM Gly-Gln used as reference responses.

To better characterize the effects of pH on the transport activity, the experiments have been conducted at the pH values of 6.0, 7.0 and 8.0, applying a voltage pulse protocol of 20 mV steps in a voltage range between -160 mV to + 20 mV. The reference substrate Gly-Gln was used at the concentration of 3mM. Figure 3.3A shows that in the absence of substrate, oocytes expressing sbPepT1 exhibit conspicuous presteady-state currents (arrows) already observed and characterized in many transporters of SLC families including mammalian PepTs (Mackenzie et al., 1996).

Upon addition of Gly-Gln, transient currents disappear with concomitant arising of large transport-associated currents (Fig 3.3B). In A and B representative traces are reported at pH 7.0. In Figure 3.3C the current-voltage relationships normalized and averaged over several oocytes are plotted and an interesting effect of pH on the transport activity is revealed. At negative voltage, the curvature of the *I/V* relationship increases with alkaline values with a crossing over around -120 mV. At positive potentials, no significant differences are detected at each pH imposed.

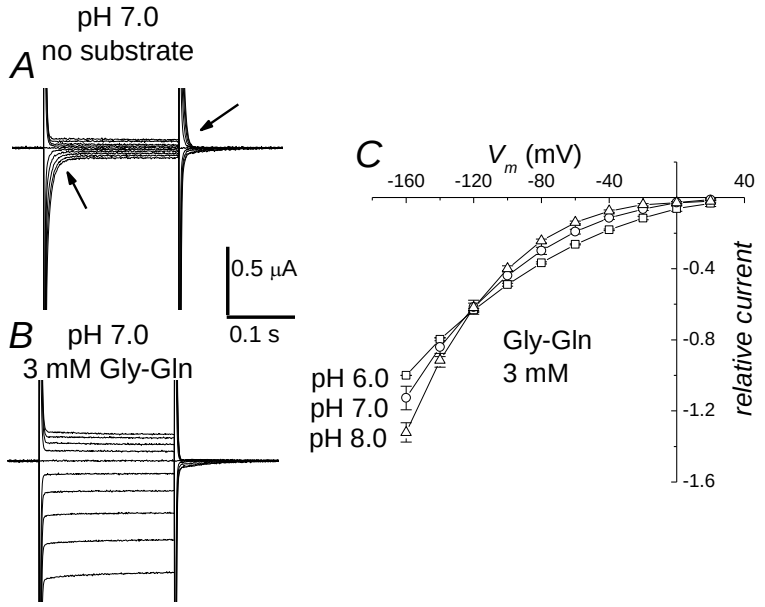

Figure 3.3. **A)** and **B)** Single current traces generated by voltage pulses in the range -160 mV to +20 mV in the absence and in the presence of substrate respectively, at pH 7.0 Arrows indicate transient currents that disappear when the substrate is added. **C)** *I/V* relationship of transport-associated current, obtained in presence of 3 mM Gly-Gln minus steady values in absence of substrate at different pH (6.0-7.0-8-0). The current amplitudes were normalized for each oocyte with respect to the value at-160 mV pH 6.0 before averaging . Data means ± SE from four oocytes.

3.1.2 Analysis of sbPepT1 transport-associated currents: apparent affinity and maximal current

The voltage and proton dependence, as well the substrate affinity and maximal transport, have been further investigated to obtain detailed information on the transport-associated currents of sbPepT1. The oocytes were tested at different concentrations of Gly-Gln between 0.03 and 3 mM and at two pH values (7.5 and 6.5). The *I/V* curves plotted in Figure 3.4A and 3.4B were normalized for each oocyte to the value of the current at -160 mV and pH 7.5.

The *I/V* plot shows:

-an increase in the curvature of *I/V* relationships at negative voltages and at higher substrate concentrations;

-for the more alkaline pH the currents at negative potentials become more conspicuous, conversely the opposite occurs at more positive potentials. The current values are replotted as function of Gly-Gln concentration and fitted with a Michaelis–Menten to get the relative maximal current (I_{max}) and the apparent affinity, reported in the graph as $K_{0.5}$, that is the substrate concentration eliciting half I_{max}.

Panels 3.4C represent the values of the maximal transport current (I_{max}) and 3.4D the apparent affinity for the substrate ($K_{0.5}$) for each potential for the two tested pH, obtained by the fitting of the dose-response curves with the Michaelis-Menten equation:

$$I = \frac{I_{max}[S]}{K_M + [S]} \qquad \text{Eq. 3.1}$$

where I_{max} is the value of the maximal current, K_M is the Michaelis-Menten constant and S is the substrate.

No significant differences are observed between I_{max} curves at the two indicated pH.

Oppositely the $K_{0.5}$ values (substrate concentration that generates half maximal current) diverge significantly at positive potentials and the apparent affinity decreases at acidic pH. This last result is in agreement with that observed for zebrafish PepT1, while the first is not. In fact in zebrafish isoform, alkaline pH was reported to significantly increase the I_{max} values (Verri et al., 2003).

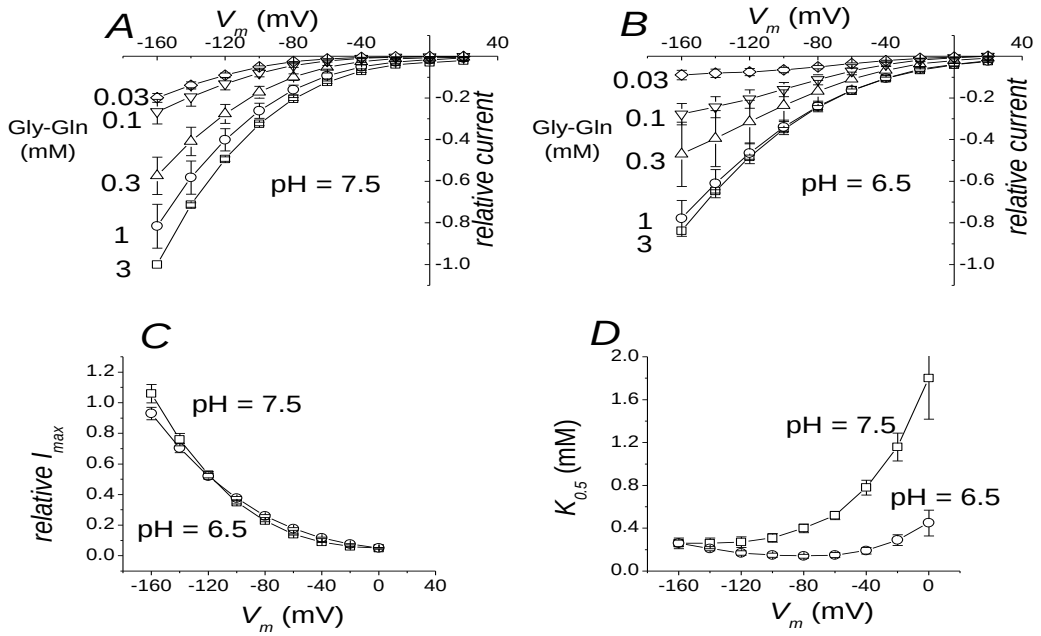

Figure 3.4. Dose-response analysis of sbPepT1 transport current. **A)** and **B)** *I/V* curves obtained from subtraction of the current traces in the absence from those in the presence of the indicated amount of dipeptides, at different potentials and at two pH values. Average data (±SE) from five oocytes. All values were normalized to that at -160 mV at pH 7.5 for each oocyte before averaging. **C)** and **D)** Relative maximal current I_{max} and the apparent affinity $K_{0.5}$ respectively at each voltage, obtained fitting the dose- response curves with a Michaelis-Menten, for the two pH values (squares pH=7.5 and circles pH=6.5)

3.1.3 sbPepT1 presteady-state currents

Figure 3.5 shows the analysis of transient currents from a representative oocyte at the two indicated pH. The presteady-state currents were separated from the endogenous oocyte capacitive currents by two different methods: 1) subtracting the current traces in the presence of saturating substrate from those in its absence and fitting the resulting traces with a single exponential; 2) fitting the transients recorded in the absence of substrate with two exponentials and considering the slow component as the presteady-state current due to the presence of the transporter in the oocyte membrane (Mackenzie et al., 1996).

Panels Aa and Ab illustrate the presteady-state currents obtained by subtracting the traces in the presence of substrate (3mM Gly-Gln) from those in its absence at pH 7.5 and 6.5 respectively. It is necessary to assume that the remaining currents represent the intramembrane charge movement converted into transport current. From V_h = -60 mV, the transient currents appear slower at acidic pH and the remaining transients are more conspicuous in response to hyperpolarizing than to depolarizing pulses (Figure 3.5 Aa and Ab).

In Figure 3.5B are shown the values of the time constants (τ) at the indicated pH values, obtained from the single-exponential fitting of the transients (open symbol). The constant τ is the time required to the transient current to decay to the steady value. At pH 7.5 the τ is faster and τ/V curve appears lower and shifted to more negative potentials than that at pH 6.5, while at pH 6.5 it is possible to appreciate the bell-shaped curve with a maximum at -130 mV (Fig. 3.5B). The solid symbols in Figure 3.5B are the τ values obtained using the two exponential fittings in which the slow component was assumed to represent the presteady-current due to the presence of the transporter on the plasma membrane. The two procedures give similar results.

At the two tested pH integrating the area under the transient (Fig. 3.5Aa and Ab) the amount of charge that moves in the electrical membrane field is obtained; plotting this quantity over the relative voltage, the *Q/V* relation can be drawn. (Fig. 3.5C). Both curves show saturation at positive potentials; at pH 7.5 the curve is shifted to more negative voltages consistently with the negative shift of the τ/V relationship. Whereas at pH 6.5 the curve *Q/V* shows a sigmoidal trend.

Confirming the capacitative nature of the transient currents, Figure 3.5D illustrates a good quantitative correlation of the “on” and “off” integrals for each voltage as observed for other transporters.

The *Q/V* relationships in Figure 3.5E were obtained fitting the transient currents with the two-exponential method. The *Q/V* curves isolated with this approach are qualitatively and quantitatively comparable to those obtained by subtraction, because of the large errors the pH-induced shift represented in Figure 3.5E is not statistically significant.

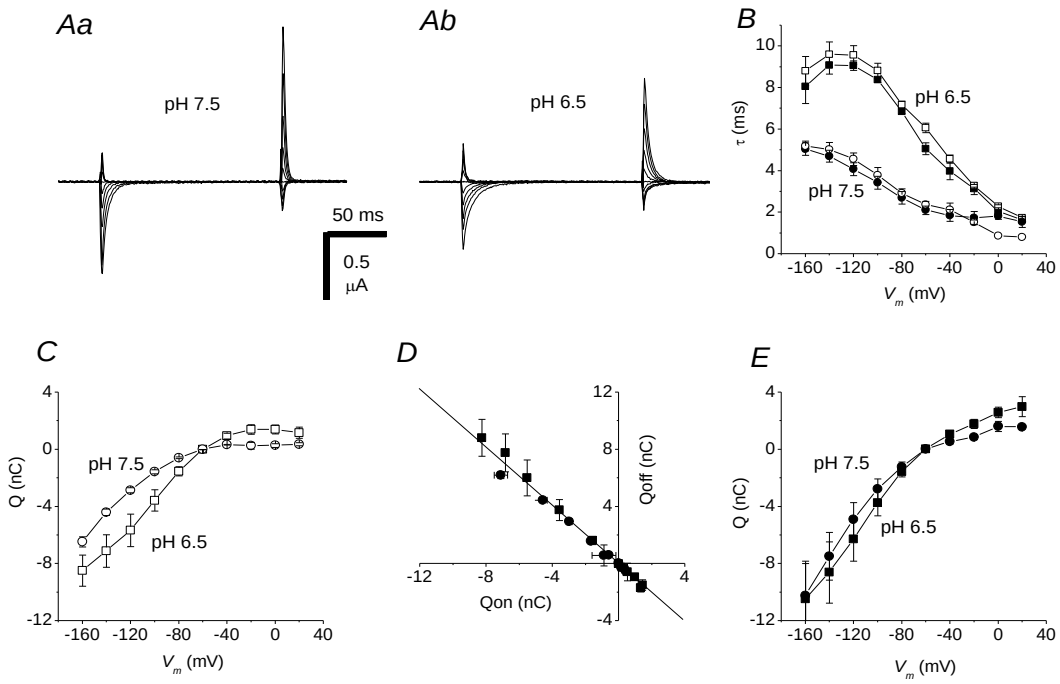

Figure 3.5. Analysis of transient currents. **Aa)** and **Ab)** Transients isolated using single-exponential fitting (subtracting the traces in presence of 3 mM Gly-Gln from those in absence of substrate) at pH 7.5 and 6.5 respectively. **B)** τ/V curves obtained from the single-exponential fitting of the transient such as in **A** (open symbols) or from a double–exponential fitting of the corresponding unsubtracted traces (filled symbols). Data are means ± SE from five oocytes. **C)** *Q/V* relationship obtained by integration of the transient isolated as in **A** at pH indicated (7.5 and 6.5). **D)** Means of Q_{on} and Q_{off} integrals plotted against each other for the same five oocytes. **E)** *Q/V* curves obtained by integration of the transient isolated using the two-exponential method at pH 7.5 and 6.5.

3.2 COMPARISON OF PepT1 ELECTROPHYSIOLOGICAL PROPERTIES FROM THREE SPECIES

PepT1 has been cloned and characterized in many species such as human, rabbit, zebrafish and sea bass (Boll et al., 1996; Fey et al., 1994; Liu et al., 1995; Covitz et al., 1998; Verri et al.; 2003; FJ237043). However, the electrophysiological results are controversial in the different species as demonstrated before in fishes, and as reported in literature for rabbit. Electrophysiological data indicate that for acidic pH I_{max} increases or does not change or decreases in zebrafish, sea bass and rabbit isoforms respectively. Uptake experiments with human PepT1 have shown instead a bell-shaped activity with an optimal between pH 5.5 - 6.0. Fujisawa and co-workers have examined the pH-dependency of transport activity by hPepT1 using CHO/hPepT1 cells. The accumulation of Gly-Sar by CHO/hPepT1 was stimulated varying pH from 8.0 to 3.5. The uptake of Gly-Sar was increased by acidification of the medium pH, but further acidification and alkalinization of the medium pH remarkably depressed the uptake. These observations indicate that the optimal pH is 5.5

and that hPepT1 expressed in CHO/hPepT1cells preserved the original characteristics of the H^+-coupled transport system (Fujisawa et al.; 2006). A similar trend has been observed for the maximal transport current in the rabbit isoform (Amasheh et al., 1997).

In this study the different functional characteristics of three isoforms (sea bass, zebrafish and rabbit) have been investigated using electrophysiological and biophysical analysis and the transport cycles compared.

3.2.1 Transport currents of PepT1

The transport currents of rabbit, zebrafish and sea bass (see above) PepT1 have been already characterized (Steel et al., 1997; Kottra and Daniel, 2001; Verri et al., 2003). Figure 3.6 shows only the electrophysiological features of rbPepT1 (similar curves can be observed for sea bass and zebrafish isoforms): in panels A and B are shown the current-voltage relationships at the two indicated pH values and in the presence of the dipeptide Gly-Gln at different concentrations (0.1,0.3,1,3 mM); in panels C and D are shown the I_{max} and $K_{0.5}$ both at pH 7.5 and 6.5 respectively. In all three species the acidic external pH causes an increase in substrate affinity. The maximal current in zebrafish isoform decreases (Verri et al., 2003), while the corresponding in rabbit and sea bass is not affected (Steel et al., 1997). In human PepT1, high acidity increases both I_{max} and $K_{0.5}$ (Fei et al., 1994; Mackenzie et al., 1996).

In figure 3.6A it is also possible to observe that low substrate concentrations elicit a small outward current already reported for the zebrafish transporter (Verri et al., 2003), but not for the human (Mackenzie et al., 1996) or sea bass isoforms (Fig.3.4).

The decrease in I_{max} at acidic pH in all three species was unexpected considering the inward proton electrochemical gradient increase.

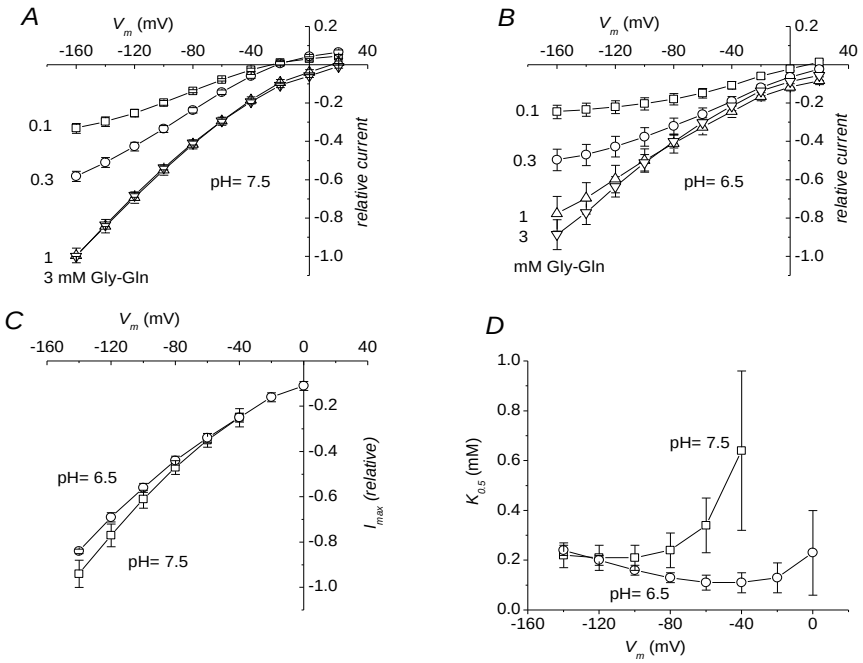

Figure 3.6. Transport-associated currents of rabbit PepT1. **A)** and **B)** *I/V* relationships at the indicated concentration of Gly-Gln and at pH 7.5 and 6.5 respectively. Data are mean values ± SE from six oocytes. All values were normalized to that at -140 mV at pH 7.5 before averaging. **C)** and **D)** values of I_{max} and $K_{0.5}$ respectively, obtained by fitting the current-voltage relationships from (A and B) with Michaelis-Menten equation. Bars are the errors from the fitting procedure.

The ratio of the relative $I_{max}/K_{0.5}$, that is the slope of the Michaleis-Menten relationship at zero substrate concentration (Fig. 3.7), represents an index of the transport efficiency.

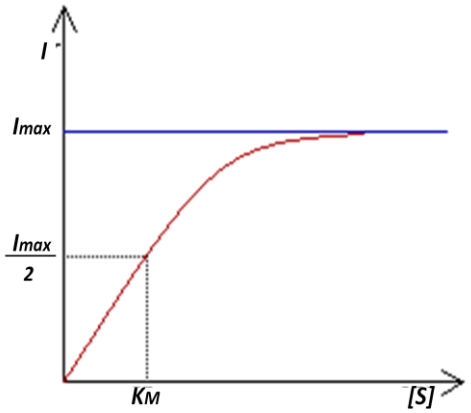

Figure 3.7. Michaelis-Menten relationship. I_{max} is the value of the maximal current, K_M is the Michaelis-Menten constant and S is the substrate.

The ratio of the relative $I_{max}/K_{0.5}$ can be described with the following equation (derivative of the Eq. 3.1):

$$\frac{dI}{dS}(S=0) = \frac{I_{max}[K_M+S] - I_{max}[S]}{[K_M+S]^2} = \frac{I_{max}K_M}{K_M^2} = \frac{I_{max}}{K_M} \qquad \text{Eq.3 2}$$

where I_{max} is the value of the maximal current, K_M is the substrate concentration that generates half maximal current and S is the substrate.

The values of the $I_{max}/K_{0.5}$ concerning the three isoforms are plotted in Figure 3.8. For rabbit the ratio of relative $I_{max}/K_{0.5}$ derived from data shown in Figure 3.6, for zebrafish from our unpublished data and for sea bass from data in Figure 3.4. In the rabbit and in the sea bass the largest difference in efficiency is observed at more acidic pH in the physiological range of potentials, while in the zebrafish isoform there is no significant difference for all the parameter tested. This is in agreement with the acidic environment of the small intestine of both rabbit and sea bass and with the alkaline pH in zebrafish (Nalbant et al., 1999).

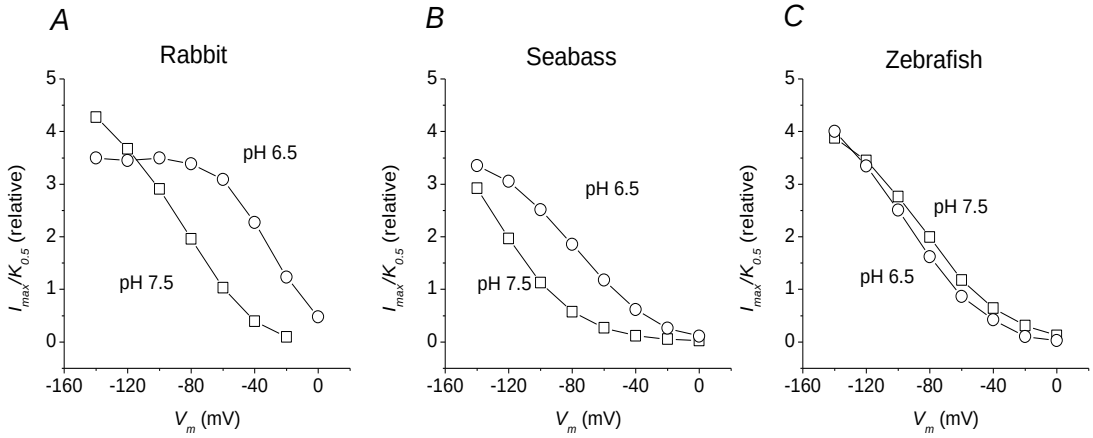

Figure 3.8. Transport efficiency. Plots of the ratio relative $I_{max}/K_{0.5}$ for rabbit ((**A**) from data in Fig 5), sea bass ((**B**) from data in reference 10) and zebrafish ((**C**) from our data not shown).The efficiency, in the physiological range of potentials, is better or equal at more acidic pH.

3.2.2 Presteady-state currents of PepT1

The presteady-state currents of rbPepT1(Nussberger et al., 1997), and sbPepT1(see above) have been already described and analyzed, while those of zfPepT1 have not been completely investigated.

The parameters that can be obtained from this currents are crucial to understand the kinetics of the transport cycle. With the goal of comparing the different PepT1 transporters, experiments on the

different isoforms were performed with a protocol of voltage pulses from -140 to +20 mV both in the absence and in the presence of saturating Gly- Gln (3mM) and at 6.5 pH.

The pH was chosen basing on the pH of the luminal surface of the mammalian small intestine (Thwaites and Anderson, 2007). In Figure 3.9 the presteady state currents of rabbit, sea bass and zebrafish PepT1 are reported. In particular, the presteady-state currents of the fish isoforms are larger at hyperpolarizing voltage values, while the rbPepT1 transient currents are about symmetrical around the -60 mV holding potential. In all the three isoforms the decay time constants of transients are slow (Fig 3.9 and top row). As expected by the previous literature data, the addition of saturating amount of substrate (Gly-Gln 3mM) generates transport-associated currents that abolished the presteady-state currents as observed in many other electrogenic transporters (Fig 3.9, bottom row). In these experiments, the "subtraction method" was used to isolate the transients. The two different methods (see sbPepT1 presteady-state currents) were tested (Mertl et al., 2008)) and the two-exponential method revealed to be less reliable when the values of the two time constants (endogenous and protein- related) are similar. In fact the time constants for charging the oocyte membrane capacity are around 1ms; thus the two-exponential method becomes defective when the decay time constant of the presteady-state currents approaches this value (i.e., 2-3 ms). This is the case of the fish species at the positive potentials. In addition, both rabbit and sea bass PepT1 exhibit an acceleration of the presteady-state currents decay at alkaline pH (Nussberger et al., 1997; data previously shown for sbPepT1).

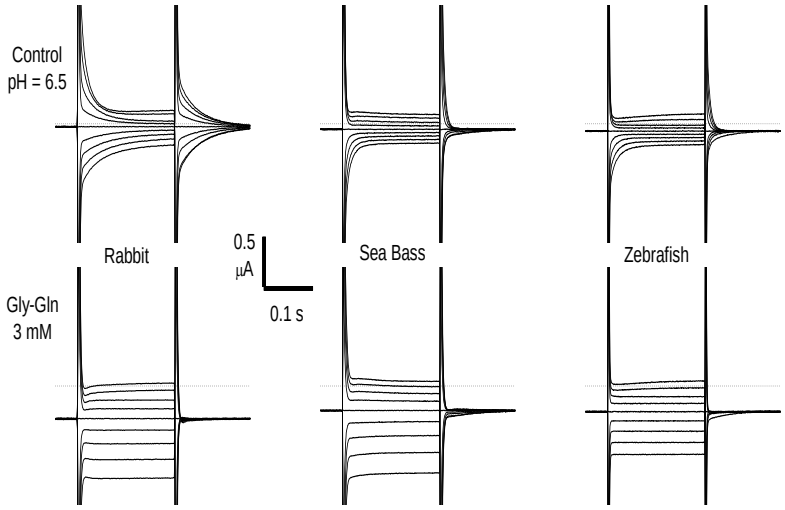

Figure 3.9. PepT1 presteady-state currents from three species. Voltage pulses in the range -140 to +20 mV applied with 20 mV steps from V_h=-60 mV and at pH 6.5. Top row shows presteady-state currents that all three transporters exhibit in the absence of substrate. The decay of the transient currents are faster in fish transporters and are lacking in the depolarizing direction. Adding 3 mM Gly-Gln induces steady currents in the same oocytes and the simultaneous disappearance of the presteady-state currents.

The amount charge that moves during the presteady-state currents can be described by the Boltzman equation:

$$Q = \frac{Q_{max}}{1+\exp\left[\frac{-(V-V_{0.5})}{\sigma}\right]} \qquad \text{Eq. 3.3}$$

where Q_{max} is the maximal moveable charge; $V_{0.5}$ is the voltage at which half of the maximal charge is moved; and $\sigma = kT/q\delta$ is the slope factor, in which k is the Boltzmann constant, q is the elementary electronic charge, T is the absolute temperature and δ is the fraction of electrical field in which the charge moves.

The Q/V curve may represent the steady state distribution of the transporter molecules between two conformations. The charge movement process may be described with the following reaction:

$$Q_{in} \underset{\text{inrate}}{\overset{\text{outrate}}{\rightleftharpoons}} Q_{out}$$

where *out-rate* and *in-rate* are the unidirectional rate constants and Q_{in} and Q_{out} are the amount of charge moving in the inward and outward position respectively in the membrane electrical field.

The two fish isoforms give very similar results (only data on zebrafish shown).

Figure 3.10 shows the voltage dependence of the decay time constant τ and of the intramembrane charge movement Q obtained from the transient currents of the rabbit and of (general) fish PepT1 at pH 6.5 and 7.5.

At pH 6.5 the rbPepT1 bell-shape τ/V curve has a maximum at about -90 mV confirming that at this pH, rabbitPepT1 transients are about symmetrical around the holding potential. In fish transporters only the right half of the bell-shaped curve is visible. In fact the sea bass transporter has the maximum of the τ/V curves shifted to more negative voltage around -140 mV. Similarly, the Q/V curve for rbPepT1 is sigmoidal, while in the fish transporters only the right part of the curve is plotted. Fitting the Q/V curves to the Eq. 3.3 gives the parameters summarized in Table 3.1.

	RABBIT		**SEABASS**		**ZEBRAFISH**	
pH	**6.5**	**7.5**	**6.5**	**7.5**	**6.5**	**7.5**
Q_{max} *(nC)*	33.2±1.9	31.5±1.2	10.2±0.3	6.8±0.9	11.0±0.3	9.9±1.1
$V_{0.5}$ *(mV)*	-41.4±2.5	-100±2.3	-98.7±1.3	-122.0±0.6	-108±1.6	-119±7.2
σ *(mV)*	42.9±3.1	39.5±1.7	23.1±0.7	23±2.7	31.1±0.9	33.5±3.3

Table 3.1. Boltzman equation parameters.

In all species, the external alkalinization strongly reduces the time constant of decay.

The τ of rbPepT1 is slower than those derived from fish data, and between these last, sbPepT1 τ is faster than zfPepT1.

Testing the PepT1 transporter at pH 7.5 changes the shape of the pre-steady state currents: the *τ/V* and *Q/V* curves are shifted to more negative voltage as is possible to appreciate in Figure 3.10, and for sea bass PepT1 in Figure 3.5.

The *outrate* and *inrate* are calculated from the experimental *Q/V* and *t/V* curves :

$$\tau = \frac{1}{outrate + inrate} \quad \text{and} \quad \frac{Q_{in}}{Q_{in} + Q_{out}} = \frac{Q_{in}}{Q_{max}} = \frac{inrate}{outrate + inrate} \qquad \text{Eq. 3.4}$$

where Q_{max} is the maximal moveable charge, determined by the fitting of the *Q/V* curve (Table 3.1). Consequently, changing the pH affects also the inward and outward rates that are sped up by external alkaline pH in all the PepT1 isoforms (Fig 3.10). These observations indicate that protonation of unidentified amino acids slows down the rates of the charge-moving conformational changes induced by membrane potential.

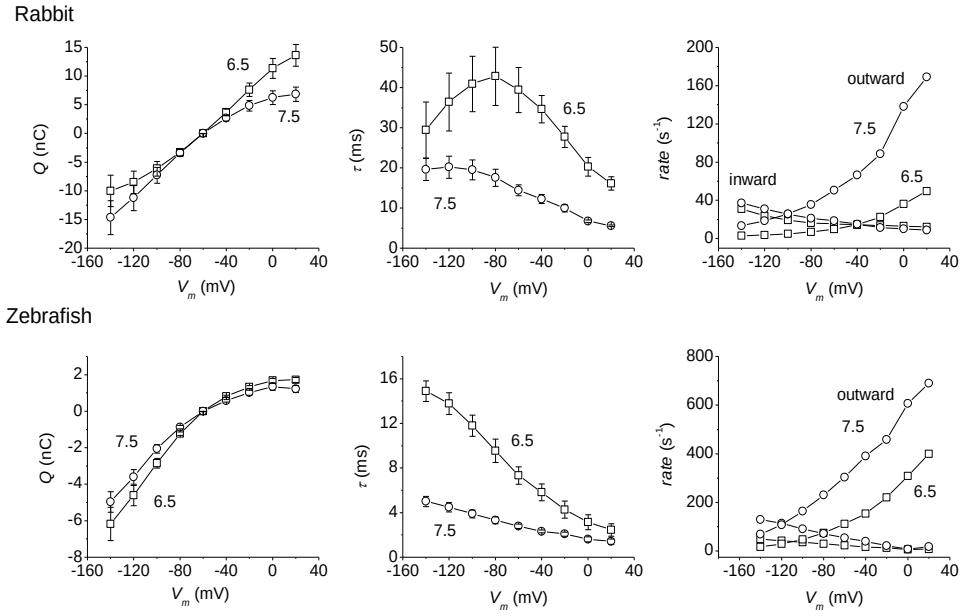

Figure 3.10. Effects of external pH on the properties of the presteady-state currents of rabbit and zebrafish PepT1. In left and in central column the *τ/V* and *Q/V* curves are shifted to more negative voltages at alkaline pH. Furthermore, the time constant of decay is strongly reduced. The right column shows the unidirectional rate constants of the intramembrane charge movement. In all plots, squares refer to data at pH 6.5 and circles represent data at pH 7.5. Data are mean ± SE from three to seven oocytes.

3.3 FUNCTIONAL KINETIC MODEL FOR PepT1

Functional kinetic models have been proposed for human and rabbit PepT1 (Mackenzie et al., 1996; (Sala-Rabanal et al., 2006); (Irie et al., 2005) but the literature transport scheme is not able to unify the characteristics revealed by the more recent works on the different isoforms.

Thus, starting from the data showed before, we proposed a new kinetic model for PepT1 able to describe the electrophysiological and biophysical differences among the three isoforms.

3.3.1 PepT1 presteady-state currents modeling

A scheme adept to simulate the observed results and in particular the effects of pH on the presteady-state currents of PepT1 transporter was proposed. The slowing effect of protonation was introduced in the scheme that was based on existing models (Mackenzie et al., 1996; Nussberger et al., 1997).

In Figure 3.11 the new kinetic model was represented:

- The intramembrane charge movement occurs between states 1 and 6 and the rearrangement of the empty transporter displaces an intrinsic net negative charge in the membrane electrical field. This transitions (green arrows) are bracketed by two proton-bound states, T2 and T7, modulating the T1↔T6 transition.

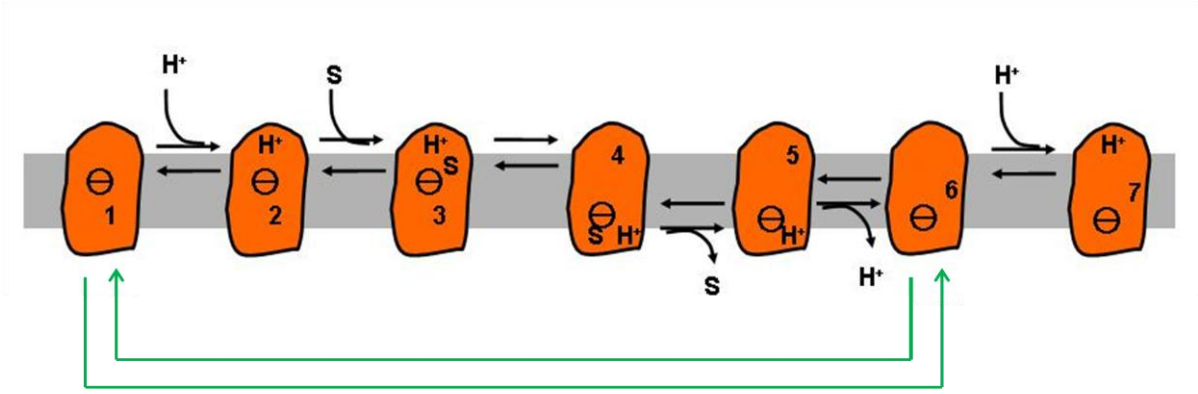

Figure 3.11. Kinetic model devised to simulate the effect of external pH on the presteady-state currents of PepT1 transporters. Transitions T1↔T6 and T3↔T4 are voltage-dependent. External protons can bind to T1 (leading to state T2) and to T6 (leading to T7). T2 and T7 slowing down both inward and outward charge movement.

- At state T2 the transporter binds the substrate leading to state T3 and causing a partial voltage-dependent conformational rearrangement from T3 and T4 states.
- In T5, the organic substrate is released in the intracellular compartment.
- The subsequent proton release leads to the empty inward-facing transporter (T6).

- The novelty is the introduction of the T7 state. This change gives reason for the effect of the slowing action of external protons on the inward rate of charge movement.
  This introduction can also explain the smaller current observed at acidic pH as already suggested for the zebrafish PepT1 (Verri et al.,2003).
  The transition to state T7 may represent a proton binding to an allosteric site. The external proton traps the transporter in an inward facing conformation, slowing down the return to the outward-facing, essential to start a new cycle.

The complete model can be described with these following equations:

$$\frac{dT_1}{dt} = -(K_{12}+K_{16})T_1+k_{21}T_2+k_{61}T_6$$

$$\frac{dT_2}{dt} = K_{12}T_1 -(K_{21}+K_{23})T_2+k_{32}T_3$$

$$\frac{dT_3}{dt} = K_{23}T_2 -(K_{32}+K_{34})T_3+k_{43}T_4$$

$$\frac{dT_4}{dt} = K_{34}T_3 -(K_{43}+K_{45})T_4+k_{54}T_5$$

$$\frac{dT_5}{dt} = K_{45}T_4 -(K_{54}+K_{56})T_5+k_{65}T_6$$

$$\frac{dT_6}{dt} = K_{16}T_1 +K_{56}T_5-(K_{61}+K_{65}+k_{67})T_6+k_{76}T_7$$

$$\frac{dT_7}{dt} = K_{67}T_6 -k_{76}T_7$$

where the T1-T7 states are the probabilities that the transporter is in a given state and the *k* values shown in Tables 2 and 3 are the rate constants, dependent or independent on the voltage and concentration. Because the parameters of the two fish species are similar, they are represented as a "generalized" fish transporter.
The unidirectional rate constants showed in Figure 3.10 were fitted with growing and decaying exponential in the form:

$$outrate = outrate^0 \exp(\delta_{out} qV/kT)$$

and

$$inrate = inrate^0 \exp(-\delta_{in} qV/kT),$$

where $outrate^0$ and $inrate^0$ are the zero-voltage rates; δ_{out} and δ_{in} (with $\delta_{out} + \delta_{in} = \delta$ in eq. 1) are the asymmetric fractional dielectric distances; ***q***, ***k*** and ***T*** have the same meaning as in Eq. 3.3;

Rates k_{16}, k_{61}, k_{12}, k_{21}, k_{67} and k_{76} were determined based on the effects of external pH and voltage on the unidirectional rate constants of Figure 3.10.

Assuming that the binding and unbinding of protons in transitions T1↔T2 and T6↔T7 is much faster than in T1↔T6, the unidirectional rate constants of charge movement *outrate* and *inrate* can be written as:

$$\boldsymbol{outrate = f_{21}\, k_{16},}$$

$$\boldsymbol{inrate = f_{76}\, k_{16},}$$

where

$$f_{21} = \frac{k_{21}}{k_{12}+k_{21}}$$

$$f_{76} = \frac{k_{76}}{k_{67}+k_{76}}$$

are modulating factors depending on the external proton concentration. Because k_{12} and k_{67} increase with acidity, the modulating factors will reduce the values of both *outrate* and *inrate*.

Rate	k_{12}	k_{21}	k^0_{16}	k^0_{61}	k_{56}	k_{65}	k_{67}	k_{76}	δ_{16}	δ_{61}	δ
Units	$M^{-1}s^{-1}$	s^{-1}	s^{-1}	s^{-1}	s^{-1}	$M^{-1}s^{-1}$	s^{-1}	s^{-1}	s^{-1}	$M^{-1}s^{-1}$	
Rabbit	$9x10^9$	750	172	10	$1x10^5$	$1.5x10^7$	$5x10^8$	400	0.45	0.26	0.71
Fish	$3.5x10^9$	750	1050	15	$1x10^4$	$1.5x10^7$	$5x10^8$	400	0.39	0.48	0.87

Table 3.2. k_{16}^0 and k_{61}^0 are the zero-voltage rates in the voltage-dependent transition T1↔T6. In the last column are indicated the value $\delta = \delta_{16} + \delta_{61}$, higher for the fish transporter and in agreement with the smaller value of σ in Table 3.1.

The results of the simulations for rabbit and the generalized fish transporter are shown in Figure 3.12. The simulations are in good qualitative, and for rabbit PepT1 also quantitative agreement with the experimental results shown in Figure 3.10.

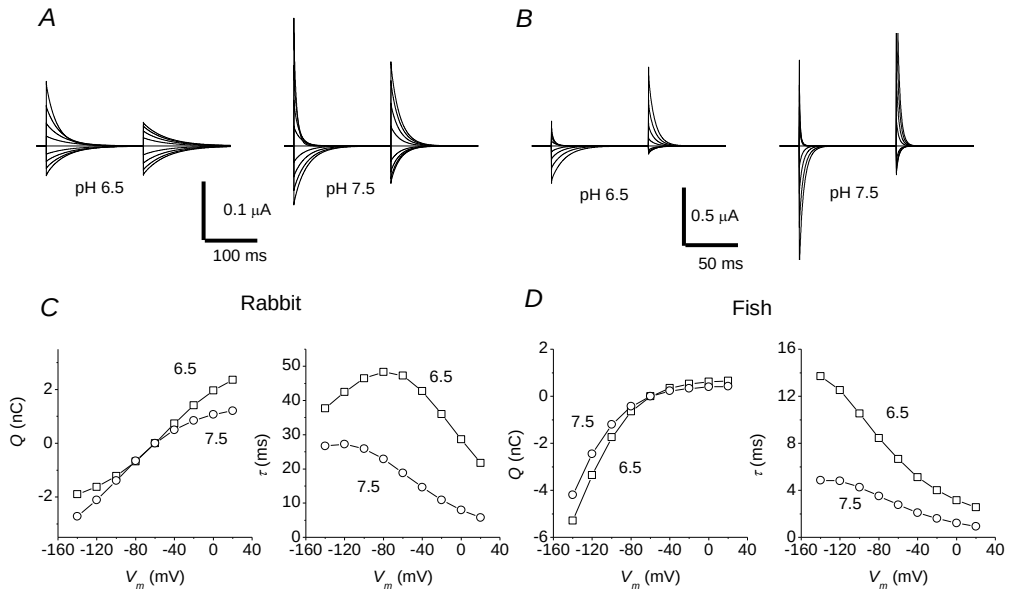

Figure 3.12. **A)** and **B)** simulated traces of presteady-state currents at two external pH values for rabbit and generalized fish, respectively. The traces in response to voltage pulses from -140 mV to +20 mV from V_h=-60 mV were analyzed following the same procedure as that was used for the experimental subtracted recordings to produce the curves shown in the bottom graphs. **C)** Rabbit results, where the symbol represent the experimental data from Fig 2 and the continuous lines are the results of the simulations. **D)** Simulations results of generalized fish. The total number of transporters was set to $24x10^{10}$ for rabbit and $10x10^{10}$ for fish, with each one carrying a single elementary charge.

3.3.2 Transport currents modeling

The presteady-state model devised above was utilized to verify its ability to reproduce the characteristics of the transport currents. The states T3 and T4, related to the outward and inward conformations of the transporter with the substrate bound, are the indispensable states inserted to complete the transport cycle. The T3↔T4 transition has a small charge movement that occurs in the membrane electrical field for rabbit and fish during substrate translocation.

Because the best fit of the experimentally observed charge movement required the transition T1↔T6 to occur over 71% of the membrane electrical field for rabbit and 87% for fish (Table 3.2), the remaining fractional voltage-dependence for protons was attributed to the T3↔T4 transition.

In Table 3.3 are reported the parameters determined to simulate the substrate binding and translocation. In particular, k_{23} and k_{32} were chosen to give a value of K_{05} consistent with the experimental observations at pH 6.5, and k_{34} and k_{43} were set to be equal to each other at 0 voltage and significantly faster than the other rates. Similarly k_{45} was set at a high value, while k_{54} was derived from the other rates to satisfy the principle of detailed balance.

Rate	k_{23}	k_{32}	k^0_{34}	k^0_{43}	k_{45}	k_{54}	δ_{34}
Units	$M^{-1}s^{-1}$	s^{-1}	s^{-1}	s^{-1}	s^{-1}	$M^{-1}s^{-1}$	
Rabbit	$2x10^5$	20	6000	6000	5000	$3.49x10^{11}$	0.29
Fish	$8x10^6$	20	6000	6000	5000	$8.89x10^{10}$	0.13

Table 3.3. Additional parameters in presence of substrate. k^0_{34} and k^0_{43} are the zero-voltage rates in the voltage-dependent transition T3↔T4. δ_{34} =1- δ is the fraction of electrical field covered by proton movement before neutralization of the intrinsic negative charge.

In Figure 3.13 the simulation curves are shown. It is possible to observe the ability of the model to simulate the pH-dependence of the I_{max} and $K_{0.5}$ parameters in the different species.

In fact fitting the simulated dose-current curves at each potential with a Michaelis-Menten equation gives correct parameters. The rabbit transporter activity is reported in the first column. The alkaline pH does not affect or slightly increases I_{max}, while the apparent affinity decreases (Steel et al., 1997; Kottra and Daniel,2001) with the increase of the pH. The central column shows the simulations extended to the generalized fish transporter. The model is able to reproduce the typical characteristics of this transporters: increase in I_{max} at alkaline pH and decrease in $K_{0.5}$ common to all species. In the last simulation (right column) we tried to verify the ability of the model to reproduce the increase in I_{max} at acidic pH, observed in human PepT1. To obtained an opposite effect of I_{max} it was sufficient to reduce the k_{67} from $5x10^8$ to $1x10^8$ (Table 3.1).

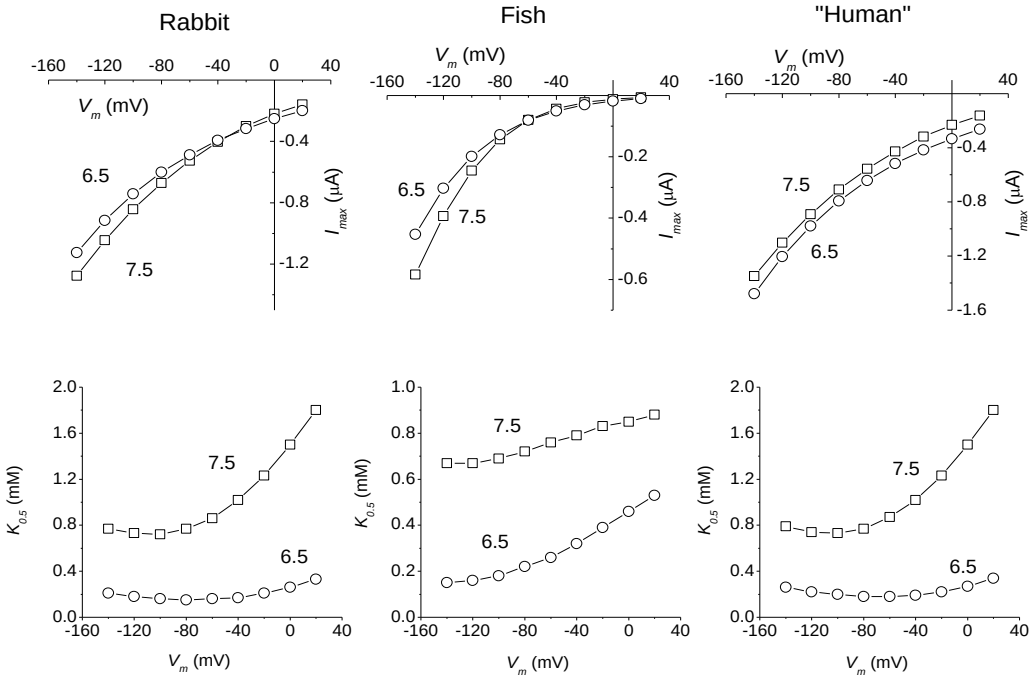

Figure 3.13. Simulation of I_{max} and $K_{0.5}$ obtained by analysis of the dose-current curves generated by the model, using the rate values indicated in Table 2 and 3 for rabbit (left column), fish (center column) and human (right column). The last simulation was used to test the ability of the model to reproduce the increase in I_{max} with acidity observed in human PepT1.

Chapter 4:

DISCUSSION

DISCUSSION

4.1 ELECTROPHYSIOLOGICAL CHARACTERIZATION OF sbPepT1

Recently the sea bass isoform sbPepT1 (FJ237043) has been cloned. In this work, sbPepT1 was successfully heterologously expressed in *Xenopus laevis* oocytes and its features investigated by the two-electrode voltage clamp technique.

4.1.1 sbPepT1 presteady-state currents

In the absence of organic substrate, sbPepT1 exhibits transient currents (I_{pre}) that are common in many different families of membrane transporters and are considered to be linked to the initial steps of the transport cycle. This type of currents have been studied in rabbit and human PepT1. They are generated when the membrane voltage is changed and correspond to the amount of charge moved in the membrane electrical field. A voltage step ΔV generates a current given by:

$$I = \frac{\Delta V}{R} \exp\left[-\frac{t}{RC} \right],$$

which declines to zero with a time constant given by $\tau = RC$ and displaces an amount of charge $Q=C\Delta V$ into the capacitor plates. In the introduction is reported the electrical circuit simulating intramembrane charge movement (Fig 1.8) (Peres et al., 2004).

The disappearance of I_{pre} upon the addition of saturating substrate indicates the conversion form an intramembrane capacitative-like charge movement to a restive-like transmembrane flux of charge when the transport cycle can be completed (Peres et al., 2004).

The presteady-state currents were isolated in this work using two different methods: the double exponential fitting (Mackenzie et al., 1996) and the subtraction of the current traces recorded in the presence of saturating substrate from those in its absence. The subtracted traces were then fitted with a single exponential. The two methods give similar results for the τ/V relationship, instead the Q/V curves obtained with the two methods are not so coincident. The isolation of the presteady-state currents using the double-exponential method produces errors larger than with the subtraction method in particular at positive potentials and as a consequence in this case a pH-induced shift was not statistically significant.

The limitation of the subtraction method is related to the saturation at positive voltage values in particular at alkaline pH.

To explain this phenomenon it is necessary to consider that it is based on the supposition that the intramembrane charge movement is completely converted into transport current in the presence of saturating substrate concentration, condition that is difficult to gather at alkaline pH and depolarized potentials. For example the data in Figure 3.4D would ideally require substrate concentration in excess of 10 mM; on the other hand the smaller charge values obtained in Figure 3.3 with the subtraction method indicate that the results of the two methods are coherent and consistent with the perspective that the 3 mM of substrate added was not fully saturating.

The electrophysiological approach used to investigate the presteady-state currents has been of particular interest in the study of the majority oligopeptide transporters independently of their belonging to different gene families and of the nature of the coupling ion (Na^+, K^+, H^+). The reason is because the control of the membrane potential allows to limit the use of strongly acidic environment, that is often not well tolerated by the cells.

4.1.2 sbPepT1 transport current

The pH sensitivity of the transport current of sbPepT1 is a point that was investigated in this work. It is known that pH affects several isoforms of PepT1, and that the potentiating effect of acidic pH on the transport current has been observed only for the human form (Mackenzie et al.; 1996), while for the rabbit isoform the published results are difficult to interpret, as they have been obtained at single substrate concentration, or at single voltage value (Amasheh et al., 1997).

Analysis of sbPepT1 currents reveals that the substrate affinity is strongly voltage and pH dependent, while the I_{max} appears substantially independent on pH. The transport current elicited by 3 mM Gly-Gln significantly increases with lower pH (see Figs 3.3C and 3.4C of this work).

This is exactly what is reported for rabbit PepT1. In fact in the study by Steel (Steel et al., 1997), the I_{max} at -50 mV appeared to be pH-independent while the transport current generated by 200 µM Gly-Leu was affected by more acidic pH.

The lack of pH dependency of the maximal current in rbPepT1 has been confirmed by Kottra and Daniel (Kottra and Daniel, 2001). These observations may be useful to reconcile some apparent differences between rabbit and zebrafish PepT1s. They show in fact that, at fixed substrate concentration, the effect of pH is voltage dependent: low pH enhances transport at depolarized potentials and depresses it at negative potentials.

In sbPepT1, this effect is explained by the observation that, although I_{max} is unchanged, the apparent affinity for the substrate is strongly decreased at alkaline pH and at depolarized potentials (Fig

3.4C, 3.4D). This implies that at pH 7.5, a 3 mM substrate concentration might be close to saturation when the voltage is kept at −160 mV, but at 0 mV only the 60% of saturation is reached, producing the enhanced curvature of the I/V relationships seen in Figures 3.3C and 3.4C. The enhancing effect of acidic pH on transport observed in the uptake experiments performed at fixed substrate concentration are in agreement with this framework; in fact in these experiments the membrane potential was not under control, and therefore, it was depolarized by the inward current generated by the transport activity itself.

4.1.3 Conclusion

In conclusion the results of this work on sbPepT1 show that:

- The transporter is electrogenic and able to generate large inward currents in the presence of several dipeptides and tripeptides, but not of tetrapeptide as Gly-Gly-Gly-Gly or histidine and threonine;
- Similarly to the most of ion-coupled, electrogenic cotransporter, sbPepT1 exhibits presteady-state currents elicited in the absence of organic substrate by voltage changes.
- These transient currents disappear when a saturating amount of substrate is added;
- Both presteady-state and transport currents are affected by external pH, although the kinetic properties vary among different species.
- These characteristics are similar to those observed for zebrafish PepT1(Verri et al., 2003), the first teleost PepT1 that has been characterized, and to those of mammalian transporters (Daniel et al., 2006).

4.2 PepT1 UNIFIED MODELING

The investigation of the PepT1 transporters of different species (human, rabbit, zebrafish, chicken and sea bass) using electrophysiological techniques have provided biophysical descriptions of their activity and details of their functionality. These studies have identified several common properties in ion-coupled transporters such as the pH-dependency of the transport with a potentiating effect of external acidic pH. However these studies have also shown some differences among the different analyzed species.

In the present work, the characteristics of presteady-state currents have been analyzed in three PepT1 isoforms (rabbit, zebrafish and sea bass) in order to unify their features in a model able to explain the different pH dependency.

4.2.1 Presteady-state currents in the different species

From the analysis of the presteady-state currents of rabbit and fishes PepT1 the time constant vs. potential (τ/V) and the charge vs. potential (Q/V) curves were obtained.

At the same external pH, τ/V and Q/V are positioned differently on the voltage axis. The zebrafish and sea bass curves are shifted to more negative values while the rabbit curves are located at more positive voltages. In addition, in the rabbit isoform the decline in the presteady-state currents, following voltage steps, are slower than in sea bass and zebrafish transporters. These observations may be explained by the different isoelectric points of the three transporters: 7.47, 6.68 and 6.0 for rabbit, sea bass and zebrafish (Daniel et al., 2006 and our calculation) respectively, suggesting that rabbit PepT1 may be protonated more easily than the fish isoforms. This protonation may explain the slower rates of charge movement observed at the same pH in the rabbit protein if it includes the residues involved in establishing states T2 and T7 of our model.

4.2.2 Effects of external pH on unidirectional rates

The unidirectional rates of the charge movement in the membrane electrical field were calculated and their dependency on external pH investigated. It was already reported that for rabbit (Nussberger et al., 1997) and sea bass (see "Results") transporters the properties of the charge movement are affected by pH through a shift along the voltage axis and with an acceleration of decay at alkaline pH. The results show that in all the three examined species, both the inward and the outward rates are slowed down by an increase in external pH (Fig. 3.9). These result suggests that the currents are mostly due to the arrangement of intrinsic transporter charges and makes unlikely that the presteady-state currents are primarily caused by the movement of external protons. The models proposed for rabbit (Nussberger et al.; 1997) and human (Fig. 4.1)(Mackenzie at al.,1996; Irie et al., 2005) sustain what observed in the results. In these models, inward and outward rates are slowed down by the binding of the internal and external protons that trap the transporters in "occluded". These models were modified in this work by adding a new state (T7 of Fig. 3.11) in which the "inward facing" transporter can bind external protons. The change was made in order to

consider the effect of the slowing down of the inward charge movement by external protons that the previous models did not account. Trapping of the transporter in state T7 by external protonation may explain the decrease in inward rate of positive charge movement caused by acidic pH in the transition T6↔T1.

The transition T3↔T4 that occurs between the outward- and inward facing conformations of the fully loaded transporter is also introduced into the model. This transition, essential to the transport cycle, includes partial fraction of voltage-dependence for protons while the major voltage-and pH-dependency of the unidirectional rates of charge movement was best fitted with a single conformational change of the intrinsically charged transporter over 71% (rabbit) or 87% (fish) of the membrane electrical field.

The presteady-state currents of rabbit and generalized fish were simulated to verify the ability of the model to reproduce the effects of changing external pH as well as the voltage dependency of the displaced charge and the decay time constants.

As shown in Figure 3.12, the kinetic scheme proposed is able to reproduce the properties of both the fish and rabbit PepT1 adjusting only some kinetic parameters (Table 3.2) derived from the experimental observations.

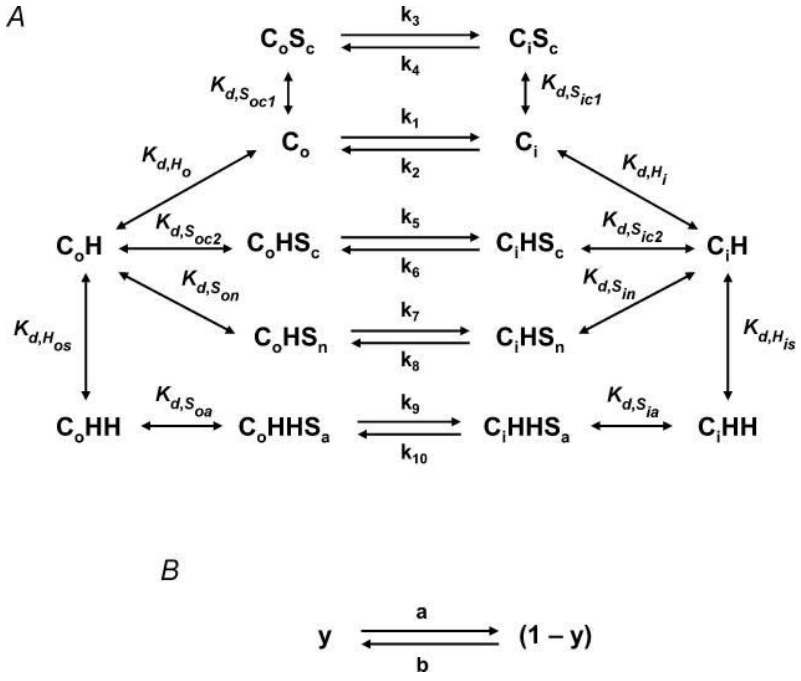

Figure 4.1. Kinetic model of PepT1. **A)** the 14- state model of PepT1. C_o and C_i represent empty PepT1 facing the exterior and interior sides, respectively. C_oX and C_iX stand for PepT1 carrying X. S and H are substrate and H^+, respectively. $K_{d,x}$ represents the dissociation constant of X, and $K_{d,Ho}$ and $K_{d,Hos}$ stand for the dissociation constants of H^+ to the H^+- and substrate, respectively. **B)** The reduced two-state model for PepT1. The 14-state model was condensed into a two-state model, which was used for simulation (Mackenzie et al.,1996).

4.2.3 PepT1 Transport currents

PepT1 is able to transport negatively or positively as well as neutrally charged oligopeptides (Mackenzie et al., 1996). To avoid excessive complications in the system, the only substrate used is the neutral dipeptide Gly-Gln at pH 6.5 and 7.5, that should represent the physiological conditions of the microenvironment in which PepT1 operates, at least in mammals (Thwaites et al., 2007). The model that explains the presteady-state currents was tested to verify its ability to reproduce the transport-associated currents. Because the model was constructed form observations of the presteady-state currents and the parameters were adjusted to simulate the characteristics of these currents, it cannot completely reproduce the behavior of the transport currents for different reasons:

- the model does not include the effects of variable percentage of charged *vs.* uncharged species of substrate at different pH;
- different substrates may present specific interactions with the transporter that are difficult to incorporate in the model.

Using additional parameters reported in Table 3.3, the simulations of mammalian and fish PepTs can reproduce the experimental observations. The results in Figure 3.13 show that there is less agreement than that obtained for the presteady-state currents especially for aspects such as changes in values of I_{max} at different pH and the common higher affinity at more acidic pH.

As already mentioned, the pH dependency of the maximal transport current of human PepT1 appears to be the opposite of that of the rabbit and fish PepT1 (Amashes et al., 1997; Verri et al., 2003). In fact a previous analysis has revealed that the pH dependency of human PepT1 was bell-shaped, with a maximal transport rate at pH 5.5. The decrease at more acidic pH is due to a change in the transporter protein itself caused by the protonation of a histidine residue near the substrate binding domain and the decrease of transport at high pH values is caused by a reduced transmembrane pH gradient (Fujisawa et al., 2006). The model presented here similarly predicts that the I_{max} should decrease at both acidic and alkaline pH for all three species. The devised model can account the differences in the pH dependencies for all of observed species, including the increase in I_{max} with acidity found in human PepT1.

The observed differences in the pH dependencies may be related to the authentic pH values in the small intestine. While in mammalian are found slightly acidic values due to the lack of the luminal expression of the sodium-proton exchanger (NHE3), in zebrafish enterocytes the microenvironment should be alkaline, reflecting the optimal conditions for peptide transporter (Verri et al., 2003).

4.2.4 Conclusion

The enhancing effect of external pH on substrate uptake has become an interesting field in the electrophysiological studies of PepT1. It has been reported that in many species (human, rabbit and sea bass), the electrophysiological properties of PepT1 is affected by external pH. A unified model has been here proposed to describe the behavior of different isoforms of PepT1 (rabbit, zebrafish and seabass) and to explain the main electrophysiological features of these transporters and their pH dependency.

The results and analysis suggest a double role of the protons in the transport cycle of PepT1:

- The protonation of the transporter breaks the transport cycle and counteracts the potentiating effects of the external acidity on the turnover rate;
- The protons are fundamental to neutralize the protein during the inward substrate translocation. The release of the protons in the cytosol reveals the net negative charge of the empty transporter. In this transition the transporter loses the energy necessary to return to the outward facing conformation (transition T6↔T1 in Fig. 3.11).

A different balance between the two actions of the protons may generate opposite effects on the maximal transporter velocity, as it is demonstrated by the kinetic scheme and by the experiments conducted on human PepT1 vs. rabbit or fish transporters.

Because the affinity and the turnover rate are generally inversely related in transport activity (Soragna et al., 2005), the two opposite roles of the protons do not affect the efficiency of substrate uptake. However, using the ratio of I_{max} to $K_{0.5}$ as an index of transport, both experimental data and our model show that PepT1 is capable to satisfy its function across species and expected physiological pH conditions.

Recently a large number of H^+-coupled cotransport mechanisms that act at the luminal side of the membrane of the mammalian small intestine cells have been identified. The work of my PhD research contributed to better characterize PepT1 transport mechanisms, not only of mammalian peptide transporters but also of two fish species. An important step was added to the previous kinetic models to solve the difference of three isoforms (zebrafish, sea bass and rabbit PepT1) and a unified kinetic scheme able to explain the electrophysiological characteristics of PepT1 in particular regarding pH effect was proposed.

The functional information obtained about sbPept1 (sea bass PepT1) are an useful tool to improve our knowledge on nutrient transport mechanisms. Fishes are known to obtain a high proportion of total energy from proteins. Detailed studies on different fish species would be of great importance

in particular in aquaculture; in fact they could help to improve the bioavailability of essential amino acids and to optimize the quantity of peptides, proteins and amino acids to support the maximum growth and the best condition to administer them. The information acquired in this work are the basis for future experimental plans.

.

Part 2:

Ion channels in touch sensation

SUMMARY

I spent part of my PhD program in Dr Bianchi's laboratory (Department of Physiology and Biophysics) at University of Miami Miller School of Medicine. In these months, I focused my research on ion channels involved in touch sensation.

The sense of touch is one of the most important senses in our everyday life. It is also a necessary component of human physical and mental development. However, it is the least understood of our senses. Touch sensation is elicited by mechanical stimuli such as stretch pressure thought to activate mechanosensitive ion channels. These channels are expressed in mechanosensory cells that convert forces into biochemical signals. However, the molecular identity of these channels has been elusive for a long time. Animal models such as C. *elegans* and *Drosophila melanogaster* have allowed to discovery of genes directly involved in touch sensation. These genes encode ion channel subunits belonging to two different families: DEG/ENaC (**Deg**enerins in C. *elegans* and the related mammalian **E**phitelial amiloride-sensitive **Na**$^{+}$ **C**hannel) and TRP (Transient Receptor Potential). Recently, the mammalian pannexins have been also shown to be sensitive to mechanical forces. However, their involvement in touch sensation has not been demonstrated.

In my study, I focused on two different channels belonging to the ENaC subfamily expressed in glia cells, which may be involved in mechanosensation: DELM-1 (**deg**enerin-**l**ike channel **m**echanosensory linked-**1**) and DELM-2 (**deg**enerin-**l**ike channel **m**echanosensory linked-**2**). These channels may have a role in touch sensation because they are expressed in socket glia cells surrounding neurons that are required for the nose touch response. Moreover, their knock-out causes nose touch insensitivity. To clarify whether they are functional channels and if they mutually interact, I tagged DELM-1 and DELM-2 with GFP in C-termini and I investigated their expression through immunochemistry analysis. Future work will be aimed to determine whether DELM-1 and DELM-2 exist as a multimeric channel complex *in vivo*.

I also started investigating the role of UNC-7 channel in *C. elegans* touch sensitivity. UNC-7 is an "innexin" subunit homologous to mammalian pannexins that is expressed in the invertebrate nervous system. In C. *elegans* there are 25 genes that encode for innexins, however little is known about their functional role. GFP expression studies show that *unc-7* is expressed in touch sensing neurons in *C. elegans*. Based on the mechanosensitivity of some pannexins and *unc-7* expression pattern, we hypothesized that UNC-7 maybe involved in mediating touch sensation. To test this hypothesis, I conducted patch clamp recording on *C. elegans* touch neurons cultured *in vitro* from wild-type (WT) and *unc-7(e5)* null mutants, and identified by expression of GFP under the touch

specific promoter *mec-4*. MEC-4 is a well-characterized DEG/ENaC sensory channel that is expressed in touch neurons and that mediates gentle touch sensation. Applying negative pressure to a touch neuron patch of membrane in inside-out configuration, I observed the activation of mechanosensitive channels. These channels are observed also in *mec-4* knock-out animals and thus they are not MEC-4. The hypothesis is that this channel may be UNC-7 and maybe required for responses to touch.

To test this hypothesis I also performed dye uptake assays in touch neurons cultured from WT and *unc-7(e5)* mutants. Indeed, innexins are large channels that are permeable to small molecules such as the dye ethidium bromide (EtBr) and such as pannexins, are inhibited by carbenoxelone (CBX).

Chapter 1:

INTRODUCTION

INTRODUCTION

1.1 TOUCH SENSATION

The sense of the touch is one of the most vital of our senses. It is essential for interaction with the outside world and it is especially important in organisms that cannot use other sense such as vision to perceive the environment. Most of our activities such as eating, drinking, driving, writing, walking, communicating would not be possible without touch. Loss of touch sensation leads to a serious inconveniences: we could not feel noxious stimuli, keep objects in our hands or coordinate fine movements. Furthermore it has been shown that touch is a significant element in human physical and mental development and it plays a key role in healthy development of preterm babies (Beachy, 2003). Despite touch being essential for all organisms, it is the least understood of our senses.

Touch sensation is elicited in response to mechanical forces like as a stretch or pressure. The mammalian organelles that detect touch are called mechanosensors. These are the Pacinian corpuscles (PCs) that sense vibration, the Meissner's corpuscles essential to the sense light touch, the Ruffini's endings that detect pressure and stretch and the Merkel receptors important for fine shape and texture discrimination. It is thought that mechanical forces are sensed by the cells through activation of mechano-sensitive channels. The genes encoding these ion channels have been very difficult to clone dues to their low level of expression and the paucity of cells that constitute the mechanosensors. Significant advancement of our understanding of mechanosensitive ion channels has come from the analysis of touch insensitive mutants in model organisms such as *Caenorhabditis elegans* and *Drosophila*.

1.2 CAENORHABDITIS ELEGANS

C. *elegans* is a powerful model organism to study the molecular and cellular bases of touch. Its genome, metabolic and biosynthetic pathways are highly conserved with vertebrates (Riddle et al., 1997). C. *elegans* is a powerful model organisms for several reasons: 1) it is small (1 mm long adult), 2) it has a rapid life cycle (3 days at 25° C), 3) it has a short life-span (2 weeks), 4) it has large number of offspring (>200), 5) it is easy to grow in a laboratory, 6) its anatomy is simple, 7) it has a small genome, and 8) transparent skin and eggshell that allow direct visualization of cellular morphology by microscopy (Fig. 1.1). *C elegans* is a hermaphrodite (XX), which is an advantage

when generating and maintaining mutant stocks. Males are also present (XY 1-2% of the population) and can be used in crosses to generate double or triple mutants.

C. *elegans* is cultured on Petri dishes or in liquid medium in the laboratory using *E. coli* as a food source.

C. *elegans* has not sense of sight, so it perceives the environment through chemosensation and mechanosensation. C. *elegans* responds to different types of mechanical stimuli: **1)** head withdrawal reflex: when touched on the ventral or dorsal side of the nose, *C. elegans* responds by turning the head away from the stimulus. **2)** Nose touch response: after a head collision with an object (for example an eyelash), C. *elegans* changes direction retracting its body, backing–up and moving away (Kaplan and Horvitz, 1993); (Driscoll and Kaplan, 1997). **3)** Tap response**:** *C. elegans* moves forward or backward when the researcher taps a Petri dish producing a diffuse mechanical stimulus (Rankin, 1991); Driscoll M. and Kaplan J., 1997)**. 4)** Gentle touch response: when gently touched by an eyelash hair on its head or tail, *C. elegans* reverses its direction. **5)** Harsh touch response: C *elegans* responds to harsh touch exerted for example by a metal wire moving away from the stimulus (Chalfie and Sulston, 1981).

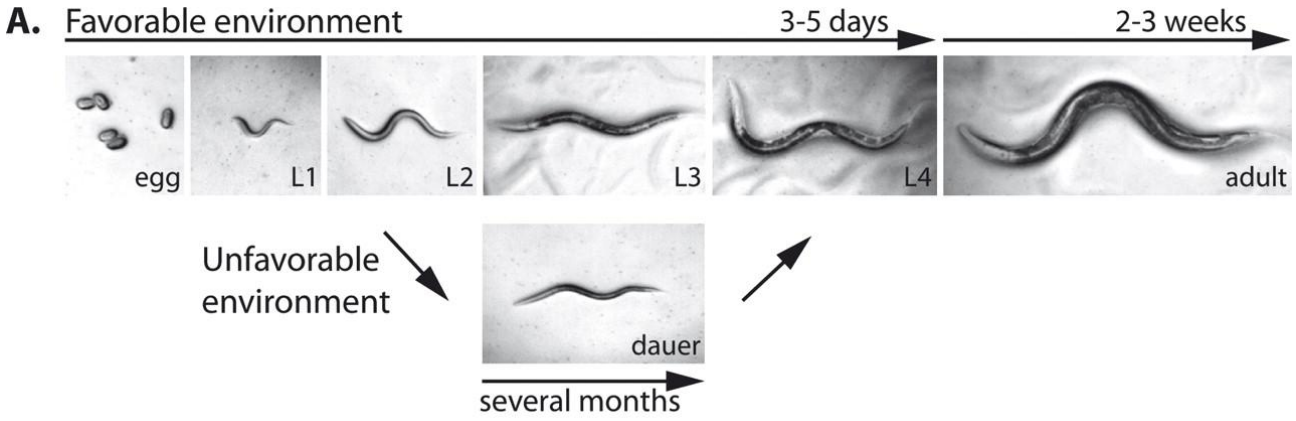

Figure 1.1. Schematic representation of *C. elegans* life cycle. It takes 3 days for *C. elegans* to develop from embryo to adult. In these 3 days *C. elegans* goes through 4 larval stages. Adult *C. elegans* lives 2-3 weeks. In unfavorable condition such as limited food, high temperature, *C. elegans* enters a specialized larval stage called dauer that can survive several months (Fielenbach and Antebi, 2008).

1.3 GENTLE TOUCH RESPONSE

When touched with a gentle stimulus such as an eyelash hair either on the anterior or on the posterior body, *C. elegans* reverses its direction. If touched on the posterior end, the worm will move forward, while if it is touched on the anterior end it will move backward (Chalfie and Sulston

1981; (Chalfie et al., 1985). There are only six touch receptor neurons involved in the gentle touch sensation. These neurons have been identified by laser ablation studies, in which each single neuron was killed by a laser beam (Chalfie et al., 1985). In the anterior part of the body AVM (**A**nterior **V**entral **M**icrotubule cell) and ALM neurons (**A**nterior **L**ateral **M**icrotubule cell) left and right mediate response to touch to the anterior part of the body. In the tail PLM left and right neurons (**P**osterior **L**ateral **M**icrotubule cells) are required for touch sensitivity to the posterior part of the body. The sixth neuron is called PVM (**P**osterior **V**entral **M**icrotubule cell) and it is located just anterior to the PLM neurons. PVM looks identical to other touch neurons but it does not mediate a gentle touch response by itself and probably it is required to some other behavioral response, for example the response to harsh touch (Fig. 1.2)(Bianchi et al., 2004). In a genetic screen on touch insensitive *C. elegans*, 16 genes have been isolated that are required for touch sensation. These genes were labeled *mec* because when mutated they produced mechanosensory abnormal behavior in the worm. Among these 16 genes, there are two channel subunits belonging to the DEG/ENaC family, that were named MEC-4 and MEC-10.

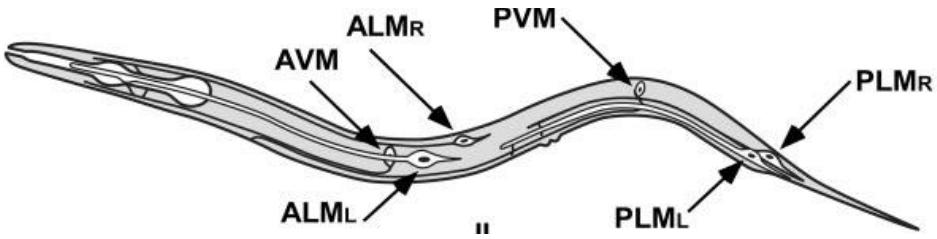

Figure 1.2. Schematic drawing that shows the position of the six neurons involved in gentle touch. (Bianchi, 2007).

1.4 DEG/ENaC CHANNELS IN TOUCH SENSATION

DEG/ENaCs channels are expressed in many organisms ranging from *C. elegans* to human and they have been involved in sensory perception including touch sensation (Price et al., 2001), thermosensation (Askwith et al., 2001), proprioception (Tavernarakis et al., 1997), pain sensation (Chen et al., 2002) and vascular and visceral mechanotrasduction (Drummond et al., 1998).

All DEG/ENaC channels show a common topology: they are 550-950 amino acid-long transmembrane proteins consisting of two transmembrane helices (MSDI and MSDII), short intracellular N- and C- termini and a large extracellular cysteine-rich domain (Jasti et al., 2007). The C- terminus has been implicated, in all organisms, in regulating channel trafficking to and from the plasma membrane.

DEG/ENaC channels are heteromeric complexes that include multiple DEG/ENaC subunits and can be divided into two groups: the epithelial, amiloride-sensitive, voltage-indipendent Na^+ channels (ENaCs), and the acid-sensing ion channels (ASICs). ENaC channels mediate Na^+ readsorbition in renal, intestinal and lung epithelia (Chalfie, 1993); (Canessa et al., 1995). ASICs channels are expressed in neurons and play a role in touch sensation (Fig. 1.3) (Wemmie et al., 2002); (Wemmie et al., 2003).

One of the best studied DEG/ENaC in *C. elegans* is the MEC touch-transducing channel complex, which includes DEG/ENaC subunits MEC-4 and MEC10, stomatin-related MEC-2 and paraoxonase-related MEC-6 (Driscoll and Chalfie, 1991); (Bianchi and Driscoll, 2006b). MEC-4 and MEC-10 are homologous proteins (48% identity) related to subunits of the ENaC channels in mammals (Canessa et al., 1994b); (Huang and Chalfie, 1994); (Hong and Driscoll, 1994). While MEC-4 is encoded only in six touch neurons, MEC-10 is expressed in six touch receptor neurons and in four other neurons (FLPs and PVDs) that function in the harsh touch and /or stretch sensitive response behaviors. Chalfie and colleagues have demonstrated that *mec-4* and *mec-10* mutants are touch insensitive showing that their touch sensory neurons are structurally normal and develop normally (Chalfie and Sulston, 1981). Goodman and colleagues showed that MEC-4 and MEC-10 expressed in *Xenopus* oocytes form a Na^+ selective channel complex. Moreover MEC-4 can form channels by itself, while MEC-10 alone does not conduct any currents (Goodman et al., 2002).

Recent studies have shown that DEG/ENaC channels are expressed in glia in mammals. For example Berdiev and colleagues showed expression of these channels in astrocytes and gliomas (Berdiev et al., 2003) and DEG/ENaCs expression has been demonstrated in both neurons and glia of rabbit retina (Brockway et al., 2002). However, virtually nothing is known about the role of DEG/ENaC channels in glia.

The Bianchi lab is using *C. elegans* to advance our understanding of the role of glial DEG/ENaC channels in the function of the nervous system. The Bianchi lab found that two novel DEG/ENaC subunits named DELM-1 (**deg**enerin-**l**ike channel **m**echanosensory linked-**1**) and DELM-2 (**deg**enerin-**l**ike channel **m**echanosensory linked-**2**) are expressed in glia associated with nose touch neurons in *C. elegans*. They also found that knock-out of *delm-1* or *deml-2* causes nose touch insensitivity. By expression in *Xenopus* oocytes, they showed that while DELM-1 is functional, DELM-2 is not. When DELM-1 and DELM-2 are co-expressed in the same oocyte, the activity of DELM-1 remains unchanged. My role in this project was to determine if DELM-2 is translated and transported to the cell surface in oocytes, to establish if lack of expression of DELM-2 currents in

oocytes is due to translation or trafficking problems, or is due to the fact that DELM-2 has a modulatory role, similarly to MEC-10 in the MEC channel complex.

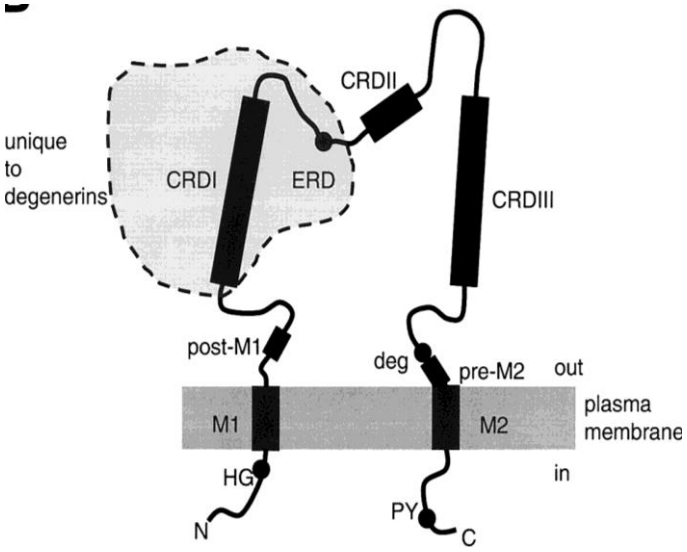

Figure 1.3. A schematic illustrating the structure of a typical DEG/ENaC channel subunit (Jasti et al., 2007).

1.5 HARSH TOUCH RESPONSE

When gentle touch neurons are killed by a laser beam, *C. elegans* still responds to probing with a platinum wire. This response is called the harsh touch response. The animal responds to anterior harsh stimulus starting backward movement while to the posterior harsh touch moving forward (Li et al., 2011). Laser ablation studies suggested that PVD, FLP and OLQ neurons are candidate harsh touch receptor neurons (Way and Chalfie, 1989). For example, animals in which PVD neurons are laser-ablated fail to respond to harsh touch to the central region of the body (Keane and Avery, 2003). Recent studies by Li and colleagues expanded these observations and identified neurons that mediate harsh touch response to other parts of the *C. elegans* body. Li and colleagues found that BDU and SDQR neurons mediate harsh touch to the right side of the body while FLP, ADE, AQR neurons mediate touch to the left. PVD and PVE neurons are needed for the harsh touch response in the posterior part of the body, and PHA and PHB mediate harsh touch to the anus. (Fig.1.4) (Li et al., 2011). Through patch clamp recordings Li and colleagues identified two family of mechanosensory channels involved in regulating harsh touch sensation in *C. elegans*: the ENaC family with the amiloride-sensitive channel MEC-10 and TRP family with TRP-4 (Li et al., 2011). These results suggests that harsh touch response is probably mediated by a different classes of ion channels. Laser ablation experiments performed by Way and Chalfie had also suggested that gentle touch neurons may participate to harsh touch sensitivity (Way and Chalfie, 1989).

Figure 1.4. *C. elegans* neurons that sense harsh body touch. A schematic illustrating the location of the sensory neurons required for harsh touch behavior. (Li et al., 2011).

1.6 INNEXIN UNC-7 IN C. ELEGANS

Innexins are homologous to mammalian pannexins which are channels that have been shown to function both as plasmamembrane ion channels and as gap junction hemichannels. In vertebrate and invertebrate, gap junctions are functionally conserved. The invertebrate pannexins are called innexins. The Innexins are oligomers of six identical or homologous subunits complexes between two neighboring cells (Fig. 1.5). Each hexamer complex is composed of proteins with four transmembrane domains coupled by two extracellular loops and one intracellular loop in addition to intracellular N and C-terminal amino acid chains. Pannexins and innexins have also two cysteine residues in each of their extracellular loops (Fig. 1.6)(Panchin et al., 2000). When they form gap junctions, they are constitutively open and they mediate communication between adjacent cells allowing passage of ions and small molecules (e.i cAMP) (Norman and Maricq, 2007). When they form plasmamembrane channels, they conduct ions and ATP and they have been shown to be activated by mechanical forces. Both pannenixs and innexins are permeable to small moleculaes including dyes and are inhibited by carbenoxelone (CBX) (Bao et al., 2004).

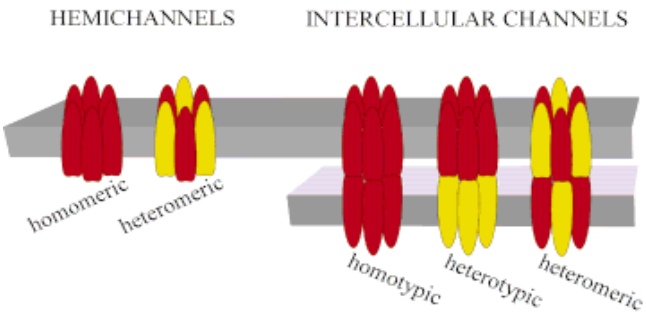

Figure 1.5. Structure of a typical gap junction. Six subunits oligomerize to form a hemichannel. Hemichannels in adjacent cells, which may be homomeric or heteromeric, form a functional intracellular channel. This channel is homotypic when the hemichannels are identical, and heterotypic or heteromeric if the hemichannels are formed by different subunits (Phelan and Starich, 2001)

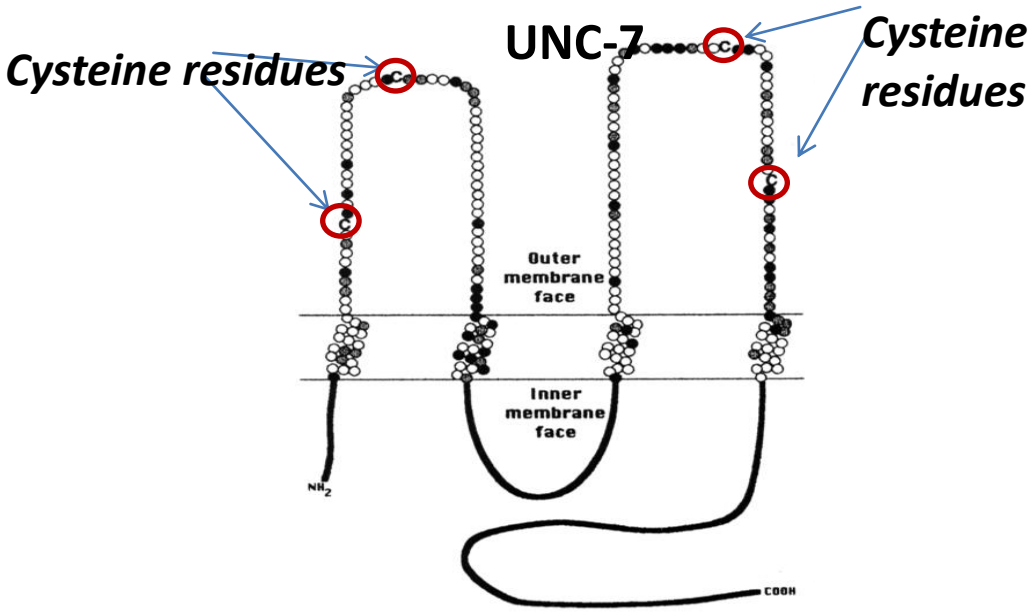

Figure 1.6. Schematic representation of an innexin. Innexins such as UNC-7 consist of four transmembrane domains, cytoplasmatic N- and C- termini, two extracellular and one intracellular loops. Many innexins including UNC-7 have two cysteine residues located in each extracellular loop (Starich et al., 1993).

Innexins were first identified in *Drosophila* and C. *elegans* (Phelan and Starich, 2001). Altun and colleagues showed that *C. elegans* innexins are expressed in many tissues throughout development and are involved in embryonic development, oogenesis, egg laying, excretion and locomotion (Altun et al., 2009). Nineteen of the 25 innexins genes of *C. elegans* are found in the nervous system. Gap junctions expressed in the mature brain, play critical roles in many physiological events such as neuronal plasticity (Landisman and Connors, 2005), REM sleep (Garcia-Rill et al., 2008) and long range calcium wave propagation (Giaume and Venance, 1998). Moreover gap junction are involved in pathological processes such as hypoxia-ischemia response (Talhouk et al., 2008) and epilepsy (Nemani and Binder, 2005). In *C. elegans*, innexins UNC-7 and UNC-9 are widely expressed and contribute to the formation of gap junctions in most neurons, glia cells (Meier and Dermietzel, 2006) and in some muscle cells (Yen and Saier, Jr., 2007). UNC-7 is expressed also in many interneurons such as AVB (Bouhours et al., 2011) and in some sensory neurons (including PVD, SDQ and PLMs) that are involved in harsh and gentle touch sensation. Because mammalian homologous channels pannexins are mechanosensitive, *unc-7* expression pattern rises the possibility that UNC-7 may mediate touch sensation.

Using northern analysis Starich and colleagues showed that mRNA of UNC.7 is present throughout development with highest expression during the early larval stages (L1-L3 larvae)(Starich et al.,

1993). The important role of UNC-7 in the neuromuscular system is underscored by the finding that *unc-7* loss-function causes defects in the neuromuscular system, such as an uncoordinated locomotion most apparent when the animals try to move forward (Fig. 1.7)(Yen and Saier, Jr., 2007), hyperactivity of the egg-laying circuit (Starich et al,;1993), and strong resistance to aldicarb, a cholinesterase inhibitor (Yeh et al., 2009).

Bouhours and colleagues recently also showed that innexin UNC-7 may form hemichannels that regulate C. *elegans*' neuronal activity (Bouhours et al., 2011).

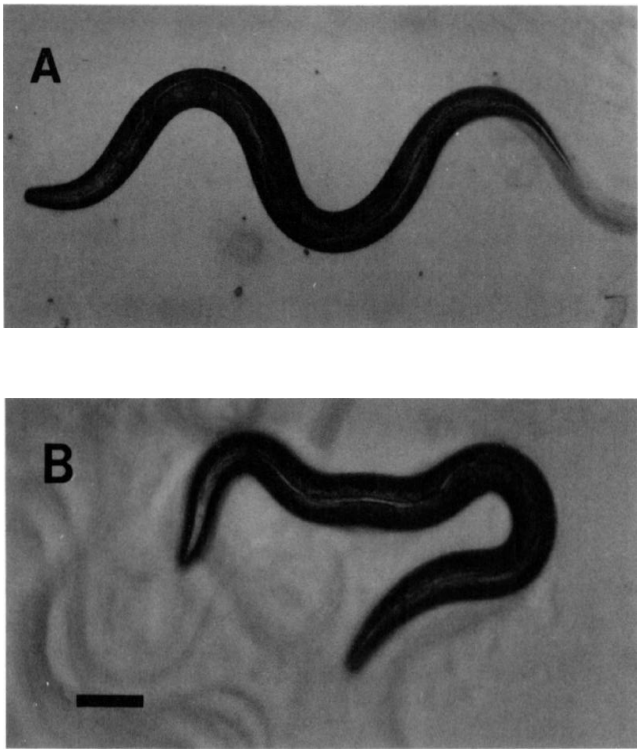

Figure 1.7. A) A typical WT worm on agar surface; B) mutant *unc-7(e5)* shows uncoordinated movement. Bar indicate 0.1mm (Starich et al,; 1993).

1.7 AIMS OF PROJECT

The sense of touch is essential for human interaction with the environment. Two ion channel families, the DEG/ENaC and the superfamilies TRPs (Transient Receptor Potential) channels have been implicated in touch sensation in both vertebrate and invertebrate. Furthermore both pannexins and innexin channels have been shown to be mechanosensitive. While in the Bianchi's laboratory I worked on both DEG/ENaC channels and innexins.

The project on DEG/ENaC channels focused on two novel *C. elegans* subunits called DELM-1 (**deg**enerin-**l**ike channel **m**echanosensory linked-**1**) and DELM-2 (**deg**enerin-**l**ike channel **m**echanosensory linked-**2**). These channels are expressed in OLQ and IL1 glia cells surrounding neurons that are required for the nose touch response. The Bianchi lab found that DELM-1 and DELM-2 are needed for nose touch response. Since DELM-1 and DELM-2 are expressed in the same cells and DEG/ENaC subunits can come together to form heteromultimers, we hypothesized that they may form a heteromultimeric channel.

My role in this project was to determine whether DELM-1 and DELM-2 form a heteromultimer. Thus, I designed two sets of experiments aimed at establishing whether DELM-1 and DELM-2 interact with each other. In the first experiment I coexpressed DELM-1 and DELM-2 in *Xenopus* oocytes and compared current properties with currents recorded from oocytes injected with DELM-1 alone. In the second experiment I fused DELM-1 and DELM-2 C-termini with two halves of GFP and made transgenic animals expressing these two constructs. If the two subunits interact *in vivo*, then GFP will be reconstituted and cells will fluoresce. In the first experiment, I found that DELM-1 currents were not changed by co-expression with DELM-2. To establish if DELM-2 is translated in oocytes and transported to the cell surface I tagged DELM-2 with GFP at the C-terminus, injected it into oocytes, sectioned them and analyzed surface fluorescence.

The project involving the study of innexins focused on a novel mechanosensitive channel that the Bianchi' laboratory recently identified in touch sensing neurons in C. *elegans*. My role in the project was to establish whether this channel is encoded by the innexin gene *unc-7*.

To test this hypothesis I conducted two types of experiments: 1) patch clamp recordings and 2) dye uptake experiments on *C. elegans* touch neurons cultured *in vitro* and identified by expression of GFP under the touch specific promoter *mec-4*.

Chapter 2:

METHODS

METHODS

2.1 CAERNORHABIDITIS ELEGANS CULTURE

C. elegans was grown on petri dishes containing NGM (nematode growth medium). NGM is composed of: NaCl, Agar, Bactopeptone, Streptomycin, $CaCl_2$ 1M, $MgSO_4$ 1M, KP Buffer 5M at pH 6.0, Cholesterol 5mg/ml, Nystatin 10mg/ml. All media and reagent used for *C. elegans* maintenance and manipulation were sterilized by autoclaving. The animals fed on *E. coli* bacteria OP50- and are generally stored at 20°C. Subculturing (chunking) of worm is done by cutting a small square of agar from a starved or crowded NMG plate and transferring it to a freshly seeded NMG plate facing down, so the worms can crawl out faster and find food source easier. Chunking in not recommended if the worms have to grow slowly. In this case the best procedure is picking, in which a thin platinum sterilized wire pick is used to transfer only few worms to a fresh plate.
Plates are stored upside-down in closed boxes to reduce condensation and contamination.

2.2 GFP REPORTER CONSTRUCT

GFP (Green Fluorescent Protein) is a protein originating from jellyfish *Aequorea Victoria* that is 230 amino acids in length and that emits fluorescent green light at 509 nm when excited by UV-light at 395 mn. The light emission is easily detected using fluorescent microscopy. GFP can also be used to study gene expression *in vivo* C. *elegans*. It is facilitated by the transparent body of the worm. In our experiments we built construct in which GFP was fused at the C- terminus of the *delm-2* cDNA to produce DELM-2 channel protein tagged with GFP.

2.3 PGEM-DELM-1-GFP AND PGEM-DELM-2-GFP CONSTRUCTS

2.3.1 Polymerase chain reaction (PCR) with gene specific primers

The PCR products, DELM-1, DELM-2 and GFP, were designed to be about 1.8Kbp and 0.7Kbp respectively and in such way that the stop codon of *delm-1* and *delm-2* genes was removed in order to have the channel-coding sequences in frame with GFP once subcloned. This method was based on fact that longer constructs would increase the probability of mutations into PCR products, since the mismatches are introduced by Taq polymerase at a frequency of 1 every 1000 nucleotides.
The specific primers designed for each one of the genes of interest are listed below:

DELM-1 primers:

- FORWARD : GGATCCatgaattcgcctcctatatcc
- REVERSE: GGTACCatatttttgtaaatttgacgatttttcggattttcctttgca

DELM-2 primers:

- FORWARD : GGATCCatgattccaacaatatcgaagccaaaaacc
- REVERSE: GGTACCgatcaaaacgctccttgatccgacg

GFP primers:

- FORWARD: GGTACCatgagtaaaggagaagaacttttcactggag
- REVERSE : AAGCTTttatttgtatagttcatccatgccatgtgtaatc

BamHI (green) and KpnI (red) restriction sites were introduced into DELM-1 and DELM-2 primers, while KpnI(red) and HindIII (yellow) restriction sites into GFP primers so that the final DNA fragments could be inserted in the pGEM oocytes vector.

The PCR reaction was prepared with cDNA of interest, forward and reverse primers, dNTPs, Taq polymerase HiFi, Taq polymerase buffer, MgSO4, sterile water. To amplify cDNA six steps were set up on the PCR machine for each one of gene of interest (Fig. 2.1). The steps a) and b) are at 94°C to denature DNA helices. The third step (c) is at a temperature which promotes the annealing of the primers to the DNA. In this step the temperature can vary depending on the length of the primers and on their sequence. The step d) is for DNA elongation and its temperature dpending on the polymerase used. Steps b),c),d) were repeated for 40 cycles prior to proceeding to step e). The last two step consisted of a seven minute elongation at 68°C to ensure that all sequences were replicated (e) and an indefinite storage temperature at 12°C (f)

DELM-2 PCR

a) 94° C x 30''
b) 94° C x 30''
c) 58° C x 30''
d) 68° C x 2'30''
e) 68° C x 7'
f) 12° C indefinitely

40

GFP PCR

a) 94° C x 30''
b) 94° C x 30''
c) 58° C x 30''
d) 68° C x 1'10''
e) 68° C x 7'
f) 12° C indefinitely

DELM-1 PCR

a) 94° C x 30''
b) 94° C x 30''
c) 58° C x 30''
d) 68° C x 2'20''
e) 68° C x 7'
f) 12° C indefinitely

40

Figure 2.1. PCR protocols to amplify *delm-1, delm-2* and *gfp* genes. a) initial denaturation step; b) denaturation step; c) annealing step; d) elongation step with Taq polymerase; e) unfinished elongation step; f) step of DNA storage. Steps b,c and d were repeated for 40 cycles.

2.3.2 Gel extraction of PCR DNA fragments.

After PCR reaction, the samples were separated on electrophoresis gel. Using the QIAquick gel extraction kit, DNAs were extracted. The PCR products were cut from the gel and put in a 1.5 microfuge tube. To this tube an amount of *gel solubilization solution* equal to three times the weight of the samples was added. The gel of each one of DNA of interest was then allowed to melt in a 60°C heating block for ten minutes. One ml of isopropanol was then added to the samples. The mixtures obtained were then applied to a QIAquick spin columns pre-treated with *column preparation solution* and spin-dry for one minute at 12.000 rpm with the aim of bind the DNA to the column. The flow-through was removed from the collection tube. To obtain a completely purified DNA, 700 µl of washing solution were added to the columns. The columns were then placed in a second fresh microfuge tube and 25 µl of sterile water were applied to the center of the column and spin-dry and left to rest for two minutes. The samples were then spin-dry at 12,000 rpm for 2 minutes to collect DNA at the bottom of the microfuge tube.

2.3.3 Topo ligation

DELM-1, DELM-2 and GFP DNA were cloned into PCR2.1 topo vector for amplification and sequencing. 0.5 to 4 µl of DNA were mixed gently with 2 µl of PCR2.1 vector and stored overnight at 4^{o}C.

In the TOPO kit the ligation is achieved through the single 3'-thymidine (T) overhangs that exist in the PCR2.1 vector. The thymidine ends of the vector are there because *Taq* polymerase has a nontemplate-dependent terminal transferase activity that adds single deoxyadenosine (A) to the 3' ends of the PCR products. These T and A overhangs allow the efficient ligation between PCR product and PCR 2.1 vector. The vector also contains a covalently bound Topoisomerase I enzyme that participate to the formation of a phosphodiester backbone between the T overhang and the next nucleic acid of the PCT products.

2.3.4 Competent cells transformation with TOPO-DELM-1, TOPO-DELM-2 and TOPO-GFP and sequencing

TOPO-DELM-1, TOPO-DELM-2 and TOPO-GFP were used to transform competent cells. 2 µl of each one of the DNA were added to a 50 µl of TOP10 competent cells and allowed to rest 30 minutes on ice to facilitate bond between DNA and the bacteria cells. The cells were heat shocked at 42°C for 45 seconds and put in ice 2 minutes. These steps are necessary to create holes through which the DNA is incorporated into the bacteria cells. 250 µl of SOC solution were added to the cells that were then incubated at 37° C in a shaker for one hour to increase the growth of bacteria cells. After one hour, cells were spread on LB plates containing ampicillin and X-gal for white/blue colony selection and incubated at 37° C over night. Topo vector contains a gene that make cells ampicillin resistant.

The day after, colonies were picked and grown in 2ml LB+ampicillin at 37°C over night.

Plasmid DNA was extracted using Quiagen Kit with the following procedure: 1,5 ml of bacteria was collected in a 2ml microfuge tube and span at 4,000 rpm for ten minutes. The LB medium was removed and the pellet at the bottom of the microfuge tube was resuspended in 100 µl of P1 solution. 200 µl of P2 solution were added to the mixture that was gently mixed. 150 µl of P3 buffer was added to the samples and samples were centrifuged at 13.000 rpm for 15 minutes. The supernatant was collected in a new centrifuge tube and mixed with 1 ml of ethanol. The mixture was centrifuged for 15 minutes at 13,000 rpm. The supernatant was removed and the precipitated DNA was allowed to dry for a few minutes on the bench. DNA was then resuspended in 70 ul of water.

Two µl of DNA was digested with EcoRI enzyme to check whether the vectors had successfully ligated the PCR products. The samples were then purified using Quiagen kit (Genelute PCR clean up kit) following standard procedures. Two to four samples were then sent for sequencing using M13 forward and reverse primers. This step was necessary to verify that our PCR products did not have any mutations, which could lead to non functional DELM-1, DELM-2 and GFP proteins.

2.3.5 Preparation of the GFP construct

Sequence-verified clones (DELM-1,DELM-2 and GFP) were removed from TOPO vector and subcloned into pGEM vector. TOPO vector containing PCR products was digested with the appropriate enzymes, BamHI and KpnI for DELM-1 and DELM-2 and KpnI and HindIII for GFP. Digestion mixes were separated on agarose gels, and appropriate bands were excised and purified.

Ligation reactions were then set up over night. The ligation reactions contained: pGEM vector, DELM-1, DELM-2 and GFP DNA, T4 ligase, the enzyme necessary for the ligation and T4.
The ligation products were then used to transform TOP10 competent cells. Colonies were picked and grown at 37 °C over night. Consequently, DNA was extracted using Qiagen miniprep kit as describe above. Two µl of DNA sample were digested with BamHI and KpnI and HindIII to ensure that pGEM vector had ligated DELM-1, DELM-2 and GFP inserts. The right samples were then purified with Qiagen kit.

2.3.6 Preparation of cRNA for injection into Xenopus oocytes

pGEM-DELM-1-GFP and pGEM-DELM-2-GFP constructs were linearized with NheI and checked for size, integrity and concentration by gel electrophoresis. Transcription reaction was performed with linear template DNA, enzyme mix, reaction buffer, NTP/CAP and nuclease free water at 37°C for 2h. One µl of TurboDnase was added to the mixture at the end of the reaction to denaturate the DNA template.
The samples were purified with RNeasy MinElute Clean up kit (Qiagen kit) with the following procedure: each sample was adjusted to a volume of 100 µl with RNase- free water. 360 µl of RTL buffer and then 250 µl of 96-100% ethanol were added to the sample. 700 µl of the sample were applied to an RNeasy MinElute Spin Column and centrifuged at 10,000 rpm for 1 minute. The flow-through was discarded and 500 µl of buffer RPE were applied two times to the column spin at 10,000 rpm for 1 minute. The flow-through was removed again and the empty column was centrifuged for two minutes. The samples were eluted with 25µl of RNase free water. To check the size and the concentration, the samples were run on an agarose/formaldhyde gel.

2.4 pCE-BIFC-VN173 AND pCE-BIFC-VC155 CONSTRUCTS

I subcloned DELM-1 and DELM-2 cDNA into two Venus cloning vectors pCE-BiFC-VN173 and pCE-BiFC-VC155. If the DELM-1 and DELM-2 interact, then the full GFP protein Venus will be reconstituted and the cells in which DELM-1 and DELM-2 are expressed (socket glia) will be fluorescent. The cloning of DELM-1 and DELM-2 into Venus vectors was performed following the procedures describe above for pGEM vector constructs.
The primers used for each one of the constructs were:

- DELM-1 Venus primers:
  delm-1 C-terminus is fused with Venus C terminus (pCE-BiCF-VC155)

Forward containing PlmI: cacgtgtgcaactccacccc

Reverse delm-1 minus stop plus VC155 sequence:

CTGGAACATCGTATGGGTACATctaatatttttgtaaatttgacgatttttcggattttcctttg

Forward VC155 start plus delm-1 sequence:

ccgaaaaatcgtcaaatttacaaaaatattagATGTACCCATACGATGTTCCAGATTACG

Reverse VC155 containing FspA1: atgcgcacttacttgtacagctcgtccatgcc

- DELM-2 Venus primers:

  <u>delm-2 C-terminus fused with Venus N-terminus (pCE-BiCF-VN173</u>)

  Forward containing BstEII: ggtaaccagttttcggcgagagc

  Reverse delm-2 minus stop plus VN173 sequence:

  AGCTTCTGCATTGATGCCATtcaaaacgctccttgatccgacg

  Forward VN173 start plus delm-2 sequence:

  gtcggatcaaggagcgttttgaATGGCATCAATGCAGAAGCTGATCTC

  Reverse VN173 containing BsaAI: tacGTGTTACTCGATGTTGTGGCGGATCTTGAAG

The steps followed to amplify each one of gene of interest are summarized in the Figure 2.2.

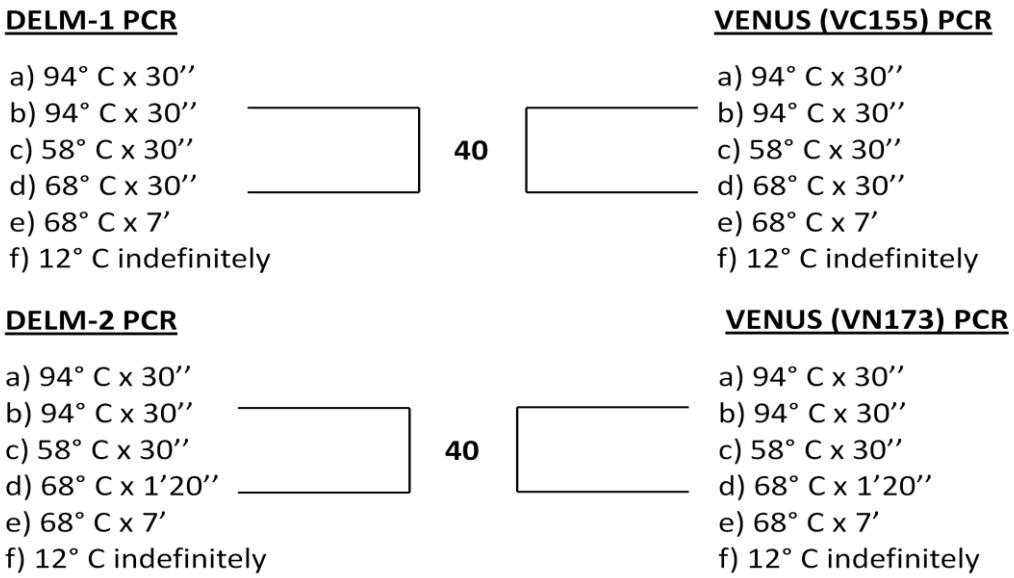

Figure 2.2. PCR protocols to amplify *delm-1*, *delm-2* and *venus (VC155 and VN173)* genes. a) initial denaturation step; b) denaturation step; c) annealing step; d) elongation step with Taq polymerase; e) unfinished elongation step; f) step of DNA storage. Steps b,c and d were repeated for 40 cycles.

2.5 OOCYTES INJECTION AND CRYOSECTIONING

In our experiments we used oocytes from *Xenopus laevis* ovaries that we acquired from NASCO. Oocytes were dissected by 2 hour collagenase treatment (2mg/ml in Ca^{2+} -free OR2 solution). Stages V-VI oocytes were manually defolliculated after selection. Oocytes were incubated in OR2 solution (82.5 mM NaCl, 2.5 mM KCl, 1 mM CaCl2, 1 mM MgCl2, 1 mM Na2HPO4, 0.5g/l polyvinyl pyrolidone and 5mM HEPES pH 7.2) containing penicillin and streptomycin (0.1 mg/ml) and 2mM Na-pyruvate for one day prior to injection. Oocytes were then injected at the concentration of 5ng/oocyte for a final volume of 69 nl of cRNA.

Injection was performed with Nanojet automated oocyte injector (Drummod Scientific, Broomall, PA) using glass capillaries pulled with a Sutter P-97 pipette puller. After injection, oocytes were incubated in OR2 solution at 20°C for 3 day before cryosectioning.

Three days after injection I prepared the oocytes for cryosectioning. I placed them in plastic molds, covered them with tissue freezing medium and incubated them over night at -20^{o}C. The following day I sectioned them using a cryostat.

2.6 GENETIC CROSS

In order to perform electrophysiological experiments on *unc-7(e5)* touch neurons, I needed to be able to recognize touch neurons of this mutant in culture. To do so, I transferred the *pmec-4::gfp* transgene that labels touch neurons with GFP to the *unc-7(e5)* mutant strain by genetic cross. I started the cross by mating *pmec-4::gfp* males with *unc-7(e5)* mutant hermaphrodites. Under standard conditions, males are only 1-2% of the total population. To obtain a larger number of males animals can be subjected to stressful conditions such a heat shock. I thus incubated L4 animals at 37 °C for 1 hour and allowed to self reproduce at 20°C. To set up the cross I transferred 15 *pmec4::gfp* males to a plate containing only 2 *unc-7(e5)* hermaphrodites. The plate had a small patch of food to maintain males and hermaphrodites close to each other and thus increase the chances of mating. After a few days I obtained the F1 generation. I picked 10 F1 fluorescent worms and I allowed them to self reproduce for another generation. Then I picked 40 fluorescent and uncoordinated F2 animals from 2 separate F1 plates. Since the allele distribution follows the

Mendelian laws, I expected that 1/4 of the animals picked would be homozygote for both *unc-7(e5)* mutation and *pmec-4::GFP*. To select for these homozygote animals, I waited until these F2s produced progeny and I kept plates in which all animals were both fluorescent and uncoordinated.

2.7 CULTURE OF EMBRYONIC C. ELEGANS CELLS

C. elegans embryonic cells were cultured from eggs of young gravid adults by removing the eggshells using a combination of enzymatic digestion and manual dissociation. Using this protocol differentiation of the major lineages and neuronal processes were observed in culture. To obtain a large quantity of gravid adult worms, I transferred them from starved plates to 10 cm 8P plates (NaCl, bactopeptone, agar, cholesterol, CaCl2 1 mM, KP buffer, MgSO4 1 mM) on a Na22 bacteria diet (grown overnight in 2XYT media pH 7.0 composed by tryptone, yeast extract, NaCl), a rich food source. After a few days I started the isolation of eggs. I collected the gravid adults worms in 50 ml tubes and I pelleted them by centrifugation at 1200 rpm for 15'. I then washed with water and repelleted the worms three times to eliminate the bacteria. I lysed the worms using a solution containing fresh Chlorox and 10 N NaOH. Released eggs and worm carcasses (Figure 2.3A) were then washed three times with sterile egg buffer (NaCl 118 mM, KCl 48 mM, $CaCl_2$ 2 mM, $MgCl_2$ 2 mM, Hepes 25 mM, pH 7.3, 340 mOsm). To separate the eggs from the carcasses I resuspended them in 30% sucrose in egg buffer and subjected them to centrifugation at 1200 rpm for 15 minutes. Eggs were collected from the supernatant (carcasses end up in the pellet) and washed three times with sterile egg buffer. Pelleted eggs were resuspended in 2 mg/ml chitinase in egg buffer and rocked for 30 min at room temperature. Chitinase is an enzyme that lyses the eggshells and functions better at acid pH (Kim et al., 2003). Figure 2.3B shows a digested eggshell. After chitinase treatment I added fresh complete medium (L-15 culture medium from Gibco, Fetal Bovin Serum, sucrose, penicillin/streptomycin 1:100) to stop the effect of the enzyme and I dissociated the cells using a syringe equipped with needle. I aspirated the suspension and released it back into the plate a couple of times and I checked for the presence of dissociated cells under the microscope (Figure 2.3D).

I filtered the suspension through a sterile 5 µm Durapore filter (Millipore) running other 3-4 ml of L-15 complete medium. Then I plated the cells on glass coverslips previously coated with peanut lectin 0.5mg/ml to increase the adhesion of the cells at the bottom of the wells. Cells must adhere to the substrate in order to differentiate (Bianchi and Driscoll, 2006a).

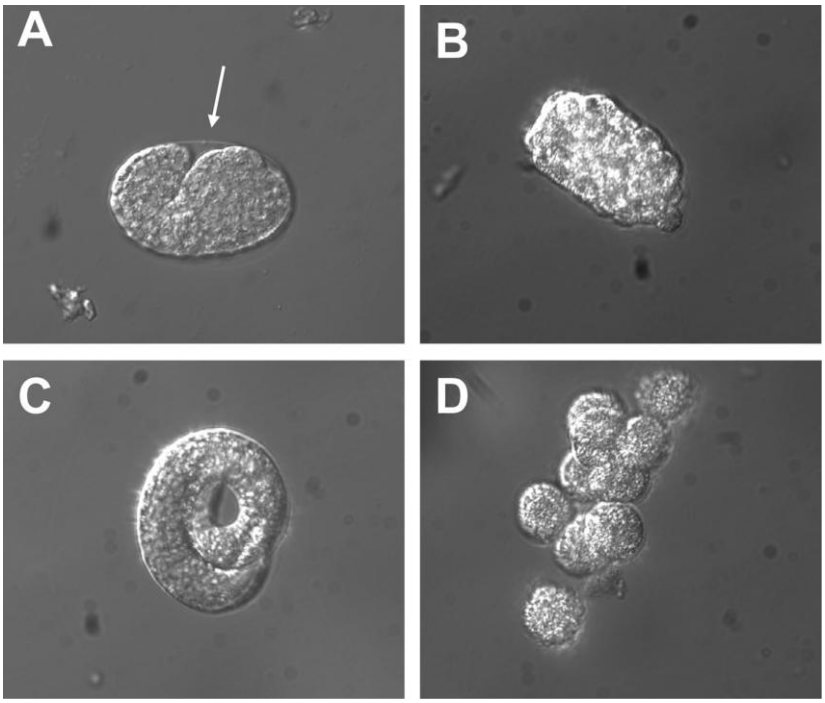

Figure 2.3. Pictures of C *elegans* eggs before and after chitinase digestion. **A)** Picture of an egg before chitinase treatment. The arrow shows the transparency of the eggshell around the embryo. **B)** An egg treated with 2mg/ml of chitinase for 25 minutes. The eggshell now has been completely digested. **C)** Three-fold embryo released from the eggshell. **D)** Picture of embryonic cells dissociated by chitinase treatment (Bianchi and Driscoll, 2006a).

2.8 PATCH CLAMP OF C. ELEGANS NEURONS

In 1976 Sakmann and Neher introduced the patch clamp technique. The patch clamp technique can be used in four different configurations: a) *cell-attached* in which the tip of the pipette is sealed with the plasma membrane of the cell and the activity of channels underneath the pipette tip is studied; b) *whole cell* in which the membrane patch underneath the tip of the pipette is broken to gain electrical access to the whole cell and thus study the activity of all the channels on the plasma membrane; c) *inside-out* in which the pipette is pulled away from the membrane from the cell attached configuration. This configuration allows to perfuse the intracellular side of the channel with different solutions and d) *outside-out*, in which the pipette is pulled away from the membrane from the whole cell configuration. This configuration allows to study the effect of different extracellular solutions on single channel activity.

Patch clamp experiments were performed using glass capillaries pulled with an horizontal Sutter P-97 pipette puller. The resistance of the pipettes was 5-7 MΩ. The pipettes were then filled with an intracellular solution (KCl 145 mM, NaCl 4 mM, $CaCl_2$ 0,6 mM, $MgCl_2$ 1mM, Hepes 10mM, D-glucose 20mM, Sucrose 25 mM at pH 7.2) filtrated with 0.2 m pore filter. The cover slide with the cells was placed into a chamber containing extracellular solution (KCl 5 mM, NaCl 145 mM, $CaCl_2$ 1 mM, $MgCl_2$ 5mM, EGTA 10mM, Hepes 10mM, Sucrose 32 mM) at pH 7.2.

Electrophysiological experiments were conducted with a patch clamp unit composed of a Faraday chamber, whose function is to minimize the outside electromagnetic noise, an inverted microscope, a system of micromanipulators to bring the pipette close to the cell, and a florescence lamp to identify touch neurons expressing GFP under the promoter of *mec-4*. Pipette were inserted into a holder containing a chlorinated Ag/AgCl wire and equipped with a small plastic tube to apply the suction. The output signals from the head-stage were sent to an amplifier (Axopatch 200B, Axon Instrument), filtered and transferred through an analogical-digital converter (Digidata 1322A, Axon Instrument) to a computer. The currents induced by potential changes are recorded at 30kHz frequency and amplified. The signal is filtered at 1 kHz in order to eliminate background noise. Membrane voltage changed to any electrode potential applied according to this formula:

$$V=Vm-Vp$$

Where V is the membrane potential of the cell, Vm is the resting membrane potential and Vp is the electrode potential. To apply the negative pressure to the cells, we used a pneumatic transducer tester.

2.9 DYE UPTAKE

Cultured *C. elegans* wild-type (WT) and *unc-7(e5)* touch neurons were washed with physiological solution to remove completely the medium. The cells were then exposed for 20 minutes to an hypotonic solution (NaCl 72,5mM, KCl 5mM, $CaCl_2$ 1mM, $MgCl_2$ 5mM, Hepes 10mM, D-glucose 20mM, Sucrose 25mM at pH 7.2) and KCl solution (NaCl 100mM, KCl 50mM, $CaCl_2$ 1mM, $MgCl_2$ 5mM, Hepes 10mM, D-glucose 20mM, Sucrose 25 mM at pH 7.2) as a control and to the same solutions plus EtBr (5µM) and EtBr (5µM) plus carbenoxelone (100 µM). After treatment cells were washed 3 times with physiological solution and then fixed with 4% paraformaldehyde.
Ethidium bromide fluorescent intensity was measured using a LEICA DMRA2 stereo fluorescence microscope. This microscope is equipped with 60 x objective, a digital camera, a LEICA GFP plus filter (460/480 nm excitation filter) and a LEICA RFP filter (535/550 nm excitation filter). The images were acquired and analyzed using Adope Photoshop.

2.10 ANALYSIS OF DATA

The oocyte sections and *C. elegans* touch neurons were analyzed using ImageJ. Patch clamp data were analyzed using Clampfit 10.2 software (Axon) and plotted using Origin 8.0 (Microcal Software Inc. Northampton, MA, USA).

Chapter 3:

RESULTS

RESULTS

3.1 DELM-1 AND DELM-2

The *C. elegans* genome contains 28 genes that encode DEG/ENaC channel subunits. These channels are trimers formed of identical or homologous subunits (Canessa et al., 1994a). In the Bianchi's laboratory I focused on two ion channels belonging to DEG/ENaC family: DELM-1(**deg**enerin-**l**ike channel **m**echanosensory linked-**1**) and DELM-2 (**deg**enerin-**l**ike cannel **m**echanosensory linked-**2**). These channels are expressed in socket glia cells associated with OLQ and IL1 neurons that mediate nose touch sensitivity. Knock-out of *delm-1* and *delm-2* causes nose touch insensitivity. Because DEG/ENaCs are trimers and DELM-1 and DELM-2 are expressed in the same cells, the Bianchi lab hypothesized that they form a heteromeric channel complex. To test this hypothesis, I expressed DELM-1 and DELM-2 alone and together in *Xenopus* oocytes and the currents were measured. The Bianchi's laboratory found that while DELM-1 forms channels by itself, DELM-2 does not. Moreover, DELM-2 does not change the properties or pharmacology of DELM-1 currents. These results could have the following explanations: 1) DELM-1 and DELM-2 do not form a heteromultimeric complexes, 2) DELM-2 may control functions of DELM-1 such as surface expression or stability that are not easily assessed in oocytes or 3) DELM-2 is not expressed on the oocytes plasma membrane. To establish if DELM-2 is at the plasmamembrane of *Xenopus* oocytes, a GFP construct in which the fluorescent protein was fused at C-terminus of *delm-2* cDNA, was built. The vector used in these experiments was pGEM vector (Fig. 3.1) in which GFP-tagged DELM-2 was subcloned.

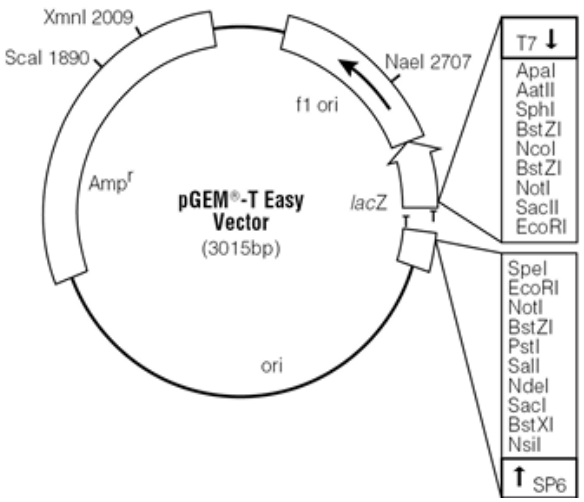

Figure 3.1. Schematic illustration of pGEM-vector using to express DELM-1 and DELM-2 in *Xenopus* oocytes.

I injected the oocytes with pGEM-DELM-2-GFP cRNA obtained through transcription reaction from PGEM-DELM-2-GFP cDNA (Fig. 3.2). Three days after injection the oocytes were prepared for cryosectioning and the presence of DELM-2 was tested in plasma membrane using LEICA DMRA2 fluorescent microscope. No fluorescence was found at the plasmamembrane, suggesting that DELM-2-GFP is either not translated or not transported to the plasma membrane (Fig. 3.3). Experiments are under way to confirm that fluorescence is visible at the plasma membrane when DELM-1-GFP is expressed and to test whether DELM-1 and DELM-2 interact *in vivo* in *C. elegans* cells. To test the interaction of DELM-1 and DELM-2 *in vivo* the BiFC (Venus-based molecular fluorescence complementation assay) technique will use. In this technique, the two proteins (in this case DELM-1 and DELM-2) are fused with N- and C-terminus of GFP. If the DELM-1 and DELM-2 interact, then the full GFP protein Venus will be reconstituted and the cells in which DELM-1 and DELM-2 are expressed (socket glia) will be fluorescent. Thus, I subcloned DELM-1 and DELM-2 cDNAs into two Venus cloning vectors pCE-BiFC-VN173 and pCE-BiFC-VC155. These two constructs will be injected into the gonads of *C. elegans* to generate transgenic animals. Transgenic animals will be analyzed using LEICA DMRA2 fluorescent microscope to determine if fluorescence is present in the socket glia. These experiments will establish if DELM-1 and DELM-2 exist as a heteromultimeric channel in glial socket cells.

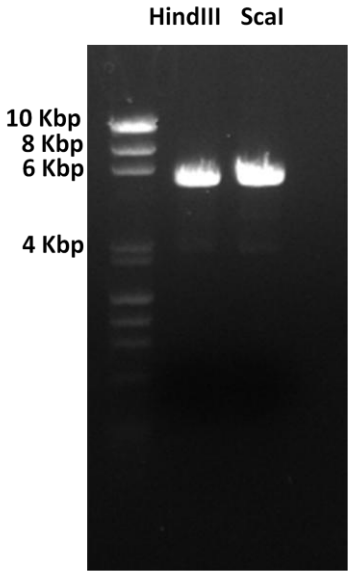

Figure 3.2. Picture of agarose gel showing the purified pGEM vector containing DELM-2-GFP linearized with HindIII and ScaI respectively. This DNA was used for *in vitro* cRNA transcription.

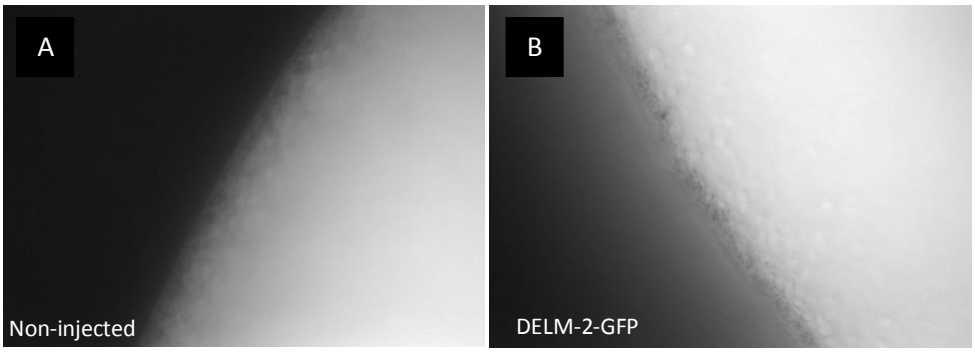

Figure 3.3. Analysis of oocytes sections by LEICA DMRA2 fluorescent microscope . **A)** Fluorescent photograph of a non- injected oocyte, showing no background fluorescence at the plasma membrane. **B**) Oocyte expressing DELM-2-GFP. Note that there is no expression of DELM-2 at the plasmamembrane.

3.2 CULTURE OF EMBRYONIC C. ELEGANS CELLS

C. elegans is a strong genetic model. However, it has some experimental limitations for the execution of electrophysiological experiments. Limitations include the fact that *C. elegans* tissues are contained within a pressurized harsh cuticle and that cells are small (a few micrometers in diameter). Christensen and colleagues recently developed a protocol (see methods) to isolate and culture *C. elegans* embryonic cells *in vitro* (Christensen et al., 2002). The culture of embryonic C. *elegans* cells is a method allows the easy application of electrophysiological techniques (Christensen et al. 2002; (Estevez et al., 2003); Bianchi et al. 2004).

I used *pmec-4::gfp* transgenic animals that express GFP in touch neurons, in order to identify touch neurons *in vitro* (Fig. 3.4).

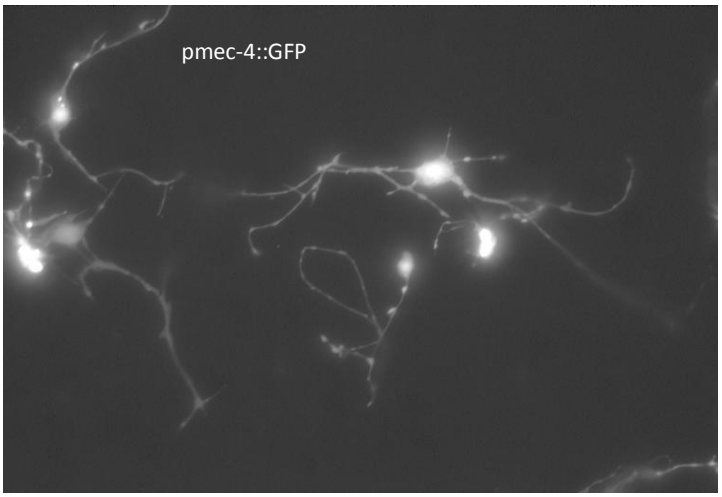

Figure 3.4. Culture of *C. elegans* touch neurons expressing GFP under the touch specific promoter *mec-4*.

3.3 INNEXIN UNC-7 IS A MECHANOSENSITIVE CHANNEL

The Bianchi's laboratory recently identified a large (300 pS) cationic channel in *C. elegans* touch neurons that is activated by stretch. Based on the fact that the channel has a large conductance, that it is non-selective and activated by membrane stretch, it was hypothesized that it is an innexin. More specifically, since innexin UNC-7 is expressed in touch neurons (Altun et al.; 2009), it was postulated that UNC-7 may underlie this conductance. To test this hypothesis I performed electrophysiological experiments on touch neurons from wild type and *unc-7(e5)* mutant animals. I cultured embryonic cells expressing PMEC-4::GFP, which is expressed in the ALMs and PLMs touch neurons. I performed electrophysiological patch clamp experiments in inside out configuration applying negative pressure on these neurons that are the 0.5% of the total number of cells (Fig 3.5) (Bianchi et al.;2004). The MEC channel is expressed in ALMs and PLMs and it is mechanosensory but cannot be activated by mechanical forces such as suction and osmotic pressure *in vitro* because it requires extracellular matrix proteins to gate (O'Hagan et al., 2005). Thus the MEC channel is typically not recorded in this type of experiments.

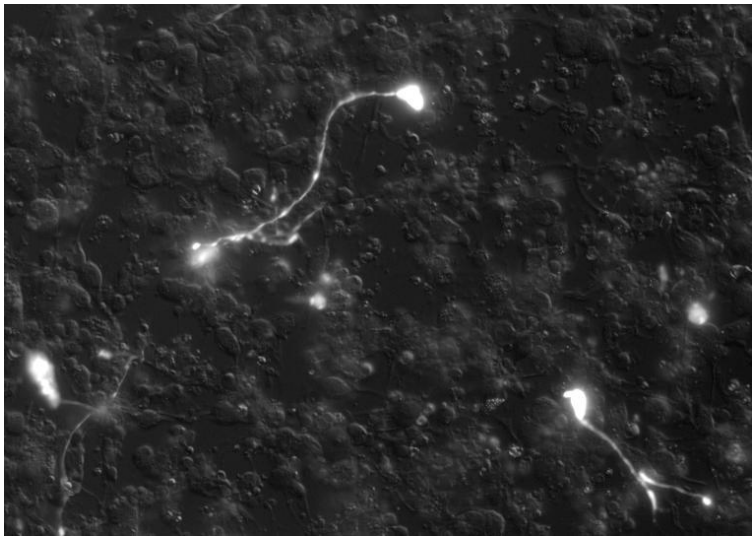

Figure 3.5. Primary of cultured *C. elegans* touch neurons expressing PMEC-4::GFP (~0,5% of the total number of the cells).

Figure 3.6 B shows a typical response of a WT touch neuron to -30 mmHg. A stretch activated channel with a conductance of 300 pS (Fig. 3.6C). As the negative pressure is maintained the channel activity declines spontaneously. When we repeated the same experiments in touch neurons from *unc-7(e5)* mutants we did not observe the same type of channel when negative pressure was applied. Rather the channel had a smaller conductance (100 pS) and opened and closed rapidly

(flickered) (Fig. 3.6D). These data suggest that UNC-7 may be part of a channel complex underlying the mechanosensitive conductance observed in cultured touch neurons (Table 3.1)

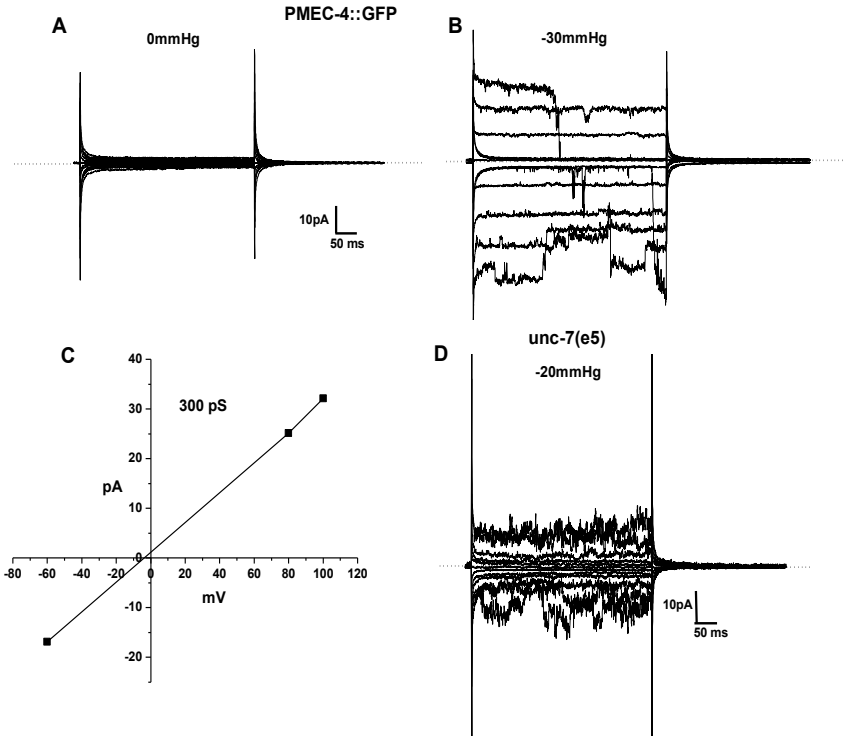

Figure 3.6. Patch-clamp recording from wild type and *unc-7(e5)* mutants cultured touch neurons expressing PMEC-4::GFP. **A)** and **B)** Patch clamp record in inside-out configuration on PMEC-4::GFP perfusing cultured cells with standard solution saline at 0mmHg and -30mmHg respectively. **C)** Single-channel current-voltage relationship estimating a conductance ~300 pS for mechanically-gated channel. **D**) Channel activity recorded from a touch neurons cultured from *unc-7(e5)* mutants while applying a negative pressure of -20mmHg.

Conductance pS	**PMEC-4::GFP** (n=36)	***unc-7(e5)*** (n=25)
10	30,5%	28%
25-40	38,8%	44%
100-300	**33,3%**	**12%**

Table 3.1. Conductance expressed in pS of all channels observed in inside out patch clamp analysis performed on both PMEC-4::GFP and *unc-7(e5)* touch neurons.

3.4 UNC-7 IS PERMEABLE TO ETHIDIUM BROMIDE

We performed dye uptake experiments in both PMEC-4::GFP and *unc-7(e)* touch neurons exposing them to a different solutions and measuring the influx of Ethidium Bromide, in the presence and absence of carbenoxelone, a pannexins and innexins inhibitor (Figure 3.7A and B).

We found that EtBr is uptaken in both wild type and *unc-7(e5)* mutant touch neurons, but that uptake is less in *unc-7(e5)* mutants. These data suggest that UNC-7 mediates part of the dye uptake. Moreover we found that in both wild type and *unc-7(e5)* mutants EtBr uptake is partially blocked by incubation with carbonoxelone, further underscoring that is mediated by innexins (Figure 3.7C and D).

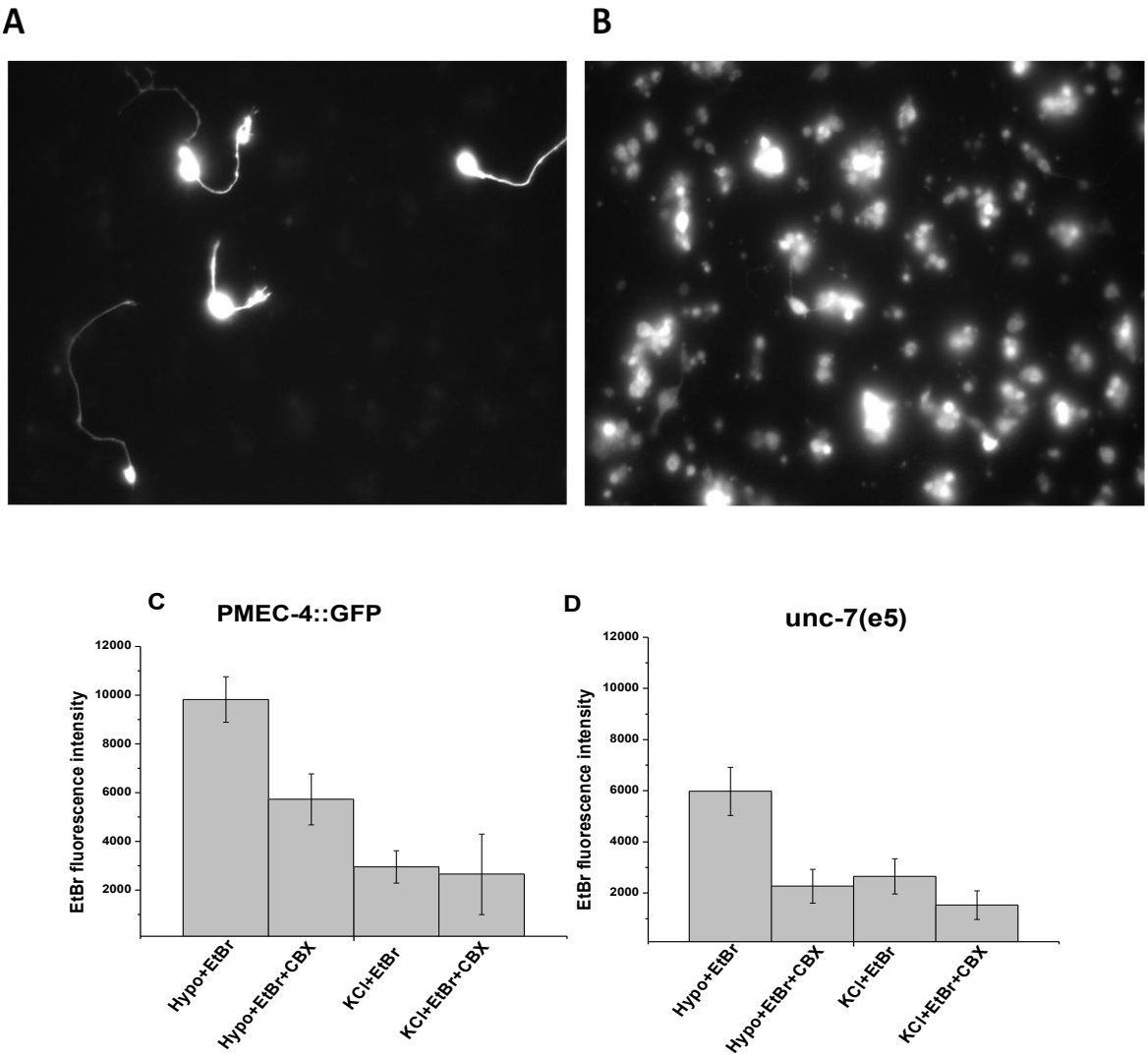

Figure 3.7. Dye uptake experiments conducted on PMEC-4:GFP and *unc-7(e5).* **A)** and **B)** Pictures of primary cultured *C. elegans* touch neurons expressing PMEC-4:GFP exposed to hypotonic solution with EtBr and acquired using GFP and RFP filter respectively. **C)** and **D)** results of dye uptake experiments from a single batch of touch neurons expressing PMEC-4:GFP and *unc-7(e5)* respectively exposed to different solutions and in presence of Etidium Bromide (EtBr) and carbenoxelone (CBX). The data were normalized to the mean value of the PMEC-4:GFP and *unc-7(e5)* touch neurons exposed to control solutions without EtBr and CBX. Data are expressed as mean ± SE, number touch neurons scored was 20 for each exposure to different solutions.

Chapter 4:

DISCUSSION

DISCUSSION

In this study I reported on ion channels implicated in touch sensation. My work was focused on DELM-1 and DELM-2 two novel channels belonging to the ENaC subfamily, and on innexin channel UNC-7. Data obtained during the time I spent in the Bianchi's laboratory provide new information ENaCs channel complex formation and on the possible role of innexin channels in mediating mechanotransduction.

4.1 DELM-1 AND DELM-2 HETEROMULTIMERIC COMPLEXES

DELM-2 does not produce measurable currents when injected alone in *Xenopus* oocytes. It is well known that some DEG/ENaC subunits are not functional on their own but can modulate the function of other DEG/ENaC subunits (Goodman et al.; 2002). Since DELM-1 and DELM-2 are expressed in the same glial cells, DELM-2 may co-assemble with DELM-1 to modulate its function. Previous studies in the Bianchi's lab had shown that DELM-2 does not change DELM-1 current amplitude, selectivity or sensitivity to amiloride. It was therefore concluded that either DELM-2 modulates properties of DELM-1 that were not initially assessed (mechanosenstivity, open probability or conductance), or that DELM-2 is not translated or transported to the plasmamembrane. My work shows that DELM-2 is likely not translated or transported to the cell surface of *Xenopus* oocytes. Interestingly, the cDNA sequence that we used for *in vitro* cRNA synthesis is capable of rescuing the nose-touch insensitive defects of *delm-2* mutants (data not shown). These data support that the cDNA that was cloned by RT-PCR in the Bianchi's lab contains a functional channel sequence. This observation refutes that problems with the cDNA that we used for in vitro cRNA synthesis may have caused lack of expression of DELM-2. We conclude that DELM-2 may need a chaperone or another protein to be efficiently transported to the cell surface. We currently do not know what this protein or factor is, but DEG/ENaC channels are known to have associated proteins including stomatins such as MEC-2 and paraoxonase-like proteins such as MEC-6 (Goodman et al., 2002,(Martinez-Salgado et al., 2007), (Brown et al., 2008). Future studies will establish if any of these proteins promotes expression of DELM-2 at the surface of oocytes. The Bianchi's lab will also test whether DELM-1 and DELM-2 interact *in vivo* in *C. elegans* glial cells using fret and BiFi.

4.2 INNEXIN UNC-7

Patch clamp experiments performed on touch neurons cultured *in vitro* show that there is a mechanosensitive channel in these neurons. This channel is likely not the MEC channel. Thus we investigated the biophysical and pharmacological features of this channel to determine if it has properties of the innexins. We observed that this channel is activated applying negative pressure to a touch neuron patch of membrane, is not selective and presents a large conductance (Fig 3.6B). These results suggest that the channel observed may be the innexin UNC-7. We performed patch clamp analysis on *unc-7(e5)* mutant touch neurons to further test the hypothesis that this channel is UNC-7. If it is UNC-7, we should not be able to see it in touch neurons of *unc-7(e5)* mutants. Our experiments show that in *unc-7(e5)* mutants the channel is activated only in 12% of patches, compared to the 33% in WT. Furthermore in mutant touch neurons the mechanosensitive channel exhibits different electrophysiological features (Fig 3.6D). These data support that UNC-7 may underlie the mechanosensitive channel found in touch neurons. Another set of experiments I performed, further supports this hypothesis. Indeed, in dye uptake experiments I found that EtBr is uptaken to a lesser degree in *unc-7 (e5)* mutants compared to WT and that the uptake is inhibited by CBX. To conclude my experiments provide evidence that the mechanosensitive channel on the membrane of touch sensing neurons of *C. elegans* is UNC-7. Further studies will determine whether UNC-7 is needed in *C. elegans* for responses to touch. If this turns out to be the case, this would be the first demonstration that a mechanosensitive innexin is directly involved in the process of touch sensation.

BIBLIOGRAPHY

1. Adibi,S.A., Schenker,S., and Morse,E. (1996). Mechanism of clearance and transfer of dipeptides by perfused human placenta. Am.J.Physiol *271*, E535-E540.

2. Altun,Z.F., Chen,B., Wang,Z.W., and Hall,D.H. (2009). High resolution map of Caenorhabditis elegans gap junction proteins. Dev.Dyn. *238*, 1936-1950.

3. Amasheh,S., Wenzel,U., Boll,M., Dorn,D., Weber,W., Clauss,W., and Daniel,H. (1997). Transport of charged dipeptides by the intestinal H+/peptide symporter PepT1 expressed in Xenopus laevis oocytes. J.Membr.Biol. *155*, 247-256.

4. Askwith,C.C., Benson,C.J., Welsh,M.J., and Snyder,P.M. (2001). DEG/ENaC ion channels involved in sensory transduction are modulated by cold temperature. Proc.Natl.Acad.Sci.U.S.A *98*, 6459-6463.

5. Bailey,P.D., Boyd,C.A., Bronk,J.R., Collier,I.D., Meredith,D., Morgan,K.M., and Temple,C.S. (2000). How to Make Drugs Orally Active: A Substrate Template for Peptide Transporter PepT1. Angew.Chem.Int.Ed Engl. *39*, 505-508.

6. Bailey,P.D., Boyd,C.A., Collier,I.D., George,J.G., Kellett,G.L., Meredith,D., Morgan,K.M., Pettecrew,R., Price,R.A., and Pritchard,R.G. (2005). Conformational and spacial preferences for substrates of PepT1. Chem.Commun.(Camb.) 5352-5354.

7. Bao,L., Locovei,S., and Dahl,G. (2004). Pannexin membrane channels are mechanosensitive conduits for ATP. FEBS Lett. *572*, 65-68.

8. Beachy,J.M. (2003). Premature infant massage in the NICU. Neonatal Netw. *22*, 39-45.

9. Berdiev,B.K., Xia,J., McLean,L.A., Markert,J.M., Gillespie,G.Y., Mapstone,T.B., Naren,A.P., Jovov,B., Bubien,J.K., Ji,H.L., Fuller,C.M., Kirk,K.L., and Benos,D.J. (2003). Acid-sensing ion channels in malignant gliomas. J.Biol.Chem. *278*, 15023-15034.

10. Bianchi,L. (2007). Mechanotransduction: touch and feel at the molecular level as modeled in Caenorhabditis elegans. Mol.Neurobiol. *36*, 254-271.

11. Bianchi,L. and Driscoll,M. (2006a). Culture of embryonic C. elegans cells for electrophysiological and pharmacological analyses. WormBook. 1-15.

12. Bianchi,L. and Driscoll,M. (2006b). Heterologous expression of C. elegans ion channels in Xenopus oocytes. WormBook. 1-16.

13. Bianchi,L., Gerstbrein,B., Frokjaer-Jensen,C., Royal,D.C., Mukherjee,G., Royal,M.A., Xue,J., Schafer,W.R., and Driscoll,M. (2004). The neurotoxic MEC-4(d) DEG/ENaC sodium channel conducts calcium: implications for necrosis initiation. Nat.Neurosci. *7*, 1337-1344.

14. Bolger,M.B., Haworth,I.S., Yeung,A.K., Ann,D., von Grafenstein,H., Hamm-Alvarez,S., Okamoto,C.T., Kim,K.J., Basu,S.K., Wu,S., and Lee,V.H. (1998). Structure, function, and

molecular modeling approaches to the study of the intestinal dipeptide transporter PepT1. J.Pharm.Sci. *87*, 1286-1291.

15. Boll,M., Herget,M., Wagener,M., Weber,W.M., Markovich,D., Biber,J., Clauss,W., Murer,H., and Daniel,H. (1996). Expression cloning and functional characterization of the kidney cortex high-affinity proton-coupled peptide transporter. Proc.Natl.Acad.Sci.U.S.A *93*, 284-289.

16. Bossi,E., Renna,M.D., Sangaletti,R., D'Antoni,F., Cherubino,F., Kottra,G., and Peres,A. (2011). Residues R282 and D341 act as electrostatic gates in the proton-dependent oligopeptide transporter PepT1. J.Physiol *589*, 495-510.

17. Bouhours,M., Po,M.D., Gao,S., Hung,W., Li,H., Georgiou,J., Roder,J.C., and Zhen,M. (2011). A co-operative regulation of neuronal excitability by UNC-7 innexin and NCA/NALCN leak channel. Mol.Brain *4*, 16.

18. Brandsch,M., Miyamoto,Y., Ganapathy,V., and Leibach,F.H. (1994). Expression and protein kinase C-dependent regulation of peptide/H+ co-transport system in the Caco-2 human colon carcinoma cell line. Biochem.J. *299 (Pt 1)*, 253-260.

19. Brockway,L.M., Zhou,Z.H., Bubien,J.K., Jovov,B., Benos,D.J., and Keyser,K.T. (2002). Rabbit retinal neurons and glia express a variety of ENaC/DEG subunits. Am.J.Physiol Cell Physiol *283*, C126-C134.

20. Brown,A.L., Liao,Z., and Goodman,M.B. (2008). MEC-2 and MEC-6 in the Caenorhabditis elegans sensory mechanotransduction complex: auxiliary subunits that enable channel activity. J.Gen.Physiol *131*, 605-616.

21. Buyse,M., Berlioz,F., Guilmeau,S., Tsocas,A., Voisin,T., Peranzi,G., Merlin,D., Laburthe,M., Lewin,M.J., Roze,C., and Bado,A. (2001). PepT1-mediated epithelial transport of dipeptides and cephalexin is enhanced by luminal leptin in the small intestine. J.Clin.Invest *108*, 1483-1494.

22. Canessa,C.M., Horisberger,J.D., Schild,L., and Rossier,B.C. (1995). Expression cloning of the epithelial sodium channel. Kidney Int. *48*, 950-955.

23. Canessa,C.M., Merillat,A.M., and Rossier,B.C. (1994a). Membrane topology of the epithelial sodium channel in intact cells. Am.J.Physiol *267*, C1682-C1690.

24. Canessa,C.M., Schild,L., Buell,G., Thorens,B., Gautschi,I., Horisberger,J.D., and Rossier,B.C. (1994b). Amiloride-sensitive epithelial Na+ channel is made of three homologous subunits. Nature *367*, 463-467.

25. Chalfie,M. (1993). Touch receptor development and function in Caenorhabditis elegans. J.Neurobiol. *24*, 1433-1441.

26. Chalfie,M. and Sulston,J. (1981). Developmental genetics of the mechanosensory neurons of Caenorhabditis elegans. Dev.Biol. *82*, 358-370.

27. Chalfie,M., Sulston,J.E., White,J.G., Southgate,E., Thomson,J.N., and Brenner,S. (1985). The neural circuit for touch sensitivity in Caenorhabditis elegans. J.Neurosci. *5*, 956-964.

28. Chatelier,A., McKenzie,D.J., Prinet,A., Galois,R., Robin,J., Zambonino,J., and Claireaux,G. (2006). Associations between tissue fatty acid composition and physiological traits of performance and metabolism in the seabass (Dicentrarchus labrax). J.Exp.Biol. *209*, 3429-3439.

29. Chen,C.C., Zimmer,A., Sun,W.H., Hall,J., Brownstein,M.J., and Zimmer,A. (2002). A role for ASIC3 in the modulation of high-intensity pain stimuli. Proc.Natl.Acad.Sci.U.S.A *99*, 8992-8997.

30. Chen,H., Wong,E.A., and Webb,K.E., Jr. (1999). Tissue distribution of a peptide transporter mRNA in sheep, dairy cows, pigs, and chickens. J.Anim Sci. *77*, 1277-1283.

31. Chen,X.Z., Steel,A., and Hediger,M.A. (2000). Functional roles of histidine and tyrosine residues in the H(+)-peptide transporter PepT1. Biochem.Biophys.Res.Commun. *272*, 726-730.

32. Christensen,M., Estevez,A., Yin,X., Fox,R., Morrison,R., McDonnell,M., Gleason,C., Miller,D.M., III, and Strange,K. (2002). A primary culture system for functional analysis of C. elegans neurons and muscle cells. Neuron *33*, 503-514.

33. Cole,K.S. and Curtis,H.J. (1941). MEMBRANE POTENTIAL OF THE SQUID GIANT AXON DURING CURRENT FLOW. J.Gen.Physiol *24*, 551-563.

34. Covitz,K.M., Amidon,G.L., and Sadee,W. (1998). Membrane topology of the human dipeptide transporter, hPEPT1, determined by epitope insertions. Biochemistry *37*, 15214-15221.

35. Daniel,H. (2004). Molecular and integrative physiology of intestinal peptide transport. Annu.Rev.Physiol *66*, 361-384.

36. Daniel,H. and Kottra,G. (2004). The proton oligopeptide cotransporter family SLC15 in physiology and pharmacology. Pflugers Arch. *447*, 610-618.

37. Daniel,H., Spanier,B., Kottra,G., and Weitz,D. (2006). From bacteria to man: archaic proton-dependent peptide transporters at work. Physiology.(Bethesda.) *21*, 93-102.

38. Doige,C.A. and Ames,G.F. (1993). ATP-dependent transport systems in bacteria and humans: relevance to cystic fibrosis and multidrug resistance. Annu.Rev.Microbiol. *47*, 291-319.

39. Doring,F., Dorn,D., Bachfischer,U., Amasheh,S., Herget,M., and Daniel,H. (1996). Functional analysis of a chimeric mammalian peptide transporter derived from the intestinal and renal isoforms. J.Physiol *497 (Pt 3)*, 773-779.

40. Driscoll,M. and Chalfie,M. (1991). The mec-4 gene is a member of a family of Caenorhabditis elegans genes that can mutate to induce neuronal degeneration. Nature *349*, 588-593.

41. Driscoll,M. and Kaplan,J. (1997). Mechanotransduction.

42. Drummond,H.A., Price,M.P., Welsh,M.J., and Abboud,F.M. (1998). A molecular component of the arterial baroreceptor mechanotransducer. Neuron *21*, 1435-1441.

43. Erickson,R.H., Gum,J.R., Jr., Lindstrom,M.M., McKean,D., and Kim,Y.S. (1995). Regional expression and dietary regulation of rat small intestinal peptide and amino acid transporter mRNAs. Biochem.Biophys.Res.Commun. *216*, 249-257.

44. Estevez,A.Y., Roberts,R.K., and Strange,K. (2003). Identification of store-independent and store-operated Ca2+ conductances in Caenorhabditis elegans intestinal epithelial cells. J.Gen.Physiol *122*, 207-223.

45. Ezra,A., Hoffman,A., Breuer,E., Alferiev,I.S., Monkkonen,J., Hanany-Rozen,N., Weiss,G., Stepensky,D., Gati,I., Cohen,H., Tormalehto,S., Amidon,G.L., and Golomb,G. (2000). A peptide prodrug approach for improving bisphosphonate oral absorption. J.Med.Chem. *43*, 3641-3652.

46. Fei,Y.J., Fujita,T., Lapp,D.F., Ganapathy,V., and Leibach,F.H. (1998a). Two oligopeptide transporters from Caenorhabditis elegans: molecular cloning and functional expression. Biochem.J. *332 (Pt 2)*, 565-572.

47. Fei,Y.J., Ganapathy,V., and Leibach,F.H. (1998b). Molecular and structural features of the proton-coupled oligopeptide transporter superfamily. Prog.Nucleic Acid Res.Mol.Biol. *58*, 239-261.

48. Fei,Y.J., Kanai,Y., Nussberger,S., Ganapathy,V., Leibach,F.H., Romero,M.F., Singh,S.K., Boron,W.F., and Hediger,M.A. (1994). Expression cloning of a mammalian proton-coupled oligopeptide transporter. Nature *368*, 563-566.

49. Fei,Y.J., Liu,W., Prasad,P.D., Kekuda,R., Oblak,T.G., Ganapathy,V., and Leibach,F.H. (1997). Identification of the histidyl residue obligatory for the catalytic activity of the human H+/peptide cotransporters PEPT1 and PEPT2. Biochemistry *36*, 452-460.

50. Fei,Y.J., Sugawara,M., Liu,J.C., Li,H.W., Ganapathy,V., Ganapathy,M.E., and Leibach,F.H. (2000). cDNA structure, genomic organization, and promoter analysis of the mouse intestinal peptide transporter PEPT1. Biochim.Biophys.Acta *1492*, 145-154.

51. Fielenbach,N. and Antebi,A. (2008). C. elegans dauer formation and the molecular basis of plasticity. Genes Dev. *22*, 2149-2165.

52. Freeman,T.C., Bentsen,B.S., Thwaites,D.T., and Simmons,N.L. (1995). H+/di-tripeptide transporter (PepT1) expression in the rabbit intestine. Pflugers Arch. *430*, 394-400.

53. Fujisawa,Y., Tateoka,R., Nara,T., Kamo,N., Taira,T., and Miyauchi,S. (2006). The extracellular pH dependency of transport activity by human oligopeptide transporter 1 (hPEPT1) expressed stably in Chinese hamster ovary (CHO) cells: a reason for the bell-shaped activity versus pH. Biol.Pharm.Bull. *29*, 997-1005.

54. Ganapathy,M.E., Huang,W., Wang,H., Ganapathy,V., and Leibach,F.H. (1998). Valacyclovir: a substrate for the intestinal and renal peptide transporters PEPT1 and PEPT2. Biochem.Biophys.Res.Commun. *246*, 470-475.

55. Ganapathy,V. and Leibach,F.H. (1982). Peptide transport in intestinal and renal brush border membrane vesicles. Life Sci. *30*, 2137-2146.

56. Ganapathy,V. and Leibach,F.H. (1983). Role of pH gradient and membrane potential in dipeptide transport in intestinal and renal brush-border membrane vesicles from the rabbit. Studies with L-carnosine and glycyl-L-proline. J.Biol.Chem. *258*, 14189-14192.

57. Garcia-Rill,E., Charlesworth,A., Heister,D., Ye,M., and Hayar,A. (2008). The developmental decrease in REM sleep: the role of transmitters and electrical coupling. Sleep *31*, 673-690.

58. Giaume,C. and Venance,L. (1998). Intercellular calcium signaling and gap junctional communication in astrocytes. Glia *24*, 50-64.

59. Gonzalez,D.E., Covitz,K.M., Sadee,W., and Mrsny,R.J. (1998). An oligopeptide transporter is expressed at high levels in the pancreatic carcinoma cell lines AsPc-1 and Capan-2. Cancer Res. *58*, 519-525.

60. Goodman,M.B., Ernstrom,G.G., Chelur,D.S., O'Hagan,R., Yao,C.A., and Chalfie,M. (2002). MEC-2 regulates C. elegans DEG/ENaC channels needed for mechanosensation. Nature *415*, 1039-1042.

61. Hauser,M., Narita,V., Donhardt,A.M., Naider,F., and Becker,J.M. (2001). Multiplicity and regulation of genes encoding peptide transporters in Saccharomyces cerevisiae. Mol.Membr.Biol. *18*, 105-112.

62. Hediger,M.A. (1994). Structure, function and evolution of solute transporters in prokaryotes and eukaryotes. [Review] [131 refs]. Journal of Experimental Biology *196*, 15-49.

63. Hediger,M.A., Coady,M.J., Ikeda,T.S., and Wright,E.M. (1987). Expression cloning and cDNA sequencing of the Na+/glucose co-transporter. Nature *330*, 379-381.

64. Henderson,P.J. (1990). Proton-linked sugar transport systems in bacteria. J.Bioenerg.Biomembr. *22*, 525-569.

65. Higgins,C.F. (1992). ABC transporters: from microorganisms to man. [Review] [236 refs]. Annual Review of Cell Biology *8*, 67-113.

66. HODGKIN,A.L., HUXLEY,A.F., and KATZ,B. (1952). Measurement of current-voltage relations in the membrane of the giant axon of Loligo. J.Physiol *116*, 424-448.

67. HOGBEN,C.A., TOCCO,D.J., BRODIE,B.B., and SCHANKER,L.S. (1959). On the mechanism of intestinal absorption of drugs. J.Pharmacol.Exp.Ther. *125*, 275-282.

68. Hong,K. and Driscoll,M. (1994). A transmembrane domain of the putative channel subunit MEC-4 influences mechanotransduction and neurodegeneration in C. elegans. Nature *367*, 470-473.

69. Huang,M. and Chalfie,M. (1994). Gene interactions affecting mechanosensory transduction in Caenorhabditis elegans. Nature *367*, 467-470.

70. Ikeda,T.S., Hwang,E.S., Coady,M.J., Hirayama,B.A., Hediger,M.A., and Wright,E.M. (1989). Characterization of a Na+/glucose cotransporter cloned from rabbit small intestine. J.Membr.Biol. *110*, 87-95.

71. Irie,M., Terada,T., Katsura,T., Matsuoka,S., and Inui,K. (2005). Computational modelling of H+-coupled peptide transport via human PEPT1. J.Physiol *565*, 429-439.

72. Jasti,J., Furukawa,H., Gonzales,E.B., and Gouaux,E. (2007). Structure of acid-sensing ion channel 1 at 1.9 A resolution and low pH. Nature *449*, 316-323.

73. Kaback,H.R. (1987). Molecular biology of active transport: from membrane to molecule to mechanism. Harvey Lect. *83*, 77-105.

74. Kalujnaia,S., McWilliam,I.S., Zaguinaiko,V.A., Feilen,A.L., Nicholson,J., Hazon,N., Cutler,C.P., and Cramb,G. (2007). Transcriptomic approach to the study of osmoregulation in the European eel Anguilla anguilla. Physiol Genomics *31*, 385-401.

75. Kaplan,J.M. and Horvitz,H.R. (1993). A dual mechanosensory and chemosensory neuron in Caenorhabditis elegans. Proc.Natl.Acad.Sci.U.S.A *90*, 2227-2231.

76. Kato,M., Maegawa,H., Okano,T., Inui,K., and Hori,R. (1989). Effect of various chemical modifiers on H+ coupled transport of cephradine via dipeptide carriers in rabbit intestinal brush-border membranes: role of histidine residues. J.Pharmacol.Exp.Ther. *251*, 745-749.

77. Keane,J. and Avery,L. (2003). Mechanosensory inputs influence Caenorhabditis elegans pharyngeal activity via ivermectin sensitivity genes. Genetics *164*, 153-162.

78. Kim,K.J., Yang,Y.J., and Kim,J.G. (2003). Purification and characterization of chitinase from Streptomyces sp. M-20. J.Biochem.Mol.Biol. *36*, 185-189.

79. Kottra,G. and Daniel,H. (2001). Bidirectional electrogenic transport of peptides by the proton-coupled carrier PEPT1 in Xenopus laevis oocytes: its asymmetry and symmetry. J.Physiol *536*, 495-503.

80. Kottra,G., Frey,I., and Daniel,H. (2008). Inhibition of intracellular dipeptide hydrolysis uncovers large outward transport currents of the peptide transporter PEPT1 in Xenopus oocytes. Pflugers Arch.

81. Kottra,G., Stamfort,A., and Daniel,H. (2002). PEPT1 as a paradigm for membrane carriers that mediate electrogenic bidirectional transport of anionic, cationic, and neutral substrates. J.Biol Chem. *277*, 32683-32691.

82. Kulkarni,A.A., Davies,D.L., Links,J.S., Patel,L.N., Lee,V.H., and Haworth,I.S. (2007). A charge pair interaction between Arg282 in transmembrane segment 7 and Asp341 in transmembrane segment 8 of hPepT1. Pharm.Res. *24*, 66-72.

83. Kulkarni,A.A., Haworth,I.S., and Lee,V.H. (2003). Transmembrane segment 5 of the dipeptide transporter hPepT1 forms a part of the substrate translocation pathway. Biochem.Biophys.Res.Commun. *306*, 177-185.

84. Landisman,C.E. and Connors,B.W. (2005). Long-term modulation of electrical synapses in the mammalian thalamus. Science *310*, 1809-1813.

85. Lee,V.H., Chu,C., Mahlin,E.D., Basu,S.K., Ann,D.K., Bolger,M.B., Haworth,I.S., Yeung,A.K., Wu,S.K., Hamm-Alvarez,S., and Okamoto,C.T. (1999). Biopharmaceutics of

transmucosal peptide and protein drug administration: role of transport mechanisms with a focus on the involvement of PepT1. J.Control Release *62*, 129-140.

86. Lester,H.A., Cao,Y., and Mager,S. (1996). Listening to neurotransmitter transporters. Neuron *17*, 807-810.

87. Li,W., Kang,L., Piggott,B.J., Feng,Z., and Xu,X.Z. (2011). The neural circuits and sensory channels mediating harsh touch sensation in Caenorhabditis elegans. Nat.Commun. *2*, 315.

88. Liang,R., Fei,Y.J., Prasad,P.D., Ramamoorthy,S., Han,H., Yang-Feng,T.L., Hediger,M.A., Ganapathy,V., and Leibach,F.H. (1995). Human intestinal H+/peptide cotransporter. Cloning, functional expression, and chromosomal localization. J.Biol.Chem. *270*, 6456-6463.

89. Liu,W., Liang,R., Ramamoorthy,S., Fei,Y.J., Ganapathy,M.E., Hediger,M.A., Ganapathy,V., and Leibach,F.H. (1995). Molecular cloning of PEPT 2, a new member of the H+/peptide cotransporter family, from human kidney. Biochim.Biophys.Acta *1235*, 461-466.

90. Lucas,M.L., Schneider,W., Haberich,F.J., and Blair,J.A. (1975). Direct measurement by pH-microelectrode of the pH microclimate in rat proximal jejunum. Proc.R.Soc.Lond B Biol.Sci. *192*, 39-48.

91. Mackenzie,B., Loo,D.D., Fei,Y., Liu,W.J., Ganapathy,V., Leibach,F.H., and Wright,E.M. (1996). Mechanisms of the human intestinal H+-coupled oligopeptide transporter hPEPT1. J.Biol Chem. *271*, 5430-5437.

92. Maffia,M., Rizzello,A., Acierno,R., Verri,T., Rollo,M., Danieli,A., Doring,F., Daniel,H., and Storelli,C. (2003). Characterisation of intestinal peptide transporter of the Antarctic haemoglobinless teleost Chionodraco hamatus. J.Exp.Biol. *206*, 705-714.

93. Mager,S., Cao,Y., and Lester,H.A. (1998). Measurement of transient currents from neurotransmitter transporters expressed in Xenopus oocytes. Methods Enzymol. *296*, 551-566.

94. Martinez-Salgado,C., Benckendorff,A.G., Chiang,L.Y., Wang,R., Milenkovic,N., Wetzel,C., Hu,J., Stucky,C.L., Parra,M.G., Mohandas,N., and Lewin,G.R. (2007). Stomatin and sensory neuron mechanotransduction. J.Neurophysiol. *98*, 3802-3808.

95. Matsumoto,S., Saito,H., and Inui,K. (1994). Transcellular transport of oral cephalosporins in human intestinal epithelial cells, Caco-2: interaction with dipeptide transport systems in apical and basolateral membranes. J.Pharmacol.Exp.Ther. *270*, 498-504.

96. Meier,C. and Dermietzel,R. (2006). Electrical synapses--gap junctions in the brain. Results Probl.Cell Differ. *43*, 99-128.

97. Meredith,D. (2004). Site-directed mutation of arginine 282 to glutamate uncouples the movement of peptides and protons by the rabbit proton-peptide cotransporter PepT1. J.Biol Chem. *279*, 15795-15798.

98. Meredith,D. and Boyd,C.A. (1995). Dipeptide transport characteristics of the apical membrane of rat lung type II pneumocytes. Am.J.Physiol *269*, L137-L143.

99. Meredith,D. and Price,R.A. (2006). Molecular modeling of PepT1--towards a structure. J.Membr.Biol *213*, 79-88.

100. Mertl,M., Daniel,H., and Kottra,G. (2008). Substrate-induced changes in the density of peptide transporter PEPT1 expressed in Xenopus oocytes. Am.J.Physiol Cell Physiol *295*, C1332-C1343.

101. Miyamoto,K., Shiraga,T., Morita,K., Yamamoto,H., Haga,H., Taketani,Y., Tamai,I., Sai,Y., Tsuji,A., and Takeda,E. (1996). Sequence, tissue distribution and developmental changes in rat intestinal oligopeptide transporter. Biochim.Biophys.Acta *1305*, 34-38.

102. Nalbant,P., Boehmer,C., Dehmelt,L., Wehner,F., and Werner,A. (1999). Functional characterization of a Na+-phosphate cotransporter (NaPi-II) from zebrafish and identification of related transcripts. J.Physiol *520 Pt 1*, 79-89.

103. Nemani,V.M. and Binder,D.K. (2005). Emerging role of gap junctions in epilepsy. Histol.Histopathol. *20*, 253-259.

104. Neumann,J. and Brandsch,M. (2003). Delta-aminolevulinic acid transport in cancer cells of the human extrahepatic biliary duct. J.Pharmacol.Exp.Ther. *305*, 219-224.

105. Newstead,S., Drew,D., Cameron,A.D., Postis,V.L., Xia,X., Fowler,P.W., Ingram,J.C., Carpenter,E.P., Sansom,M.S., McPherson,M.J., Baldwin,S.A., and Iwata,S. (2011). Crystal structure of a prokaryotic homologue of the mammalian oligopeptide-proton symporters, PepT1 and PepT2. EMBO J. *30*, 417-426.

106. Norman,K.R. and Maricq,A.V. (2007). Innexin function: minding the gap junction. Curr.Biol. *17*, R812-R814.

107. Nussberger,S., Steel,A., Trotti,D., Romero,M.F., Boron,W.F., and Hediger,M.A. (1997). Symmetry of H+ binding to the intra- and extracellular side of the H+-coupled oligipeptide cotransporter PepT1. J.Biol.Chem. *272*, 7777-7785.

108. O'Hagan,R., Chalfie,M., and Goodman,M.B. (2005). The MEC-4 DEG/ENaC channel of Caenorhabditis elegans touch receptor neurons transduces mechanical signals. Nat.Neurosci. *8*, 43-50.

109. Panchin,Y., Kelmanson,I., Matz,M., Lukyanov,K., Usman,N., and Lukyanov,S. (2000). A ubiquitous family of putative gap junction molecules. Curr.Biol. *10*, R473-R474.

110. Parent,L., Supplisson,S., Loo,D.D., and Wright,E.M. (1992). Electrogenic properties of the cloned Na+/glucose cotransporter: I. Voltage-clamp studies. J.Membr.Biol. *125*, 49-62.

111. Paulsen,I.T. and Skurray,R.A. (1994). The POT family of transport proteins. Trends Biochem.Sci. *19*, 404.

112. Peres,A., Giovannardi,S., Bossi,E., and Fesce,R. (2004a). Electrophysiological insights into the mechanism of ion-coupled cotransporters. News Physiol Sci *19*, 80-84.

113. Peres,A., Pisani,R., Soragna,A., and Fesce,R. (2004b). Biophysical approaches to the study of ion coupled transport protein. Recent Res.Devel.Membrane Biol. *2*, 1-19.

114. Phelan,P. and Starich,T.A. (2001). Innexins get into the gap. Bioessays *23*, 388-396.

115. Price,M.P., McIlwrath,S.L., Xie,J., Cheng,C., Qiao,J., Tarr,D.E., Sluka,K.A., Brennan,T.J., Lewin,G.R., and Welsh,M.J. (2001). The DRASIC cation channel contributes to the detection of cutaneous touch and acid stimuli in mice. Neuron *32*, 1071-1083.

116. Ramamoorthy,S., Liu,W., Ma,Y.Y., Yang-Feng,T.L., Ganapathy,V., and Leibach,F.H. (1995). Proton/peptide cotransporter (PEPT 2) from human kidney: functional characterization and chromosomal localization. Biochim.Biophys.Acta *1240*, 1-4.

117. Rankin,C.H. (1991). Interactions between two antagonistic reflexes in the nematode Caenorhabditis elegans. J.Comp Physiol A *169*, 59-67.

118. Renna,M.D., Oyadeyi,A.S., Bossi,E., Kottra,G., and Peres,A. (2011). Functional and structural determinants of reverse operation in the pH-dependent oligopeptide transporter PepT1. Cell Mol.Life Sci. *68*, 2961-2975.

119. Riddle,D.L., Blumenthal,T., Meyer,B.J., and Priess,J.R. (1997). Introduction to C. elegans.

120. Roman,G., Meller,V., Wu,K.H., and Davis,R.L. (1998). The opt1 gene of Drosophila melanogaster encodes a proton-dependent dipeptide transporter. Am.J.Physiol *275*, C857-C869.

121. Romano,A., Kottra,G., Barca,A., Tiso,N., Maffia,M., Argenton,F., Daniel,H., Storelli,C., and Verri,T. (2006). High-affinity peptide transporter PEPT2 (SLC15A2) of the zebrafish Danio rerio: functional properties, genomic organization, and expression analysis. Physiol Genomics *24*, 207-217.

122. Ronnestad,I., Gavaia,P.J., Viegas,C.S., Verri,T., Romano,A., Nilsen,T.O., Jordal,A.E., Kamisaka,Y., and Cancela,M.L. (2007). Oligopeptide transporter PepT1 in Atlantic cod (Gadus morhua L.): cloning, tissue expression and comparative aspects. J.Exp.Biol. *210*, 3883-3896.

123. Rubio-Aliaga,I. and Daniel,H. (2002). Mammalian peptide transporters as targets for drug delivery. Trends Pharmacol.Sci. *23*, 434-440.

124. Saito,H., Okuda,M., Terada,T., Sasaki,S., and Inui,K. (1995). Cloning and characterization of a rat H+/peptide cotransporter mediating absorption of beta-lactam antibiotics in the intestine and kidney. J.Pharmacol.Exp.Ther. *275*, 1631-1637.

125. Sakata,K., Yamashita,T., Maeda,M., Moriyama,Y., Shimada,S., and Tohyama,M. (2001). Cloning of a lymphatic peptide/histidine transporter. Biochem.J. *356*, 53-60.

126. Sala-Rabanal,M., Loo,D.D., Hirayama,B.A., Turk,E., and Wright,E.M. (2006). Molecular interactions between dipeptides, drugs and the human intestinal H+ -oligopeptide cotransporter hPEPT1. J.Physiol *574*, 149-166.

127. Shiraga,T., Miyamoto,K., Tanaka,H., Yamamoto,H., Taketani,Y., Morita,K., Tamai,I., Tsuji,A., and Takeda,E. (1999). Cellular and molecular mechanisms of dietary regulation on rat intestinal H+/Peptide transporter PepT1. Gastroenterology *116*, 354-362.

128. Smith,D.E., Pavlova,A., Berger,U.V., Hediger,M.A., Yang,T., Huang,Y.G., and Schnermann,J.B. (1998). Tubular localization and tissue distribution of peptide transporters in rat kidney. Pharm.Res. *15*, 1244-1249.

129. Soragna,A., Bossi,E., Giovannardi,S., Pisani,R., and Peres,A. (2005). Relations between substrate affinities and charge equilibration rates in the rat GABA cotransporter GAT1. J Physiol *562*, 333-345.

130. Starich,T.A., Herman,R.K., and Shaw,J.E. (1993). Molecular and genetic analysis of unc-7, a Caenorhabditis elegans gene required for coordinated locomotion. Genetics *133*, 527-541.

131. Steel,A., Nussberger,S., Romero,M.F., Boron,W.F., Boyd,C.A., and Hediger,M.A. (1997). Stoichiometry and pH dependence of the rabbit proton-dependent oligopeptide transporter PepT1. J.Physiol *498 (Pt 3)*, 563-569.

132. Steiner,H.Y., Naider,F., and Becker,J.M. (1995). The PTR family: a new group of peptide transporters. Mol.Microbiol. *16*, 825-834.

133. Talhouk,R.S., Zeinieh,M.P., Mikati,M.A., and El Sabban,M.E. (2008). Gap junctional intercellular communication in hypoxia-ischemia-induced neuronal injury. Prog.Neurobiol. *84*, 57-76.

134. Tamai,I., Nakanishi,T., Hayashi,K., Terao,T., Sai,Y., Shiraga,T., Miyamoto,K., Takeda,E., Higashida,H., and Tsuji,A. (1997). The predominant contribution of oligopeptide transporter PepT1 to intestinal absorption of beta-lactam antibiotics in the rat small intestine. J.Pharm.Pharmacol. *49*, 796-801.

135. Tavernarakis,N., Shreffler,W., Wang,S., and Driscoll,M. (1997). unc-8, a DEG/ENaC family member, encodes a subunit of a candidate mechanically gated channel that modulates C. elegans locomotion. Neuron *18*, 107-119.

136. Terada,T., Saito,H., and Inui,K. (1998). Interaction of beta-lactam antibiotics with histidine residue of rat H+/peptide cotransporters, PEPT1 and PEPT2. J.Biol.Chem. *273*, 5582-5585.

137. Terada,T., Sawada,K., Irie,M., Saito,H., Hashimoto,Y., and Inui,K. (2000). Structural requirements for determining the substrate affinity of peptide transporters PEPT1 and PEPT2. Pflugers Arch. *440*, 679-684.

138. Thamotharan,M., Bawani,S.Z., Zhou,X., and Adibi,S.A. (1999). Hormonal regulation of oligopeptide transporter pept-1 in a human intestinal cell line. Am.J.Physiol *276*, C821-C826.

139. Theis,S., Doring,F., and Daniel,H. (2001). Expression of the myc/His-tagged human peptide transporter hPEPT1 in yeast for protein purification and functional analysis. Protein Expr.Purif. *22*, 436-442.

140. Thwaites,D.T. and Anderson,C.M. (2007). H+-coupled nutrient, micronutrient and drug transporters in the mammalian small intestine. Exp.Physiol *92*, 603-619.

141. Thwaites,D.T., Ford,D., Glanville,M., and Simmons,N.L. (1999). H(+)/solute-induced intracellular acidification leads to selective activation of apical Na(+)/H(+) exchange in human intestinal epithelial cells. J.Clin.Invest *104*, 629-635.

142. Uchiyama,T., Kulkarni,A.A., Davies,D.L., and Lee,V.H. (2003). Biophysical evidence for His57 as a proton-binding site in the mammalian intestinal transporter hPepT1. Pharm.Res. *20*, 1911-1916.

143. Verri,T., Kottra,G., Romano,A., Tiso,N., Peric,M., Maffia,M., Boll,M., Argenton,F., Daniel,H., and Storelli,C. (2003). Molecular and functional characterisation of the zebrafish (Danio rerio) PEPT1-type peptide transporter. FEBS Letters *549*, 115-122.

144. Vig,B.S., Stouch,T.R., Timoszyk,J.K., Quan,Y., Wall,D.A., Smith,R.L., and Faria,T.N. (2006). Human PEPT1 pharmacophore distinguishes between dipeptide transport and binding. J.Med.Chem. *49*, 3636-3644.

145. Walker,D., Thwaites,D.T., Simmons,N.L., Gilbert,H.J., and Hirst,B.H. (1998). Substrate upregulation of the human small intestinal peptide transporter, hPepT1. J.Physiol *507 (Pt 3)*, 697-706.

146. Wang,H., Fei,Y.J., Ganapathy,V., and Leibach,F.H. (1998). Electrophysiological characteristics of the proton-coupled peptide transporter PEPT2 cloned from rat brain. Am.J.Physiol *275*, C967-C975.

147. Watanabe,K., Sawano,T., Terada,K., Endo,T., Sakata,M., and Sato,J. (2002). Studies on intestinal absorption of sulpiride (1): carrier-mediated uptake of sulpiride in the human intestinal cell line Caco-2. Biol.Pharm.Bull. *25*, 885-890.

148. Way,J.C. and Chalfie,M. (1989). The mec-3 gene of Caenorhabditis elegans requires its own product for maintained expression and is expressed in three neuronal cell types. Genes Dev. *3*, 1823-1833.

149. Wemmie,J.A., Askwith,C.C., Lamani,E., Cassell,M.D., Freeman,J.H., Jr., and Welsh,M.J. (2003). Acid-sensing ion channel 1 is localized in brain regions with high synaptic density and contributes to fear conditioning. J.Neurosci. *23*, 5496-5502.

150. Wemmie,J.A., Chen,J., Askwith,C.C., Hruska-Hageman,A.M., Price,M.P., Nolan,B.C., Yoder,P.G., Lamani,E., Hoshi,T., Freeman,J.H., Jr., and Welsh,M.J. (2002). The acid-activated ion channel ASIC contributes to synaptic plasticity, learning, and memory. Neuron *34*, 463-477.

151. Wenzel,U., Diehl,D., Herget,M., Kuntz,S., and Daniel,H. (1999). Regulation of the high-affinity H+/peptide cotransporter in renal LLC-PK1 cells. J.Cell Physiol *178*, 341-348.

152. Yamashita,T., Shimada,S., Guo,W., Sato,K., Kohmura,E., Hayakawa,T., Takagi,T., and Tohyama,M. (1997). Cloning and functional expression of a brain peptide/histidine transporter. J.Biol.Chem. *272*, 10205-10211.

153. Yang,C.Y., Dantzig,A.H., and Pidgeon,C. (1999). Intestinal peptide transport systems and oral drug availability. Pharm.Res. *16*, 1331-1343.

154. Yeh,E., Kawano,T., Ng,S., Fetter,R., Hung,W., Wang,Y., and Zhen,M. (2009). Caenorhabditis elegans innexins regulate active zone differentiation. J.Neurosci. *29*, 5207-5217.

155. Yen,M.R. and Saier,M.H., Jr. (2007). Gap junctional proteins of animals: the innexin/pannexin superfamily. Prog.Biophys.Mol.Biol. *94*, 5-14.

156. Yuen,B.B., Wong,C.K., Woo,N.Y., and Au,D.W. (2007). Induction and recovery of morphofunctional changes in the intestine of juvenile carnivorous fish (Epinephelus coioides) upon exposure to foodborne benzo[a]pyrene. Aquat.Toxicol. *82*, 181-194.

157. Zeng,H., Parthasarathy,R., Rampal,A.L., and Jung,C.Y. (1996). Proposed structure of putative glucose channel in GLUT1 facilitative glucose transporter. Biophys.J. *70*, 14-21.

158. Zhang,E.Y., Emerick,R.M., Pak,Y.A., Wrighton,S.A., and Hillgren,K.M. (2004). Comparison of human and monkey peptide transporters: PEPT1 and PEPT2. Mol.Pharm. *1*, 201-210.

159. Zhu,T., Chen,X.Z., Steel,A., Hediger,M.A., and Smith,D.E. (2000). Differential recognition of ACE inhibitors in Xenopus laevis oocytes expressing rat PEPT1 and PEPT2. Pharm.Res. *17*, 526-532.

160. Zucchelli,M., Torkvist,L., Bresso,F., Halfvarson,J., Hellquist,A., Anedda,F., Assadi,G., Lindgren,G.B., Svanfeldt,M., Janson,M., Noble,C.L., Pettersson,S., Lappalainen,M., Paavola-Sakki,P., Halme,L., Farkkila,M., Turunen,U., Satsangi,J., Kontula,K., Lofberg,R., Kere,J., and D'Amato,M. (2009). PepT1 oligopeptide transporter (SLC15A1) gene polymorphism in inflammatory bowel disease. Inflamm.Bowel.Dis. *15*, 1562-1569.